Aus der Herzchirurgischen Klinik und Poliklinik

Klinik der Ludwig-Maximilians-Universität München

Vorstand: Prof. Dr. med. Christian Hagl


# *Novel transvalvular ventricular assist device (VAD) as new surgical treatment strategy in acute terminal heart failure, as LVAD or RVAD, in acute adult porcine models – initial experiences*

Dissertation
zum Erwerb des Doktorgrades der Medizin
an der Medizinischen Fakultät der
Ludwig-Maximilians-Universität zu München

vorgelegt von

Maks Mihalj
aus
Ljubljana, Slowenien

Jahr 2021

Mit Genehmigung der Medizinischen Fakultät
der Universität München

| | |
|---|---|
| Berichterstatter: | Prof. Dr. med. Paolo Brenner |
| Mitberichterstatter: | Prof. Dr. Michael Näbauer |
| | Priv.Doz. Dr. med. Peter Steinbigler |
| | Prof. Dr. Wolfgang von Scheidt |
| | Prof. Dr. Berhard Zwißler |
| Dekan: | Prof. Dr. med. dent. Reinhard Hickel |
| Tag der mündlichen Prüfung: | 24.06.2021 |

*Dedicated to most loved ones*

*To my mom and Hiroki*

# Table of contents

**TABLE OF CONTENTS** ..... I

**1 INTRODUCTION** ..... 1

**1.1 HEART FAILURE** ..... 1
***1.1.1 Epidemiology*** ..... *1*
***1.1.2 Pathophysiology*** ..... *1*
***1.1.3 Classification*** ..... *2*
***1.1.4 Treatment options for advanced heart failure*** ..... *3*
**1.2 DURABLE MECHANICAL CIRCULATORY SUPPORT SYSTEMS (MCS)** ..... 4
***1.2.1 Brief history of MCS*** ..... *4*
***1.2.2 MCS implementations*** ..... *6*
***1.2.3 Treatment options in advanced heart failure with MCS*** ..... *6*
**1.2.3.1 Jarvik 2000© Flowmaker LVAD** ..... 8
**1.2.3.1.1 Technical specifications** ..... 8
**1.2.3.1.2 Components** ..... 9
**1.2.3.1.3 Implantation technique** ..... 10
**1.2.3.2 Impella© - a percutaneous transaortic short-term mechanical circulatory support system for acute heart failure** ..... 11

**2 INVESTIGATED DEVICE: NOVEL TRANSVALVULAR AXIAL CONTINUOUS FLOW VENTRICULAR ASSIST DEVICE (TVAD; TRANSVALVULAR VAD)** ..... 13

**2.1 PUMP DESIGN** ..... 14
**2.2 ANIMAL MODEL** ..... 17
***2.2.1 Animal experiments in LVADs so far*** ..... *17*
**2.2.1.1 Bovine models** ..... 17
**2.2.1.2 Porcine models** ..... 18
***2.2.2 Ways of inducing heart failure in large animal models*** ..... *18*

**3 METHODOLOGY** ..... 19

**3.1 CHOOSING THE ANIMAL MODEL USING EX-VIVO MODELS** ..... 20
***3.1.1 Bovine model*** ..... *20*
***3.1.2 Porcine model*** ..... *21*
**3.2 ANESTHESIA** ..... 23
**3.3 SURGICAL IMPLANTATION TECHNIQUE** ..... 24
***3.3.1 Transvalvular LVAD in aortic position and biological aortic valve replacement*** ..... *24*
***3.3.2 Transvalvular LVAD in aortic position*** ..... *25*
***3.3.3 Transvalvular RVAD in pulmonary position*** ..... *25*
**3.4 INTRAOPERATIVE TIMELINE PROTOCOL** ..... 27

**4 RESULTS** ..... 29

**4.1 TRANSVALVULAR LVAD IN AORTIC POSITION AND BIOLOGICAL AORTIC VALVE REPLACEMENT – PROSTHETIC VALVE PUMP (TLVAD WITH AVR, PVP)** ..... 29
***4.1.1 LAD Occlusion*** ..... *35*
**4.2 TRANSVALVULAR RVAD IN PULMONARY POSITION IN NATIVE PULMONARY VALVE (TRVAD)** ..... 38
**4.3 TRANSVALVULAR LVAD IN AORTIC POSITION IN THE NATIVE AORTIC VALVE (TLVAD)** ..... 41
***4.3.1 LAD-Occlusion*** ..... *43*

**5 DISCUSSION** ..... 47

**5.1 SURGICAL FEASIBILITY** ..... 50
**5.2 HEMODYNAMICS** ..... 52
***5.2.1 Transvalvular LVAD*** ..... *54*

5.2.1.1 Induction of acute heart failure by surgical LAD-occlusion ..... 57
*5.2.2 Transvalvular RVAD* ..... *58*
5.3 IMPLICATIONS FOR THE FUTURE ..... 60
6 CONCLUSIONS ..... 63
7 ACKNOWLEDGMENTS ..... 65
8 APPENDIX ..... 67
8.1 LIST OF ABBREVIATIONS ..... 67
8.2 INDEX OF IMAGES ..... 69
8.3 INDEX OF GRAPHS ..... 69
8.4 INDEX OF TABLES ..... 69
8.5 INDEX OF PUBLICATIONS ..... 69
8.6 "EIDESSTATTLICHE VERSICHERUNG" ..... 71
9 REFERENCES ..... 73

# 1 Introduction

## 1.1 Heart failure

### 1.1.1 Epidemiology

Heart failure (HF) is a major cause of death in the western world, affecting over 23 million people worldwide[1], with trends indicating rapid increase in its prevalence.[2] In the USA, the overall lifetime risk of developing HF is 20% for individuals ≥40 years of age[3]. In Germany, the overall lifetime prevalence of major cardiovascular disease in 2012 was 12%, however with steep rise in the prevalence with increasing age, reaching 45% of individuals ≥80 years of age.[4] The rate was 2.6% higher in men (13.3%) than in women (10.7%).

The 5-year mortality rate for HF after the initial diagnosis lies at 50%.[5] In the ARIC study, the 30-day, 1-year, and 5-year overall mortality rates after hospitalization for HF were 10.4%, 22%, and 42.3%, respectively.[6] In another population cohort study with 5-year mortality data, survival ranged from 97% and 96 % in ACC/AHA HF[12] stages A and B, to 75% and 20% in stages C and D, respectively.[7] Approximately 7% of all cardiovascular deaths are due to HF, with cardiovascular diseases being the most common cause of death in the western world.[9]

The increased severity of the disease with age and time requires repeated hospitalizations despite best medical therapy with resulting substantial health care costs as well as a decrease in quality of life for the patients. HF is the primary diagnosis in over 1 million hospitalizations yearly in the USA alone. Patients with HF are at high risk for all-cause rehospitalizations, with a 1-month readmission rate of 25%.[8] It is associated with growing economic burden on the health care systems globally, in Germany alone the hospitalization costs in 2006 were estimated to 2.9 Billion Euros [23 24], in USA the yearly costs for hospitalizations due to HF are estimated at over 18 Billion USD.[2 9]

### 1.1.2 Pathophysiology

HF is defined as is a complex clinical syndrome of symptoms and signs that suggest impairment of the heart supporting physiological circulation, caused by structural or functional abnormalities of the heart, resulting in the impairment of ventricular filling or ejection of blood, and thus in the inability of the heart to supply the peripheral tissues with sufficient blood, resulting in insufficient tissue metabolism at rest and/or at exertion.

From the pathophysiological point of view, HF can be divided in three main types: left-sided HF, right-sided HF, and congestive HF. While the causes vary, it is associated with wide spectrum of myocardial functional and structural abnormalities, ranging from patients with normal ventricular size and preserved ejection fraction (EF), to patients with severe ventricular dilatation, and severely impaired EF. In most patients, abnormalities of systolic and diastolic dysfunction coexist, irrespective of EF. EF however has an important role in the classification and identification of patients, because most clinical trials and thus recommendations on differing patient demographics, comorbid conditions, prognosis, and response to therapies[10] are based on the EF.

The symptoms most commonly observed include dyspnea and fatigue, which may limit exercise intolerance, and fluid retention, which may lead to pulmonary, systemic or peripheral congestion. There is no single diagnostic test for HF as it is largely a clinical diagnosis based on a careful history and medical examination, although some pharmacological and physical diagnostic tests can imply to HF, such as right sided heart catheterization, and proBNP serum levels.

The clinical syndrome of HF may result from any structural or functional of the heart and include, but are not limited to, disorders of the pericardium, myocardium, endocardium, heart valves, or great vessels or from certain metabolic abnormalities, resulting in an impaired left ventricular (LV) myocardial function in most cases. While HF does not imply to the presence of either cardiomyopathy or LV dysfunction, however these structural and functional disorders can be attributable to the development of HF.

### 1.1.3 Classification

The international consensus recognizes two classifications systems for the severity of HF. The international classification of American College of Cardiology (ACC) and American Heart Association (AHA) divides HF in four progressive stages ranging from A to D, emphasizing on the development and progression of the disease and can be used to describe populations or individuals.[11] [12] The functional New York Heart Association (NYHA) classification ranging from functional class I to IV provides useful and complementary information about the presence and severity of HF, focusing on exercise capacity and the symptomatic status of the disease, and is thus more subjective and can change over a short periods of time.[13] The objective ACC/AHA stages of HF recognize that both risk factors and abnormalities of cardiac structure are associated with HF. Once a patient moves to a higher stage, regression to an earlier stage is not observed – meaning the ACC/AHA stages of HF are progressive and inviolate.[12]

The natural history of HF develops from AHA Stage A HF (no structural heart disease), to AHA stage B HF (structural heart disorders), to AHA Stage C HF (structural heart disorders with symptoms). By AHA Stage C HF, etiologic factors are addressed and optimal medical therapy is titrated accordingly. However, a progressive decline to advanced HF (defined as AHA Stage D HF) is the rule. [14] [15]

Chronic HF is a process in which cardiac remodeling plays a crucial role. Remodeling is part of a vicious circulus vitiosus where the myocardial ventricle starts to dysfunction, initially observed in ventricular dilatation with increased wall stress and myocardial stretch, leading to systemic neurohumoral activation and in a long-term process resulting in myocyte death and toxicity and ultimately leading to altered gene expression resulting in ventricular remodeling. The chronic process often results in pathophysiological complex syndrome of cardiomyopathy, with dilative cardiomyopathy (DCM) and ischemic cardiomyopathy (ICM) being most commonly observed in patients with chronic HF. ICM is primarily caused by ischemic disorders, commonly caused by coronary artery disease and is often the cause of a myocardial infarction. DCM refers to a large group of heterogeneous myocardial disorders that are characterized by ventricular dilation and depressed myocardial contractility in the absence of abnormal loading conditions such as hypertension or valvular disease.[16] [17]

Patients with advanced HF suffer from decreasing levels of activity (NYHA IIIB, IV), recurrent hospitalizations for volume overload, rhythm management and complications of HF and HF therapy (cardiorenal syndrome, medication side effects, anti-coagulation complications and others) and marked increases in the level of outpatient visits in efforts to avoid hospitalizations.

### 1.1.4 Treatment options for advanced heart failure

Accordingly to the progression of symptoms and the severity of the impaired LV function, the multiple modalities of treatment available to treat HF include but are not limited to lifestyle modifications, pharmacologic agents, device therapies such as implantable cardioverter-defibrillator (ICD), and cardiac resynchronization therapy (CRT). With further progression of symptoms w/o further decline of impaired LV- and/or RV-function, further escalation of the therapy is necessary.

While treatment strategies for advanced HF vary, cardiac transplantation remains not only the treatment of choice in applicable patients, but also presents the only curable option.[18] [19] With the improvement in immunosuppressive therapies in the recent decades, overall survival after cardiac transplantation is over 85% at one year post-transplant, and approximately 70 to 75% at 5 years post-transplant, and over 50% at 10 years post-transplant.[20] This survival is superior to the dismal prognosis of 75% mortality at one year with optimal medical therapy as reported in the REMATCH trial in 2001.[21]

Unfortunately, there is a discrepancy between organ demand and organ availability. Eurotransplant, the European international non-profit organization responsible for coordination of all organ transplantations in its eight member countries in Europe, states in their annual report 2016[22] that in Germany alone there were 725 patients listed on the active transplantation list for cardiac transplantation, whereas only 297 heart transplantations were performed in 2016 in Germany. Furthermore, in Germany alone, 113 patients listed for cardiac transplantation deceased in 2016, and there were 458 new listings for cardiac transplantation added in 2016 in Germany alone, with yearly-observed growing median age of deceased donors, as well as growing demand of organ transplantations, without growing numbers of organ availability.[22]

The median recipient age for adult transplants is 55 years, and the proportions of patients aged 60 to 69 years and ≥ 70 years are increasing.[20] With the growing organ donor shortage, marginal donor organs may be increasingly accepted. Particularly in Europe, the medial donor age has increased dramatically in the recent years, from median age of 30 years in the early 90s, to median donor age of 45 years in 2015.[20]

With the ageing population, a growing part of especially elderly population is not eligible for cardiac transplantation.[23] [24] In those eligible for a heart transplantation, there are strict allocation and matching criteria in place, as well as strict inclusion and exclusion criteria for patients with end-stage heart failure to be listed for a heart transplant. [23]

However, due to organ shortage and strict allocation criteria to match the best suitable donor and recipient, the waiting time is often too long and a progressive decline in cardiac function and thus overall health decline is a growing problem. In those selected cases mechanical circulatory systems (MCS) may be used, either as a bridging strategy until a suitable donor heart is found (i.e. bridge to transplant; BTT), or as a destination therapy (DT), if a patient does not (anymore) qualify for a heart transplantation. The global proportion of transplant recipients bridged with mechanical circulatory support (MCS) has increased dramatically since 2007, especially in older recipients, with currently 50% of heart transplantations being treated with MCS as a BTT strategy prior to transplant.[20]

## 1.2 Durable mechanical circulatory support systems (MCS)

### 1.2.1 Brief history of MCS

Dr. D. A. Cooley and Dr. D. Liotta in Houston, Texas, USA successfully implemented the first implantation of a mechanical heart pump that replaces the heart in the 1969 with the implantation of a pneumatically driven total artificial heart (later known as Liotta Heart). After a 64-hour support, the patient received a heart transplant. The first successful long term support with a total artificial heart (TAH) came with the first human implantation of the Jarvik 7 Heart in 1982 by Dr. DeVries, the patient survived for 112 days. These initial devices were focusing on “replacing” the heart function in biventricular end-stage heart failure, rather than “assisting” it.

*Image 1. Jarvik 7 total artificial heart (TAH).*

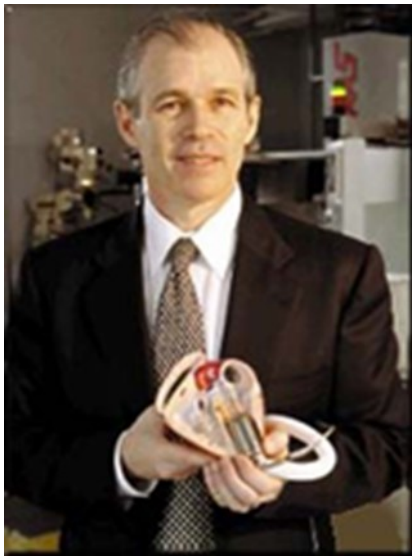

*Image 2. Dr. Robert Jarvik holding the Jarvik 2000 Flowmaker LVAD in a heart model.*

The beginnings of the left ventricular assist devices (LVAD) started with the first temporary LVAD implant by Dr. Liotta in 1963. During the first decades many pulsatile mechanical circulatory support (MCS) systems for treating chronic end stage heart failure emerged, and have undergone extensive in vitro and in vivo testing.

Over the next decades, many ventricular assist devices (VAD) emerged, and after their efficacy and safety was established, the U.S. Food and Drug Administration (FDA) approved a number of these devices for clinical use in the 1990s (e.g. Heart Mate IP©, Thoratec VAD©, Novacor©). The problem of these first generation ventricular assist devices however was their size, weight and durability of its pneumatically driven membranes, resulting in ultimately poor clinical outcomes and high morbidity and mortality rates.

Although the first-generation VADs significantly advanced heart failure therapies at that time, they had several limitations. The devices were large pneumatically driven VADs to produce a pulsatile flow (pf) profile, with large consoles, complex handling and short durability due to pneumatically driven moving membranes prone to wearing off. The large size of these devices limited patient selection to those of larger size.[25] Additionally, through a pneumatically driven system the devices created a loud sound and through their large extracorporeal units resulted in very limited patient mobility, affecting patients' quality of life.[26] The pulsatility design required a pneumatically driven membrane with multiple moving parts, thus reducing device durability leading to increased frequency of device replacement.[27] Consequently, 21% of patients had to undergo device replacement.[21] Because of the growing prevalence of HF and the limitations of first-generation VADs, the need for smaller, more durable devices was realized.

The breakthrough came in the end of 1990s, with the emergence of second generations of ventricular assist devices. These second generation VADs are electrically driven rotary axial flow pumps with a continuous flow pattern, rather than a pneumatically driven pulsatile flow of the 1st generation VADs. The best known second generation LVADs are the Jarvik 2000© Flowmaker LVAD, and the Heart Mate II© LVAD. As the HeartMate II remains the most implanted LVAD to this date, most clinical trials compare the novel devices to the HeartMate II© as the control group.

In the 2nd generation cfLVADs, the limitations including stroke, driveline infections, and right-ventricular failure (RVF) persisted, and an abrupt increase in pump thrombosis from 2011–2013[28] highlighted the need for improvements in LVAD device design, perioperative management, and patient selection.[29] To address the growing concern of pump thrombosis and stroke in chronic HF support, as well as with increasing trends of LVAD patients as a DT strategy, the need for devices that were more durable was necessary. This led to the development of 3rd generation LVADs.

The 3rd generation LVADs are centrifugal-flow fully magnetically levitating centrifugal rotor pumps, producing a continuous flow pattern. Through the magnetically levitating centrifugal pumps, the bearings are omitted and thus improving the hemocompatibility, as well as improving the long-term durability of the pump. The first 3rd generation LVAD clinically in use today are the HeartWare© HVAD, followed by the development and use of HeartMate 3©.

### 1.2.2 MCS implementations

As mentioned above, one needs to differentiate between the etiology of the heart failure, meaning a left- right- or biventricular heart failure. Accordingly, the different ventricular assist devices (VADs) are used as left ventricular assist device (LVAD), right ventricular assist device (RVAD) and biventricular assist devices (BiVAD), respectively. In specific cases of advanced severe biventricular heart failure, a complete heart replacement using a total artificial heart (TAH) may be considered.

Furthermore, one differentiates the durable MCS between pulsatile working displacement pumps with a pneumatically or hydraulically driven membrane (first generation VADs and TAH), from rotary pumps, which produce a continuous flow of blood, through an electromagnetically or electromechanically driven system (second and third generation VADs).

Depending on the MCS system, the pumps are either extracorporeal (e.g. some first generation VADs; e.g. Thoratec VAD©), paracorporeal (e.g. Berlin Heart Excor©, Centrimag©, DeltaStream DP3©, Levitronix©) or intracorporeal (e.g. some first generation VADs (HeartMate IP©, Novacor©), TAH (e.g. Syncardia©), and most 2nd and 3rd generation VADs (e.g. Jarvik 2000©, HeartMate II©, HeartWare©, HeartMate 3©). The paracorporeal systems are intended for medium-term cardiac support, the intracorporeal systems are all intended for long-term use.

### 1.2.3 Treatment options in advanced heart failure with MCS

In chronic end-stage HF, as well as in acute-on-chronic end-stage HF in patients in AHA HF stage D, few treatment options remain and are limited to the use of continuous inotropes, VAD implantation (either as LVAD, RVAD or BiVAD), total artificial heart (TAH) implantation, and heart transplantation, with latter presenting the only curative option.[30] In patients with end-stage, chronic or acute-on-chronic HF with imminent end-organ failure in whom all conventional pharmacological, anti-arrhythmic and surgical options have been exhausted, ventricular assist device (VAD) support should be considered, either as a destination- (DT) or as a bridge-to-transplantation (BTT) strategy.[83]

Despite the limitations of the 1st generation pulsatile VADs, the landmark REMATCH trial in 2001 demonstrated a significant increase in one year survival of end-stage HF patients implanted with pulsatile HeartMate XVE LVAD© (Abbott, Lake Bluff, IL, USA) compared to medical therapy alone (52% vs. 25%). The overall survival at two-years also showed significant benefit, with (23% in LVAD group versus 8% in medical therapy group, and an overall mortality reduction of 48% in LVAD group.[21] The quality of life was also significantly improved at one year in the device group.[31]

Restoring circulation in advanced stage of HF can dramatically improve the overall condition and functional status of these severely ill patients. As showed by the 7th Annual Report of Interagency Registry for Mechanically Assisted Circulatory Support (INTERMACS) from 2015, which included over 15 000 patients in 158 participating cardiac centers in USA, the overall survival of Patients who received a continuous flow devices at 1 and 2 years is 80% and 70%, respectively.[32]

The improvement of overall survival with cfLVADs has led to increasing implantations not only as a bridge to transplant (BTT), but also to increased number of patients as a destination therapy (DT) – in 2014 nearly 46% of cfLVADs in USA were designated as DT. [32]

MOMENTUM 3 trial compared the short-, medium- and long-term outcomes in patients who underwent implantation of HeartMate 3 centrifugal-flow LVAD to patients who underwent implantation of HeartMate II axial-flow LVAD. At 6-months follow up, there were 0% vs 10.1% of occurred pump thrombosis in centrifugal-flow vs axial-flow pump group ($p<0.001$). At two year follow up, the composite of survival free of disabling stroke or reoperation due to device malfunction was 79.5% in centrifugal-flow- pump vs 60.2% in axial-flow pump ($p<0.001$ for noninferiority). The study showed a significant risk reduction in centrifugal-flow pump and a significant superiority of centrifugal-flow pump, compared to axial-flow pump (HR 0.46, CI 0.31-0.69, $p<0.001$ for superiority), which the authors interpret due to better hemocompatibility of the centrifugal-flow pump with resulting fewer reoperations due to pump malfunction and significantly less pump thrombosis, compared to axial-flow pump. [33]

Thus, despite significant improvement in the current LVAD systems, the overall survival is defined by the main complications associated with LVAD therapy: major bleeding (42%), major stroke (between 4-16% per patient year)[34] [35] [36], major infection (driveline infection or pump pocket infection; between 2-7% per patient year), device malfunction or pump thrombosis (between 1-15% per 2 years).

### *1.2.3.1 Jarvik 2000© Flowmaker LVAD*

Jarvik 2000© Flowmaker LVAD (Jarvik Heart, Inc, New York, NY, USA) is a miniaturized blood pumps intended for the use as a left ventricular assist device (LVAD) creating sufficient levels of cardiac support, with first clinical implantations since the year 2000. To this date, it remains one of the smallest assist devices on the market. It is an axial-flow pump that is durable (longest support in a patient lasted 9.5 years[37]), quiet, easy to implant and operate. It is powered electrically via a tunneled cable, connected to the controller unit through a retroauricular connector.[38] Due to its small size and weight, it is placed intraventricularly, omitting the need for inflow cannula, thus simplifying the implantation technique, reducing the wound surface and thus reducing the risk for perioperative bleeding, thus reducing the implantation time and surgical recovery time. As it is placed inside the ventricle, it is exposed to continuous blood flow, thus reducing the formation of blood clots.

#### 1.2.3.1.1 Technical specifications

The Jarvik 2000© Flowmaker LVAD weighs 90 g, measures 2.5 cm in diameter, is 5.5 cm long and displaces 25 mL of volume. The light weight and small size of the device not larger than an AA battery, allows an intracardiac implantation, rather than intrapericardial or extracorporeal as in some other devices. The outer shell of the blood pump is constructed of welded titanium granulate surface, which is hermetically sealed and contains an electromagnetic direct current motor. The rotor includes titanium impeller blades, and is held in place by two ceramic bearings. The pump also includes outflow stator blades downstream from the impeller. The electromagnetically powered rotating impeller rotates at speeds between 8,000 to 12,000 rpm, thus producing a maximum blood flow of around 7 L/min against physiologic resistance. All blood-contacting surfaces are made of smooth titanium. Through the intracardiac placement of the blood pump the need for an inflow cannula is omitted. The blood exits the blood pump through an outflow cannula made of Dacron® prosthesis, which is then implanted end-to-side either in the ascending aorta or in the descending aorta, depending on the surgical access chosen for the implantation procedure, respectively.

The blood pump is connected to the extracorporeal controller via a driveline cable, which is coated in a silicon tube. There are two variations of the placement of the driveline – either tunneling it through the subcutaneous tissue from the blood pump and exiting close to the umbilicus, or via tunneling it through the subcutaneous tissues cranially, fixating it in the base of the skull, before exiting retroarticular. The latter option for driveline placement is available to this date only in Jarvik 2000© Flowmaker LVAD. Despite being technically more challenging and thus prolonging the implant procedure time, this technique is associated with the lowest rate of infections.[39] [40]

*Image 3. Jarvik 2000© Flowmaker LVAD compared to a standard AA battery*

A further development in the design of the Jarvik 2000© Flowmaker LVAD is a miniaturized version for pediatric use in infants. This novel miniature pediatric Jarvik 15mm© LVAD system is only 15mm in diameter, and about the size of AAA battery. The working principle of the Jarvik 15mm© LVAD is in its design similar to the Jarvik 2000© Flowmaker LVAD. It is an axial rotary continuous flow LVAD. It is usually implanted in the apex of the LV and pumping the blood in the aorta via outflow graft. It provides more blood flow as the pump speed is increased by adjustment of the control system, so as the child grows, so does the blood flow. The device is designed for patients under one year up to about age ten and may provide long-term support in children for whom no donor heart becomes available.[37]

*Image 4. Jarvik 15 mm© LVAD and Jarvik 2000© Flowmaker LVAD compared in size.*

#### 1.2.3.1.2 Components

The Jarvik 2000© Flowmaker LVAD system consists of following main components:[41]

- intracorporeal: blood pump, outflow conduit, driveline cable;
- extracorporeal: driveline connector, extension cable, pump controller, Li-Ion batteries (x2), Y-cable for batteries


*Image 5. Components of the Jarvik 2000© Flowmaker LVAD system.*
*1 blood pump, 2 outflow conduit, 3 driveline connector, 4 driveline, 5 extention cable, 6 controller, 7 Li-Ion battery.*
*Adopted from Jarvik Heart, I., 333 West 52nd Street, 10019 New York. "User Manual Guide" The Jarvik 2000; Version March 2009.*

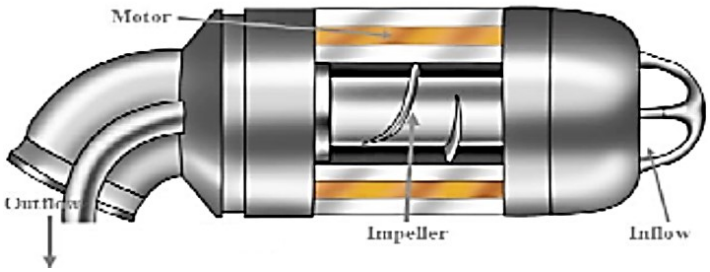


*Image 6. Jarvik 2000© Flowmaker LVAD.*
*Inner view of the pump components.*
*Adopted from Jarvik Heart, I., 333 West 52nd Street, 10019 New York. "User Manual Guide" The Jarvik 2000; Version March 2009.*

#### 1.2.3.1.3 Implantation technique

The implant procedure depends on the type of device intended to use – either as an LVAD, RVAD or as BiVAD.

In the case of LVAD implantation without any concomitant surgical procedures, the pump may be implanted via left anterolateral thoracotomy in the 6$^{th}$ intercostal space approach. This necessitates the use of double lumen endotracheal intubation, allowing for a single lung ventilation. Partial cardiopulmonary bypass support is used when the apex of the left ventricle is cored under induced ventricular fibrillation. The outflow graft if then anastomosed in the descending aorta under partial clamp occlusion.

This implant procedure differs from the more commonly used approach via median sternotomy, which allows for better exposure of the heart, allowing for concomitant surgical procedures, as well as implantation of the Jarvik 2000© Flowmaker as LVAD, RVAD or BiVAD. Partial cardiopulmonary bypass support is used when the apex of the left ventricle is cored under induced ventricular fibrillation. To secure the pump in place, a sewing cuff ring is anastomosed to the apex of the heart. The outflow graft is then anastomosed in the ascending aorta under partial clamp occlusion. In RVAD implantation, the pump is placed in right ventricle near the apex parallel to the interventricular septum, and the outflow graft anastomosed in the pulmonary truncus.

The heart is then defibrillated, and air is evacuated from the left ventricle and blood pump. Any residual air is removed from the graft with a 19-gauge needle. The Jarvik 2000© pump is then activated, and the patient is weaned from cardiopulmonary bypass.

The Jarvik 2000© Flowmaker LVAD has been in clinical use for over 15 years, with granted CE mark for Europe in 2005, and Shonin mark in Japan in 2013. It has been implanted in over 1000 patients worldwide. The Jarvik 2000© LVAD system remains to this date the smallest and lightest permanent LVAD system for adult patients in the world.[37]

In the department of cardiac surgery at Klinikum Grosshadern of the Ludwig-Maximilians-University in Munich, 21 Jarvik 2000© Flowmaker LVADs were implanted between the years 2008 and 2011. Thus, the surgical and anesthesiologists team had the necessary surgical and perioperative experience to perform the experiments.

### *1.2.3.2 Impella© - a percutaneous transaortic short-term mechanical circulatory support system for acute heart failure*

The Impella© (Abiomed, Inc., Danvers, Massachusetts, USA) devices are percutaneous intracardiac continuous flow axial pumps, used for ventricular unloading in acute heart failure. They can be used either for the treatment for left- or for right-sided heart failure. The pump is positioned transvalvular, either through the aortic valve for left ventricular unloading, or through the pulmonary valve for right ventricular unloading. There are several Impella devices available on the market (Impella 2.5 L/min©, Impella CP© (Cardiac Power), and Impella 5.0 L/min© for left-sided AHF, and Impella RP© (Right Percutaneous) for right-sided AHF). Depending on the Impella device used, these pumps rotate at 33,000 to 51,000 rpm – compared to 7,000 to 14,000 rpm in Jarvik 2000©.

In left ventricular support, the devices are inserted percutaneously, via the femoral or axillary artery, and are advanced retrograde across the aortic valve. Similar to the intra-aortic balloon pump (IABP), the LV-Impella unloads the distressed LV through decreasing the LV pressures and increasing the stoke volume by pumping the blood from the inlet area located in the LV, directly into the aorta. Through the unloading of the LV it decreases the myocardial oxygen consumption and demand. It also increases the mean arterial pressure (MAP) in the aorta, thus increasing the systemic and end-organ perfusion, as well as increasing the coronary flow.

Obvious contradictions for the implantation of the LV-Impella include significant aortic valve disease, mechanical aortic valve and intracardiac thrombi, as well as peripheral vascular disease and the inability to tolerate systemic anticoagulation. Some Impella© devices are CE-approved for use of up 14 days, giving the myocardium time to recover or acting as a bridge to definite surgical or interventional therapy. The devices have large bore cannulas and require strict systemic anticoagulation.[42]

The common complications from Impella© support include limb ischemia, bleeding, vascular injury, infection, thromboembolic events and hemolysis. [43] In general, Impella devices are associated with the highest rate of hemolysis amongst other percutaneous mechanical circulatory devices for short-term support (i.e. IABP, ECMO etc.), with some studies suggesting hemolysis occurring in 5 – 10 %.[44] [45] This has been associated with the high revolutions per minute (up to 51,000 in Impella 2.5©). Other complications include LV perforation, vascular injury and aortic valve dysfunction due to Impella placement. Proper placement of Impella© is critically important and requires close monitoring as migration can occur.

In a meta-analysis of the three randomized trials (n=100) comparing percutaneous VADs (pVADs) (including Impella 2.5©) to IABP for cardiogenic shock, the pVAD group had more bleeding (HR 2.35 [1.40–3.93], p<0.01) and a trend towards more limb ischemia (HR 2.59 [0.75–8.97]).[46] Also, as in every LVAD, a detrimental complication may be the worsening of the RV function due to increased volume overload.

Studies have shown that in patients in acute HF the use of percutaneous MCS (pMCS) show an improvement in hemodynamics, however without a clear survival benefit.[43] [46] [47] [48] Nevertheless, data suggest that the use of pVADs has increased 30-fold from 2007 to 2011.[49]

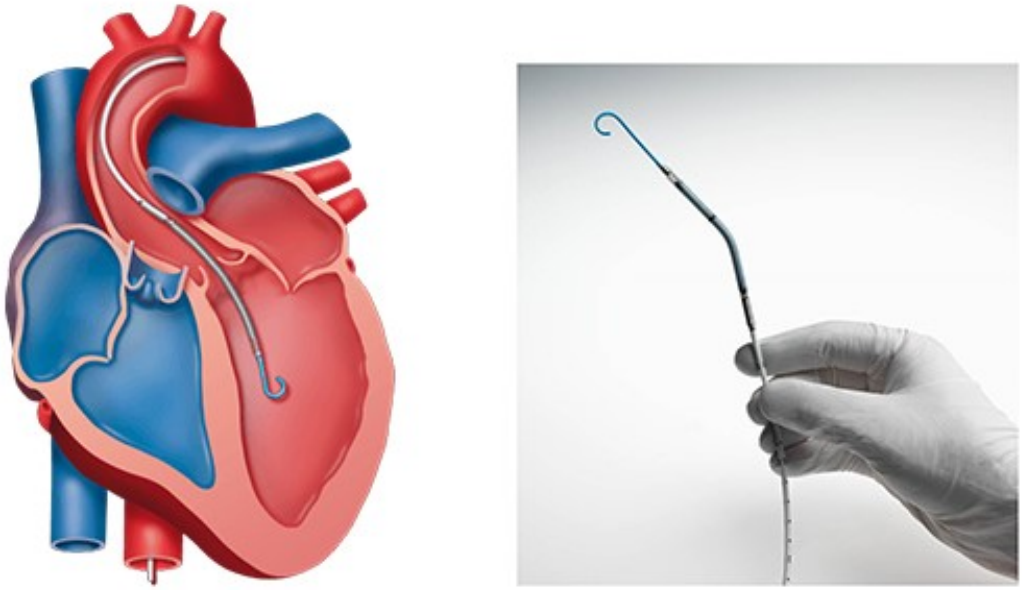

*Image 7. Image 2. Schematic illustration on the placement of Impella for left-sided ventricular support. Adopted from http://www.ch-aix.fr/wp-content/uploads/2018/02/.*

# 2 Investigated Device: novel transvalvular axial continuous flow ventricular assist device (tVAD; transvalvular VAD)

Together with Robert Jarvik we have evaluated the specially developed transvalvular ventricular assist device (tVAD), for the use in acute left- and in right-sided acute heart failure, in acute animal testing using adult porcine models.

The pump was designed and developed as an idea collaboration between our Department of cardiac surgery at Ludwig-Maximillians-University Munich and Walter Brendel Center of Experimental Medicine, represented by Professor Dr. Paolo Brenner, and between Jarvik Heart Inc, represented by Dr. Robert Jarvik. Following many years of idea exchange, the first prototype was developed in autumn 2012 by Robert Jarvik. The full details of the pump design and mechanics remain undisclosed, as it is a product still in development by Dr. Robert Jarvik and his company. There is no financial agreements between Dr. Robert Jarvik and any of our team members, none of our team members has any financial disclosures with the participating parties. This research was of purely academic purpose. The idea for the design of the experiment was made by Dr. Paolo Brenner, and is his intellectual property.

The novel transvalvular valve pump developed by Dr. Robert Jarvik combines the previously used principle of a transvalvular pump as disclosed in the US Patent 5,888,241 by Dr. Robert Jarvik in 1999, with the technological advancement and miniaturization of the pediatric Jarvik 15mm© LVAD.

## 2.1 Pump design

In its basic design the novel transvalvular VAD system was adopted by the pediatric Jarvik 15mm© LVAD system that is used in infants. The working principle of the Jarvik 15mm© LVAD is in its design similar to the Jarvik 2000© Flowmaker LVAD. It is an axial rotary continuous flow blood pump of second generation VADs. It is powered by an electromagnetic motor. The rotor blades are wielded in place by ceramic bearings (thus second generation VAD), all blood-contacting surfaces are made from titanium.

The form of the blood pump is adapted however in such a form, that it can be positioned through a functional aortic valve. For this purpose, the part where the cusps of the aortic valve would come in contact with the blood pump upon valve closure, the area was held as small in diameter as possible. The electromagnetic motor is accordingly placed in the wider area before and after this transvalvular part of the blood pump. The size of the transvalvular VAD is 64 mm of length, and 14 mm in outer diameter. At the transvalvular part of the pump, the outer diameter narrows down to 7 mm. The narrowest part of the VAD is to be positioned on the annular level, allowing for the valve leaflets to come together upon end of the systole and thus keeping the valve functional.

The Image 8 below illustrates the basic outer design of the pump.

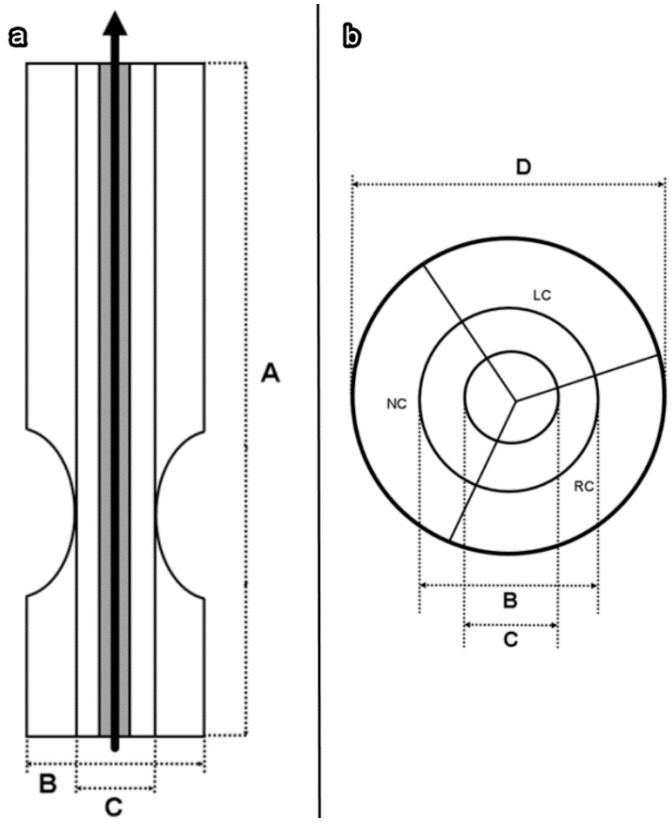


*Image 8. The basic design of the investigated transvalvular VAD. Panels a and b.*
*a: longitudinal section of the transvalvular VAD. Length (A) of 64 mm, outer width (B) of 14 mm, outer width at its narrowest part (C) 7 mm. Note the narrowing of the pump outer design at the lower transition lower 1/3 to upper 2/3 of the pump length – this part is to be places on the annular level, to allow the valve leaflets to come "laying" down upon valve closure. b: cross section of the transvalvular VAD on the annular level through aortic valve (here pictured with three aortic valve leaflets: NC non-coronary leaflet, RC right-coronary leaflet, LC left-coronary leaflet). Note the cross section distribution of the valve orifice area, and the orifice area taken by the pump. B=outer width of the pump (14mm), C=outer width of the pump at its narrowest point (7mm).*

Similar to the Jarvik 15mm© LVAD it is operated by a special controller, which was adapted by the Jarvik 2000© controller. Accordingly, it has five levels at which it operates, with corresponding increases of the rpm between 14,000 rpm and 22,000 rpm, resulting in changes of generated blood flow, as illustrated in the Table 1. Similar to the Jarvik 2000© Flowmaker LVAD, it has an intermittent low speed (ILS) function integrated in its operating system, which can be turned on or off by a medical professional using the special controller. When then ILS mode is on, the pump speed decreases to 8,000 rpm. This results in immediate decrease of the pump flow, thus resulting in decreases in LV unloading and thus allowing the ventricle to eject, following the Frank-Starling mechanism. As the ventricle ejects through the transvalvular LVAD, and through the aortic valve, it not only results in increased pulsatility, but also generates a wash-out effect around the aortic valve. The ILS mode occurs every 60 seconds, and lasts for 8 seconds.

| Operating level of the investigated transvalvular VAD | Pump speed [Revolutions per minute; rpm] | Output of Water without resistance [L/min] | Input Power in viscosity test fluid at Flow of 3 L/min [Watts] [average] |
|---|---|---|---|
| Level 1 | 14,000 | 4.5 | 2.4 |
| Level 2 | 16,000 | 4.5 | 3.1 |
| Level 3 | 18,000 | 5.6 | 4.1 |
| Level 4 | 20,000 | 6.4 | 5.2 |
| Level 5 | 22,000 | 7.2 | 6.8 |
| ILS | 8,000 | | |

*Table 1. Speed and flow characteristics of the investigated transvalvular VAD.*

The special adaptation is also the development of a bioprosthetic aortic valve, which has a mounting system in its subvalvular apparatus that allows for placement of the transvalvular LVAD (tLVAD). The valve pump is secured in its position via screwing mechanism placed in the subvalvular apparatus of the bioprosthetic valve. The bioprosthetic valve designed was bovine stented tri-leaflet aortic valve. Prior to pump implantation, the bioprosthetic valve replacement in aortic position needs to be performed. The Illustration below indicates this valve-pump principle (Image 9).

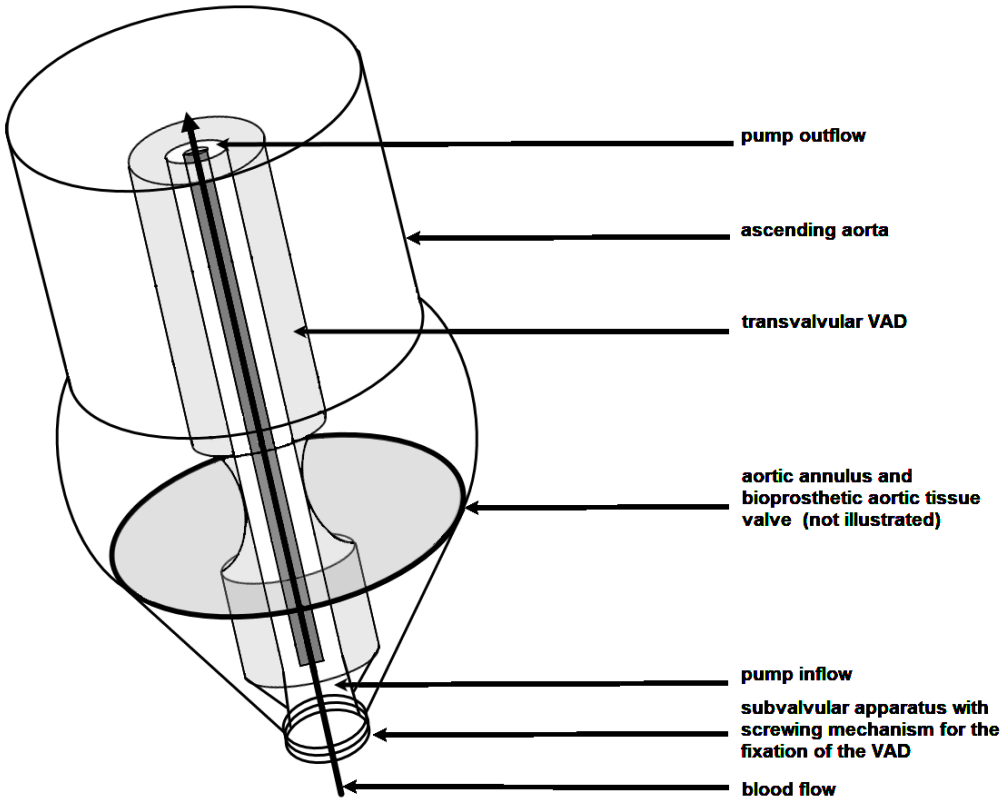


*Image 9. Positioning of the investigated transvalvular VAD in aortic position in a three-dimensional illustration. Note the positioning of the VAD to the aortic annulus and the aortic valve (aortic valve not illustrated) in such a way that the aortic valve leaflets come to "lay down" on the curved concave surface of the VAD. Note the special subvalvular placing apparatus with a centered screwing mechanism, onto which the VAD is mounted on.*

The remaining components of the transvalvular VAD remain unchanged to the pediatric Jarvik 15mm© LVAD and Jarvik 2000© Flowmaker LVAD, respectively.

The terms transvalvular VAD, tLVAD, tRVAD, valve pump, tVAD pump and tVAD valve pump in this work all relate to the investigated transvalvular ventricular assist device.

## 2.2 Animal model

### 2.2.1 Animal experiments in LVADs so far

The need for temporary support, replacement, and recovery therapies in heart failure has been driving advances in cardiac assist devices over the past decades. Before development, a new device typically undergoes computer-based testing upon the design of the first prototype. This is followed by in vitro mock circulatory flow loop models, followed by acute and finally chronic in vivo animal models, before the first human trials can begin.

In vivo testing of an LVAD requires firstly an animal model comparable in size as to represent an adult human device recipient, and secondly inducing the otherwise healthy animals to heart failure, thus representing the human heart failure patient as closely as possible. Furthermore, the animal model needs to be technically and financially possible to perform and maintain.

Device and cannula design, fit, surgical approach, performance, and the integration within the cardiovascular system must translate from the animal to the human patient. Thus, most device implant studies have been using adult large animals who in terms of the basic pathophysiology and cardiac anatomy mimic that of the human, as well as the size proportions of the heart and of the great vessels do not differ too greatly from that of the adult human.

For most device implant studies, healthy animals have been used. The optimal combination of an appropriate animal species with a clinically relevant method of creating HF is necessary for elucidating insights into novel cardiac assist devices and their impact on the cardiac function, and the overall patient outcomes and quality of life.[50]

For testing the transvalvular LVAD in acute animal model, one needs to consider the interspecies differences including the overall size of the animal, anatomical variations (thorax dimensions, cardiac anatomy, coronary anatomy, perfusion and valvular function) and similar pathophysiology. The important correlation observed in other animal studies is the correlation between the weight of these animals and the size of their hearts and great vessels of the heart.[51] [52] [53] [54] In acute animal models, the animals are normally sedated/anaesthetized, followed by a controlled euthanasia upon termination of the acute experiment. After a thorough review of the literature, and after consulting with the technical possibilities of the local animal research facility (Walter Brendel Center for Experimental Medicine at LMU Munich), we evaluated two animal models for this study. We agreed on aiming for animals weighing about 70-90 kg, as their weight correlates with the size of their heart and great vessels, and at 70-90 kg resembles the proportions of an adult 70 kg human male the most.

#### *2.2.1.1 Bovine models*

Their large size and thoracic cavity make them excellent models for device-related studies, and they possess large peripheral vessels that facilitate vascular access for device cannulation, graft anastomosis, instrumentation, and blood collection. Calves (4–6 months) are more suitable than adult cattle for approximating the human body size (70–100 kg) and are physically easier to handle by study personnel. Anatomical differences include a common brachiocephalic trunk that divides into the subclavian, vertebral, and carotid arteries - this dissimilar anatomy may influence device cannulation/graft sites.[55] The bovine pericardium is thicker than other large animal species but relatively compliant.[56] The cost of acquisition and maintenance, as well as adequate animal cage and surgical space required for this model, is considerable, and specific study supplies (large animal laryngoscope blades and endotracheal tubes) may be required.

#### *2.2.1.2 Porcine models*

Pigs are a popular species for animal model development in cardiovascular research because of their ease of procurement. The porcine aortic valve is most similar to humans[57] and has been a critical component of transplantation research. Porcine coronary artery distribution and perfusion is right-dominant as in humans.[51] The anatomical differences include the presence of three pulmonary vein ostia on both sides the left atrium and sharper angles that the vena cava enter the right atrium[58] The peripheral vessels of pigs are small and deep, presenting some challenges in vascular access particular in studies where repeated procedures or sampling is involved.

### 2.2.2 Ways of inducing heart failure in large animal models

Mechanical circulatory support devices are indicated in acute or chronic advanced heart failure. The novel devices undergo severe testing, including studies on large animals. Therefore determining the appropriate technique to create a clinically relevant large animal HF model for LVAD is critical to the success of the study. Most LVAD implantation studies have been performed in healthy animal models.[59] [60] There are many different well-established techniques for creating HF in large animals, including pacing (nonischemic, reversable)[61], cardiotoxins (it affects the whole animal and is not limited to the heart alone, let alone specific regions of the heart, irreversible),[62] [63] and immediate ventricular dysfunction via oxidative damage (e.g. ligation of a coronary artery, partially reversible).

The latter options is most controllable to specific areas of the heart. There are three most established techniques. The interventional selective coronary embolization of microspherical particles can effectively produce numerous focal microinfarctions, resulting in diffuse area of ischemia. Most common particles include selective injection of Microspheres© in the left anterior descending coronary artery (LAD), however in most cases needs to be performed approximately 2-3 weeks prior to the LVAD surgery, with the resulting EF dropping to 30 % or less.[64] The surgical technique of ligating the corresponding coronary artery is a popular technique, as it can be performed during the LVAD surgery, and results in instant myocardial infarction (MI) and subsequent reduction of the corresponding ventricular function.[65] Another surgical option is the induction of sudden severe mitral valve regurgitation, via surgically cutting the chordae tendinae (chordae rupture), thus resulting in rapid decline of the LV function.[66] [67]

# 3 Methodology

The animal models were obtained in accordance with the regional animal safety standards, and registered as a surgical training experiments. All animals were treated in accordance with the training protocol and in accordance with the Protection of Animals Act of the State of Bavaria (Tierschutzgesetz der Regierung von Oberbayern).

The animals were obtained one week prior to the surgery from the local animal husbandry of the University of Munich (Lehr- und Versuchsgut der LMU München Oberschleißheim, St.-Hubertus- Str. 12, 85764 Oberschleißheim, Germany). They were then held at the in the stables of the Walter Brendel Center for experimental medicine, where they were held in animal boxes (1.5 x 2.0 m), until the surgery. In each box there were two animals. Each box had open access to 4 x 4 m unroofed section for recreation.

To simulate the adult human patient, we selected animal models with corresponding weight to that of the average adult human patient – weight of approximately 80 kg.

The experiments and surgery all took place in specially designed operating room for large animals at the Walter Brendel Center for experimental medicine at the University of Munich, located at Campus Grosshadern in Munich.

## 3.1 Choosing the animal model using ex-vivo models

For the selection of the animal model, we evaluated two animal models – calves and porcine model. With a specific design of the transvalvular VAD we intended on testing on adult animal models, we needed to inspect the ex vivo hearts and great vessels of the selected animals on the feasibility of the implantation of the device, as well as choosing the size of the bioprosthetic valve based on the findings of the inspected aortic valves and annular sizing on these ex vivo hearts. The ex vivo hearts were taken from slaughtered animals, provided by the local slaughterhouse in Munich (Fleischgrosshandel Valentin Hahn, Schlachthof München). The ex vivo hearts and great vessels were then taken to the Walter Brendel Center, where they were inspected. Upon inspection the animal tissues were disposed of in specially designed containers and destroyed.

### 3.1.1 Bovine model

For the bovine model, we evaluated three ex vivo hearts and great vessels of calves weighting 100 to 130 kg. Upon inspection, the size of the hearts of the three calves was much larger then that normally found in adult human patients. Also, the left main coronary artery seems very large in all three inspected models (outer diameter of LCA of 12 mm). The ascending aorta is very short, with the brachiocephalic trunk branching off in median 45 to 50 mm above the aortic annulus. The short ascending aorta would mean little operating space, since the implantation is primarily focused around the aortic valve and ascending aorta. In the inspected three hearts there were no atrial or ventricular septal defects. The aortic and tricuspid valves were all tricuspid, the annular size of both aortic and pulmonary valves did not differ, and the median annular size was 33 mm.

For sizing of the bioprosthetic aortic valve in the experiment, three cylinder models of 21 mmh, 23 mm and 27 mm outer diameter were used. It was placed transaortically, as well as through the pulmonary valve. In all three models all sizing models passed through both valves without any resistance.

Considering the design of the transvalvular Jarvik pump with approximately 4 cm of blood pump reaching above the aortic valve and aortic annulus, thus potentially causing a malperfusion by entering into one of the aortic bifurcations, this option was soon abandoned.

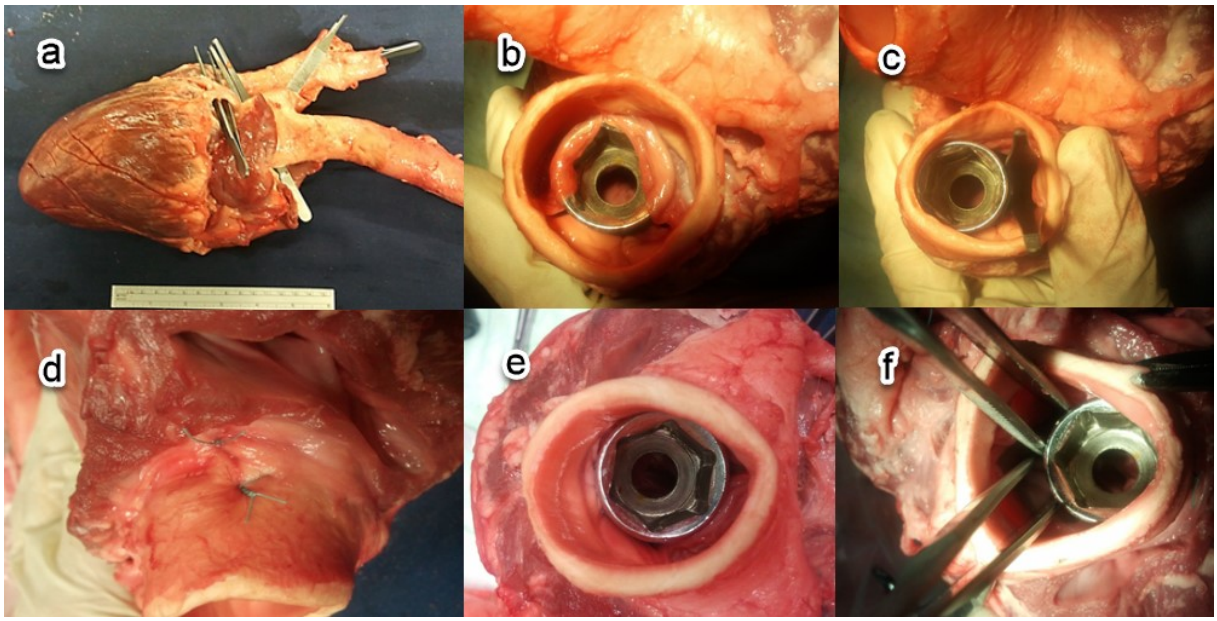


*Image 10. Evaluation of ex-vivo bovine hearts; a-f.*
*a: bovine heart after preparation oft aorta and pulmonary truncus. Note the special anatomy with short ascending aorta before the branching of the bicarotid truncus. b: pulmonary truncus with the placed 23 mm sizer model. Note the free space between the aortic wall and the sizer model. Pulmonary truncus diameter was 33 mm in this picture. c: pulmonary truncus with the placed 23 mm sizer model. Note the free space between the aortic wall and the sizer model, indicated by the forceps in-between. d: 23 mm sizer model placed through the aortic valve, and secured through two 1-0 Ethibond sutures to the aortic wall. Aortic size 31 mm. e: 23 mm sizer model placed through the aortic valve. Note the loose space between the sizer model and aortic annulus. f: 23mm sizer model placed transaortically. Note the loose space between sizer and aortic annulus, indicated by the two forceps in-between.*

### 3.1.2 Porcine model

For the porcine model, we evaluated six ex vivo hearts and great vessels of slaughtered adult pigs (breed Deutscher Landesschwein). We were able to collect three ex vivo heart with great vessels from pigs of 80-90 kg of weight, and three of pigs which weighted around 100-110 kg.

The observed anatomy is similar to the human anatomy, including similar size of the hearts and the great vessels in both weight categories of the inspected pigs. The size of the hearts correlated with the size of the hearts normally found in human patients.

The anatomy of the coronary arteries is similar to those in humans. The ascending aorta has similar anatomy as in humans. The brachiocephalic trunk branched off in median at 40 mm above the aortic anulus. There were no atrial or ventricular septal defects. The aortic and pulmonary valves were all tricuspid, the median anular size of aortic valves was 18.5 mm. The median anular size of the pulmonary valve was 19.5 mm.

For sizing of the bioprosthetic valve we used 4 cylinder models with outer diameters of 19 mm, 21 mm, 23 mm and 27 mm. Then the cylinder models were placed through the aortic and through pulmonary valve. If the sizer passed through the aortic valve, in also passed through the pulmonary valve. The 19 mm and 21 mm sizers passed through the valves without any resistance, despite the aortic anulus measuring only 18.5 mm on average. The 23 mm sizer also passed through the aortic valve in all hearts, however with more resistance. The 27 mm sizer did not pass through any aortic or pulmonary valves.

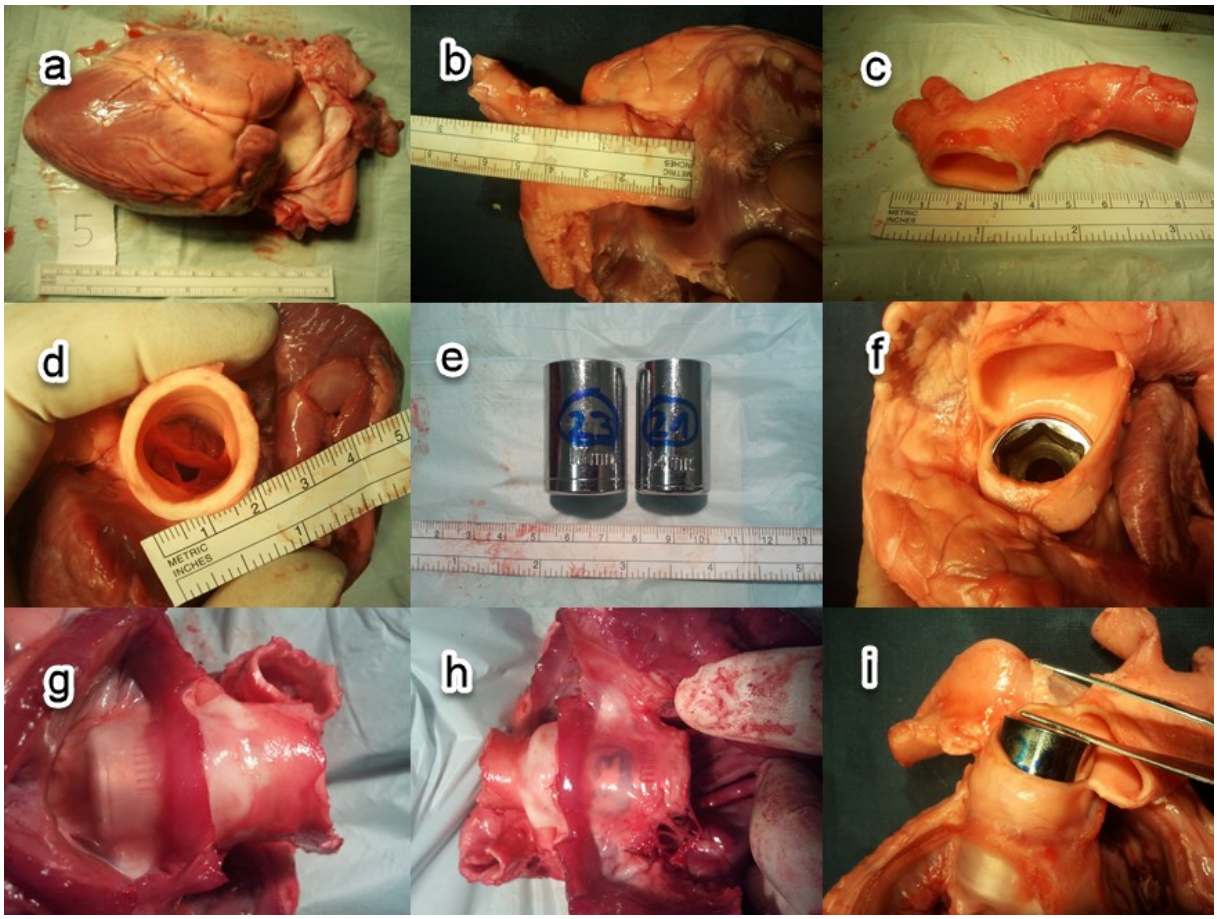


*Image 11. Evaluation of porcine ex-vivo hearts. a-i.*
*a: porcine heart. b: the short length of porcine ascending aorta from aortic annulus to the branching of the bicarotid truncus (ca. 4 cm in length). c: Anatomy of the porcine aortic arch, with short ascending aorta (excised and not shown), and bicarotid truncus. d: the principle of measuring the diameter oft ascending aorta after the sinotubular section. e: sizing models for the valve size. The numbers 23 and 21 indicate the outer diameter of the sizing model in millimeters. f: 21 mm sizing model positioned through the aortic valve. g: 21 mm sizing model positioned through the aortic valve. h: 23 mm sizing model positioned through the aortic valve. i: 21 mm sizing model positioned through the aortic valve.*

Upon inspection of these findings, we decided to use German land pig (Deutsches Landrasseschwein) of 80 kg of weight as our acute animal training model. Given the findings of the annular sizings for the bioprosthetic aortic valve, and taken into considerations of the outer diameters of the transvalvular Jarvik VAD we intended on implanting, we decided to use the 23 mm size of the bioprosthetic valve. Through the selection of the 23 mm valve, we postulated the minimal patient-prosthesis mismatch, as well as smallest transvalvular gradients.

## 3.2 Anesthesia

The surgery is performed under general anesthesia. The animals are sedated through intramuscular injections of Ketamine (10-20 mg/kg body weight), Azaperone (Stressnil; 10 mg/kg body weight) and Atropinsulfate (1.0 mg). Once sufficient depth of the anesthesia is achieved, the animals receive the intravenous line inserted in the auricular vein, and the narcotics are switched to the continuous intravenous application via of propofol (6-12 mg/kg body weight/h) and bolus-wise application of fentanyl (5-7 µg/kg body weight). This follows an endotracheal intubation, and the animals are put on mechanical ventilation and are monitored in their oxygen saturation levels, $CO_2$ expiration levels, blood pressure and regular arterial blood gas analyses. Then the electrodes are placed on the lateral sides of the torso, for continuous electrocardiographic monitoring of the heart. For the substitution of the fluids, continuous crystalloids and colloids are given intravenously. For hemodynamic stability, intravenous catecholamines were used (noradrenaline, adrenaline).

Through the surgical team, an arterial line is placed surgically via right-sided axillary cutdown in the right common carotid artery, and secured with multiple ligatures. Then the central venous line is placed in the internal jugular vein through the surgical team, and also secured in place with multiple ligatures.

Upon completion of the surgical experiment, the animal is left under deep narcosis and analgesia and given intravenously systemically pentobarbital as well as intracardially 20-30 ml of highly concentrated potassium chloride (1 mmol/ml), upon which the heart drops in immediate irreversible ventricular fibrillation followed by cardiac arrest. This timepoint marks the controlled euthanasia of the animal.

## 3.3 Surgical implantation technique

When the animal is in deep general anesthesia (including no reaction to pain) the animal is placed on its back, shaved on the ventral part of its torso, and sterile covers placed in orderly way and surgical part of the training starts.

Firstly, via surgical cutdown the arterial line is placed in the right common carotid artery, and the central venous line is placed in the right internal jugular vein, for the hemodynamic monitoring and fluid application. These lines are positioned in place through two or more ligatures.

Median sternotomy is performed, sternal retractor is placed and the chest spread apart. The pericardium is opened, followed by intravenous administration of heparin (400 IE/kg body weight). This is followed by arterial cannulation high in the aortic arch and the venous cannulation in the right atrium, as well as inserting the LV-vent through the upper right pulmonary vein, as well as inserting the aortic-root vent in the ascending aorta. Then these cannulas are attached to the extracorporeal circulation (heart-lung machine; ECC), the ascending aorta is cross-clamped just under the brachiocephalic trunk and the cardioplegic solution (1000 ml cold Bretschneider© blood cardioplegia) is administered through the aortic root vent. This brings the heart to in a cardioplegic arrest.

Then there are three operative variations according to the intended use of the transvalvular VAD. Each used only once in corresponding animal model.

### 3.3.1 Transvalvular LVAD in aortic position and biological aortic valve replacement

In the first setting, the transvalvular VAD is used as an LVAD, and a replacemet of the aortic valve with a 23 mm stentet biological valve prothesis made of porcine pericardium is performed. The biological aortic valve prothesis is equipped with a subvalvular apparatus with a centrally mounted screw drill, onto which the transvalvular LVAD is screwed onto and fixed in the center position of the prosthetic valve. This transvalvular left ventricular assist device (tLVAD) system with bioprosthetic aortic valve deployment system can be termed as “prosthetic valve pump”, or PVP.

For this purpose, a cross incision is performed in the ascending aorta and the native aortic valve is excised. The biological porcine pericardial stented aortic valve prothesis, which is 23 mm in size is placed in typical surgical technique in the aortic anulus via multiple teflon-pledges-armed aortic valve sutures. The valve is checked for paravalvular leakage. Upon securing the bioprothesis, the transvalvular LVAD is carefully placed through the center of the bioprothesis whilst displacing all three valve cusps to the side, and sliding the tLVAD retrogradely in the subvalvular apparatus of the bioprothesis. Then it is screwed onto the subvalvular apparatus of the bioprothesis. The tLVAD is also secured supraannularly using two 3-0 teflon-pledged armed sutures through the aortic wall, choosing the direction furthest away from the two coronary ostia (prefereaby in the acoronary sinus). The aortomy incision is closed using double-winding continuous suture technique with 4-0 Prolene, enhanced with Teflon-pledges especially in the place where the driveline cable exits the aorta. Then the heart is carefully filled with blood and deaired using the aortic root vent. This is followed by removing the aortic crossclamp and thus allowing for the reperfusion of the heart.

Pressure lines are inserted directly in the LV-apex, in the ascending aorta and in the left atrium, and fixated with tourniquets. It is important to consider the proximity of the tLVAD, and trying to keep as greatest distance to the tLVAD inflow and outflow areas while positioning these pressure lines. The ECC is slowly reduced and stopped. ECC cannulas are clamped, but left in situ in case of sudden need for repeated ECC start.

Then the pump is started and gradually increased to different levels, whilst measuring the corresponding parameters. For the induction of the acute heart failure, a direct ligation of the left anterior descending (LAD) coronary artery using 2-0 Ethibond on a tourniquet was used.

Upon completion of the experiment, the right atrium was decannulated from the ECC, protamine was administered, followed by the decannulation of the aortic arch. This ends the surgical training and the animal is euthanized.

### 3.3.2 Transvalvular LVAD in aortic position

In the second setting, the transvalvular VAD is used as an LVAD, and the native aortic valve is not replaced. The transvalvular LVAD (tLVAD) is carefully positioned retrogradely through the native valve whilst displacing the aortic cusps to the sides, and fixating the transvalvular tLVAD supraannularly in the acoronary sinus through two 3-0 Ethibond Teflon-pledged armed sutures through the aortic wall.

For this purpose, a cross incision is performed in the ascending aorta. The tLVAD is carefully positioned retrogradely through the native valve whilst displacing one aortic cusp to the side of the aortic wall, preferably the acoronary cusp. Great care must be given to treat the native valve cusps as diligently as possible. The tLVAD is then fixated supraanularly in the acoronary sinus through two 3-0 Ethibond Teflon-pledged armed sutures through the aortic wall. Attention must be given to choose the position of the tLVAD in such a way that the pump is placed furthest away from both coronary ostia. The aortomy incision is closed using double-winding continuous technique with 4-0 Prolene sutures enhanced with Teflon-pledges especially in the place where the driveline cable exits the aorta. Then the heart is carefully filled with blood and de-aired using the aortic root needle vent. This is followed by removing the aortic crossclamp and thus allowing for the reperfusion of the heart.

Pressure lines are inserted directly in the LV-apex, in the ascending aorta and in the left atrium, and fixated with tourniquets. It is important to consider the proximity of the transvalvular LVAD, and trying to keep as greatest distance to the LVAD inflow and outflow areas while positioning these pressure lines. The ECC is slowly reduced and stopped. ECC cannulas are clamped, but left in situ in case of sudden need for repeated ECC start.

Then the pump is started and gradually increased to different levels, whilst measuring the corresponding parameters. For the induction of the acute heart failure, a direct ligation of the left anterior descending (LAD) coronary artery using 2-0 Ethibond on a tourniquet is performed.

Upon completion of the experiment, the right atrium was decannulated from the ECC, protamine was administered, followed by the decannulation of the aortic arch. This ends the surgical training and the animal is euthanized.

### 3.3.3 Transvalvular RVAD in pulmonary position

In the third setting, the transvalvular VAD is used as an RVAD positioned through the pulmonary valve. The pulmonary valve is not replaced. The tRVAD is carefully positioned retrogradely through the native valve whilst displacing one pulmonary cusp to the sides, and fixating the transvalvular tRVAD in the ventral part of the pulmonary truncus through two 3-0 Ethibond Teflon-pledged armed sutures through the wall of the pulmonary truncus. This technique allows for being used on a beating heart or without applying cardioplegic solution, as well as without the need for aortic crossclamp.

For this purpose, a cross incision is performed in the pulmonary truncus. The tRVAD is carefully positioned retrogradely through the native valve whilst displacing the pulmonary cusps to the sides. Great care must be given to treat the native valve cusps as diligently as possible. The transvalvular tRVAD is then fixated supraanularly in the ventral part of the pulmonary truncus, through two 3-0 Ethibond Teflon-pledged armed sutures through the wall of the pulmonary truncus. Attention must be given to choose the position of the transvalvular tRVAD in such a way that the pump is placed furthest away from aorta, thus omitting the proximity of coronary arteries and choosing the axis of the RVOT. The cross-incision or the pulmonary truncus is closed using double-winding continuous technique with 4-0 Prolene sutures enhanced with Teflon-pledges especially in the place where the driveline cable exits the pulmonary truncus. Then the heart is carefully filled with blood and de-aired using the aortic root vent. This is followed by removing the aortic crossclamp and thus allowing for the reperfusion of the heart.

Pressure lines are inserted directly in the RV-apex, in the pulmonary artery and in the right atrium, and fixated with tourniquets. It is important to consider the proximity of the transvalvular RVAD, and trying to keep as greatest distance to the RVAD inflow and outflow areas while positioning these pressure lines. The ECC is slowly reduced and stopped. ECC cannulas clamped, but left in situ in case of sudden need for repeated ECC start.

Then the pump is started and gradually increased to different levels, whilst measuring the corresponding parameters. For the induction of the acute heart failure, a direct ligation of either right coronary artery (RCA) or of the circumflex coronary artery (RCX) using 2-0 Ethibond on a tourniquet can be performed.

Upon completion of the experiment, the right atrium was decannulated from the ECC, protamine was administered, followed by the decannulation of the aortic arch. This ends the surgical training and the animal is euthanized.

## 3.4 Intraoperative timeline protocol

Upon implantation of the transvalvular VAD with or without the valve replacement as left or right ventricular support, respectively, the experiment underwent following time sequences in following chronological order:

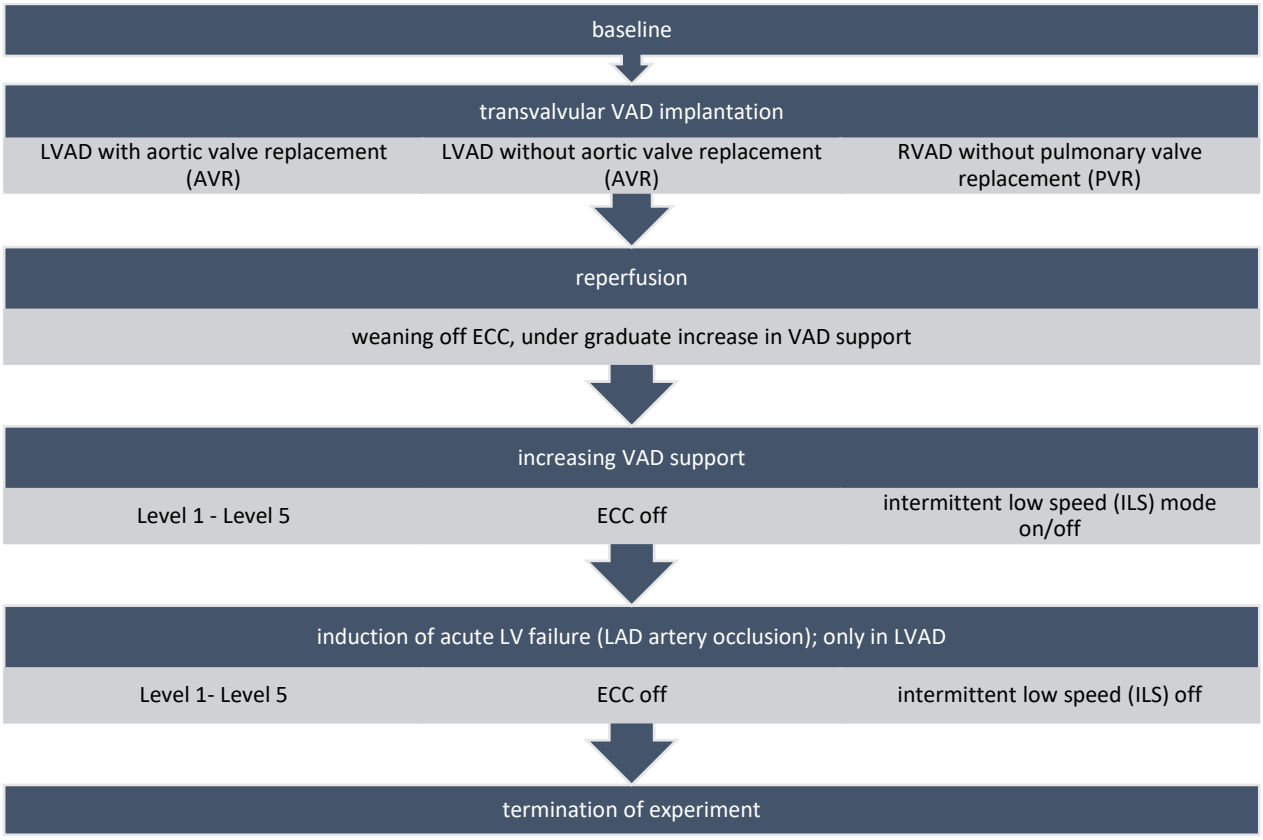


Legend to the intraoperative timeline protocol:

- baseline: before ECC start,
- timepoint T0: weaning off ECC, no coronary artery occlusion, VAD off,
- timepoint T1: ECC off, no coronary artery occlusion, ILS mode switched on, gradual increase of VAD from speed level 1 to speed level 5,
- timepoint T2: ECC off, no coronary artery occlusion, ILS mode switched off, gradual increase of VAD from speed level 1 to speed level 5,
- timepoint T3: ECC off, induction of coronary artery occlusion (in LVAD setting the occlusion is performed on LAD, in RVAD setting the occlusion is performed on RCA or RCX), ILS mode switched off, gradual increase of VAD from speed level 1 to speed level 5,
- timepoint T4: ECC off, induction of coronary artery occlusion, VAD switched off.

Upon each section of the experiment, we analyzed the following parameters (Table 2):

| | |
|---|---|
| hemodynamics | LV-pressure (in LV-apex; [mmHg]) |
| | aortic pressure (in ascending aorta, [mmHg]) |
| | central venous pressure (CVP [mmHg]) |
| | pulmonary arterial pressure (PA; [mmHg]) |
| | RV-pressure (in RV; [mmHg]) |
| | cardiac output (CO) [L/min] |
| | heart rate (HR) [ /min] |
| VAD parameters | speed Level [1-5] |
| | power [watt] |
| | ILS mode switched on or off |
| transepicardial echocardiographic imaging | LVEF per visual assessment [%] |
| | presence of aortic regurgitation (AR) or mitral regurgitation (MR) [mild, moderate, severe] |
| | RV-function impaired per visual assessment [mild, moderate, severe] |
| | septal suctions observed [yes/no] |
| | filling status of the ventricles |
| | valve pump position correct [yes/no] |
| laboratory parameters via arterial blood gas analysis (BGA) | hemoglobin [mg/dL] |
| | hematocrit [%] |
| | $pO_2$ [mmHg] |
| | $pCO_2$ [mmHg] |
| | bicarbonate [mmol/L] |
| | base excess |
| | pH |
| | lactate [mmol/L] |
| | glucose [mmol/L] |

*Table 2. Intraoperative parameters assessed at timepoints baseline, T0, T1, T2, T3, T4*

The continuous measurement of the hemodynamic parameters was recorded through direct pressure line inserted in the respected area, and recorded by implantable data transmitter (Data Sciences International (DSI)© of St. Paul, MN, USA). All other parameters were manually recorded in the respected protocol sheets that were designed for this study.

As this entire experiment is a dynamic process, in case of either a technical difficulty or hemodynamic instability, deviations to the described intraoperative protocol and timeline may be necessary, and need to be taken into consideration.

# 4 Results

## 4.1 Transvalvular LVAD in aortic position and biological aortic valve replacement – Prosthetic Valve Pump (tLVAD with AVR, PVP)

In this first part, the replacement of the aortic valve with 23 mm bioprosthetic porcine aortic valve was performed, followed by the implantation of the valve pump through the prosthetic valve and whilst using it as an LVAD. The animal model used was adult pig of 100 kg with BSA of 1.51 $m^2$.

The surgery time was 422 minutes, the ECC time for the implantation of the bioprosthetic aortic valve and the Jarvik valve pump was 167 minutes, with aortic cross-clamp time of 120 minutes. The time for the implantation of the bioprosthetic valve and valve pump from aortotomy to closure of the aorta was 25 minutes. Upon declamping the aorta, the heart was reperfused for 20 minutes, after which the weaning of the ECC gradually began.

Prior to cannulation and ECC start, the baseline hemodynamics were physiological, with average aortic pressure at 58/92/42 mmHg (mean/systolic/diastolic pressures), CVP at 12 mmHg, and the average heart rate at 90/min. The PCWP was 12 mmHg, and the measured CO was 9.10 L/min. The calculated total peripheral resistance (TPR) (using the standard formula $TPR = \frac{MAP \times 80}{CO}$) was 509 dyn · sec · $cm^{-5}$, and the CI was 6.03 L· $min^{-1}$ · $m^{-2}$. The pressure curves were physiological (Graph 1).

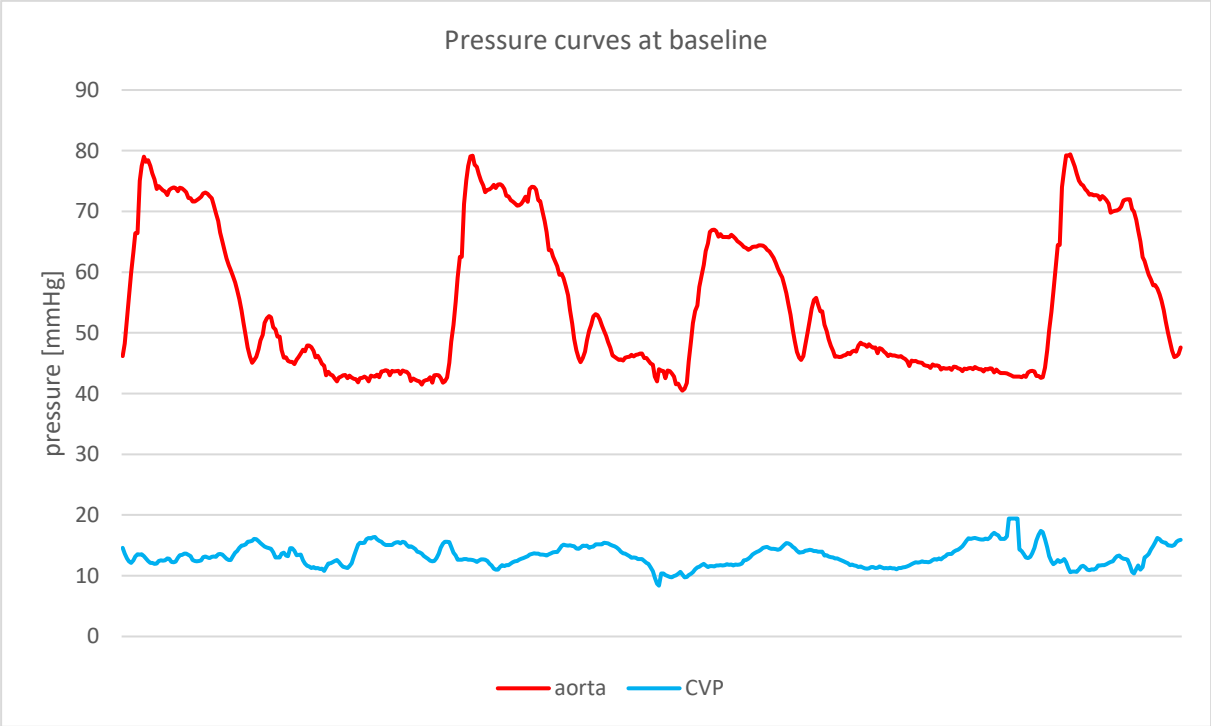


*Graph 1. tLVAD with AVR. Pressure curves at baseline*

The heart was echocardiographically physiological, with visual LVEF of 60 %, no aortic or mitral regurgitation, the calculated AVA was at 3.8 $cm^2$. The baseline hemoglobin was at 12.4 g/L, and baseline lactate at 5.95 mmol/L.

During the implantation under full support of ECC under cross clamped aorta and cardioplegic heart with Bretschneider cardioplegic solution, the hemodynamics were stable and no surgical complications were encountered. The average hemodynamics during this phase were MAP of 29 mmHg, mean PAP of -8 mmHg, mean LV pressure of 4 mmHg, and CVP of 4 mmHg (Graph 3, Panel A). During this phase we observed increase of lactate levels to 11.3 mmol/L, and a drop in hemoglobin to 10.3 g/L.

Upon successful implantation of the bioprosthetic aortic valve and the LVAD valve pump, the reperfusion of the heart was initiated. The average aortic pressures were 59/98/49 mmHg (m/s/d), mean PAP 24 mmHg, LV pressures were 28/129/-5 mmHg (m/s/d), and CVP at 13 mmHg (Graph 3, Panel B). The average heart rate was 100/min, hemoglobin and lactate levels were stable at 11.1 g/L and 12.15 mmol/L, respectively.

After 20 min of reperfusion we then stopped the ECC support and started the LVAD valve pump to level 1, with ILS mode switched on. The power indicated on the pump was fluctuating between 3 and 4 Watt, and no alarms. The echocardiographic imaging showed presence of low grade aortic regurgitation, as well as low grade mitral regurgitation, and low LV filling, but no septal suction. During the ILS phases, the mitral and aortic regurgitation were not observed, and the LV filling improved echocardiographically. The left ventricular hemodynamics changed, with drop of average aortic pressures to 42/50/37 mmHg (m/s/d), and decrease of the LV filling pressures to 9/42/-5 mmHg (m/s/d), but there were no significant changes to mean PAP at 15 mmHg and no change in CVP at 11

With stable hemodynamics for 8 minutes, we increased the valve pump to level 3, with ILS mode turned on. The power increased to 8 Watt, echocardiographically there was no aortic regurgitation, however we observed a worsening of the mitral regurgitation to medium grade, with worsening of the LV-filling and presence of the septum suction was observed after a few seconds. The aortic MAP remained stable at 45 mmHg, the systolic LV pressure dropped significantly to 30 mmHg, with no change in diastolic LV pressures (reduction of LV pressure amplitude). The pulmonary artery pressures and the CVP did not change. The following Graph 2 illustrates the rapid decrease of LV pressures:

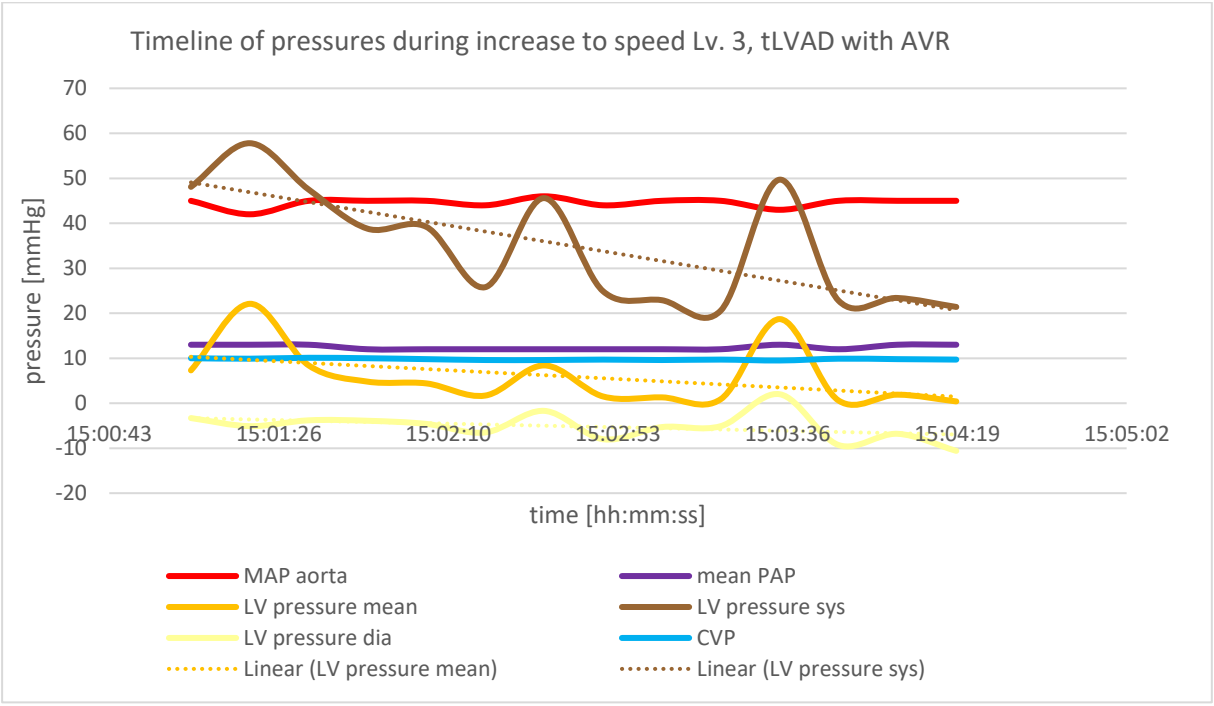


*Graph 2. tLVAD with AVR. Timeline of pressures after increase to level 3, T1, tLVAD at level 3.*

To stabilize the situation the valve pump was reduced to level 1, and the ECC support was reestablished. Under partial ECC-support the valve pump remained at level 1 and stable power between 3 and 4 Watt. Under partial ECC-support, and after 4 minutes of valve pump support at speed level 1, we increased the valve pump again to level 3, at 8 Watt, and observed septal suction in an empty LV as well as presence of medium grade mitral regurgitation, despite unloading through the ECC. Upon speed reduction of valve pump to level 1, the septal suction, mitral regurgitation and filling of the LV all improved. When increasing the valve pump to level 2, the power increased to 6 Watt, without significant change in systemic arterial pressure (MAP remained unchanged at 51 mmHg). The LV pressures dropped significantly to -8/15/20 mmHg (m/s/d). There was no worsening of the mitral regurgitation, and no septal suctions observed. The Panels D and E of the Graph 3 demonstrate the difference in pressure between valve pump operating at level 1 during ILS phase (Graph 3 Panel D) and operating at level 2 without ILS phase (Graph 3 Panel E). The Panel F of Graph 3 demonstrates the directly observed hemodynamic impacts in pressure curves during the start of the ILS mode, with increase of endsystolic LV pressures, with increase of overall pulsatility.

Twenty five minutes after reestablishing the partial ECC support, we were able to wean off the ECC, under continuation of valve pump support running at level 1 at stable 4 Watt. At this point we measured the cardiac output, which was merely 3.6 L/min, the CI was calculated at 2.38 $L \cdot min^{-1} \cdot m^{-2}$, and the TPR was 800 $dyn \cdot sec \cdot cm^{-5}$. The average pressures in aorta over the next 17 minutes were 44/77/32 mmHg (m/s/d), in LV 23/82/0 mmHg (m/s/d), in PA 23/28/18 mmHg (m/s/d) and in CVP 13 mmHg.

Afterwards we turned the valve pump off (Graph 3 Panel G). There was no significant change of pressures, without changing the titration of catecholamines. The recorded hemodynamics were stable, at 42/67/32 mmHg (m/s/d) in aorta, 26/77/5 mmHg (m/s/d) in LV, 24/26/22 mmHg (m/s/d) in PA, and 14 mmHg in CVP.

Afterwards we tested the hemodynamics and echocardiographic parameters after restarting the valve pump at level 1, and gradually increasing the pump speed. The pump valve was operating at different levels between 5 and 10 minutes each, before increasing it up one level.

Running at level 1, the power remained stable at 3 Watt, CO was measured at 4.7 L/min, which equivalents to CI of 3.11 $L \cdot min^{-1} \cdot m^{-2}$, and TPR of 851 $dyn \cdot sec \cdot cm^{-5}$. The average pressures in aorta were 47/80/35 mmHg (m/s/d), in LV 25/84/2 mmHg (m/s/d), in PA 24/27/21 mmHg (m/s/d), and CVP at 14 mmHg. The hemodynamics as demonstrated by the pressure curve is demonstrated in Graph 3 Panel H.

At speed level 2, the power increased to 6 Watt, CO was measured at 4.6 L/min, which equivalents to CI of 3.05 $L \cdot min^{-1} \cdot m^{-2}$, and TPR of 956 $dyn \cdot sec \cdot cm^{-5}$. The average pressures in aorta were 51/83/37 mmHg (m/s/d), in LV 25/80/3 mmHg (m/s/d), in PA 25/27/21 mmHg (m/s/d), and CVP at 20 mmHg. No alarms, septum suction, or aortic regurgitation was observed, and a low grade mitral regurgitation with good fillings of the LV were present.

At speed level 3, the power increased to 8 Watt, CO was measured at 5.1 L/min, which equivalents to CI of 3.38 $L \cdot min^{-1} \cdot m^{-2}$, and TPR of 910 $dyn \cdot sec \cdot cm^{-5}$. The average pressures in aorta were 55/86/39 mmHg (m/s/d), in LV 24/76/0 mmHg (m/s/d), in PA 26/29/23 (m/s/d), and CVP at 17 mmHg. No alarms, aortic regurgitation or septum suction were observed, and the low-grade mitral regurgitation remained stable, however the LV was significantly less well filled. The pressure curves at this stage is demonstrated in Graph 4 Panel I.

At level 4, the power increased to 10 to 11 Watt (intermittently fluctuating between 10 and 11 Watt), CO was measured at 5.9 L/min, which equivalents to CI of 3.91 L· $min^{-1}$ · $m^{-2}$, and TPR of 840 dyn · sec · $cm^{-5}$. The average pressures in aorta were 54/83/43 mmHg (m/s/d), in LV 22/82/4 mmHg (m/s/d), in PA 27/32/22 (m/s/d), and CVP at 15 mmHg. No alarms, aortic regurgitation or septum suction was observed, with stable low-grade mitral regurgitation. The LV-enddiastolic filling remained echocardiographically stable to the stage observed at speed level 3. The pressure curves at this stage is registered in Graph 4 Panel J.

At tLVAD operating at speed level 5, the power increased to 13 Watt, CO was measured at 6.5 L/min, which equivalents to CI of 4.30 L· $min^{-1}$ · $m^{-2}$, and TPR of 763 dyn · sec · $cm^{-5}$. The average pressures in aorta were 56/77/45 mmHg (m/s/d), in LV 21/66/2 mmHg (m/s/d), in PA 30/33/25 (m/s/d), and CVP at 16 mmHg. Unchanged to the prior stages at lower pump speeds, no alarms, septum suction, or aortic regurgitation was registered, with stable low grade mitral regurgitation, and stable low enddiastolic LV-fillings.


*Graph 3. Pressure curves at timepoints T0-T3 for tLVAD with AVR, Part I, Panels A-H.*
*Panel A: during aortic crossclamp. Panel B: timepoint T0, during reperfusion, tLVAD turned off. Panel C: timepoint T1, tLVAD at level 1. Panel D: timepoint T1, tLVAD at level 1, during ILS phase and partial ECC support. Panel E: timepoint T1, tLVAD at level 2, under partial ECC support. Panel F: timepoint T1, tLVAD at level 1, during start of ILS mode (marked), ECC support off. Panel G: timepoint T1, tLVAD switched off, ECC support off. Panel H: timepoint T1, tLVAD at level 1, ECC support off. (Legend: aorta: aortic pressure; PA: pulmonary artery; LV: left ventricle; CVP: central venous pressure)*


*Graph 4. Pressure curves at timepoints T0-T3 for tLVAD with AVR, Part II, Panels I-P.*
*Panel I: timepoint T1, tLVAD at level 3, ECC support off. Panel J: timepoint T1, tLVAD at level 4, ECC support off. Panel K: timepoint T2, tLVAd at level 2, ILS mode off, ECC support off. Panel L: timepoint T2, tLVAD switched off, ECC support off. Panel M: timepoint T2, tLVAD at level 3, ILS mode off, ECC support off. Panel N: timepoint T3, prior to 2nd LAD occlusion, tLVAD switched off, ECC support off. Panel O: timepoint T3, during 2nd LAD-occlusion, tLVAD at level 3, ECC support off. Panel P: timepoint T3, during 2nd LAD-occlusion, tLVAD at level 4, ECC support off. (Legend: aorta: aortic pressure; PA: pulmonary artery; LV: left ventricle; CVP: central venous pressure).*

Afterwards the phase T2 of the experiment began. The speed of the valve pump was reduced to level 2, and the ILS mode was switched off. Then the pump was left at speed level 2 for 12 minutes, with stable power consumption of 6 Watt, and stable hemodynamics, to allow for conditioning of the LV. The average pressures in aorta were 58/87/44 mmHg (m/s/d), in LV 23/73/2 mmHg (m/s/d), in PA 31/33/24 (m/s/d), and CVP at 16 mmHg. The pressure curves are demonstrated in Graph 4 Panel K. No alarms, septum suction or aortic regurgitation was observed, with good enddiastolic fillings of the LV. Mitral regurgitation remained stable and classified as low grade.

Afterwards the valve pump was switched off, resulting in pressure curves as demonstrated in Graph 4 Panel L. During the phase where the valve pump was switched off, the CO was measured at 5.5 L/min, which equivalents to CI of 3.64 $L \cdot min^{-1} \cdot m^{-2}$, and TPR of 669 $dyn \cdot sec \cdot cm^{-5}$. The average pressures in aorta were 44/73/27 mmHg (m/s/d), in LV 33/109/4 mmHg (m/s/d), in PA 31/33/24 (m/s/d), and CVP at 16 mmHg. No alarms, septum suction, mitral or aortic regurgitation, was observed, with visually good filling of the LV.

Four minutes after switching valve pump off, the valve pump was turned on again, directly to speed mode at level 3. Power consumption was 8 Watt, echocardiographically septum suction and low LV-filling with kissing ventricle phenomenon was observed. There were no presence of aortic regurgitation, however a low grade mitral regurgitation. The CO was measured at 6.3 L/min, which equivalents to CI of 4.17 $L \cdot min^{-1} \cdot m^{-2}$, and TPR of 800 $dyn \cdot sec \cdot cm^{-5}$. The average pressures in aorta were 67/87/40 mmHg (m/s/d), in LV 35/92/0 mmHg (m/s/d), in PA 30/34/22 (m/s/d), and CVP at 20 mmHg. The pressure wave forms is demonstrated in Graph 4 Panel M.

### 4.1.1 LAD Occlusion

The next step was the phase T3 of the experiment, with induction of acute heart failure via surgical LAD occlusion. For this phase of the experiment, the ILS mode was turned off.

Prior to LAD-occlusion the valve pump speed was reduced to level 2. Power consumption dropped to 6 Watt, the pressures in aorta measured 57/82/54 mmHg (m/s/d), in LV 29/96/6 mmHg (m/s/d), in PA 26/34/22 mmHg (m/s/d), and CVP at 15 mmHg.

Upon induction of LAD-occlusion with surgical ligation of the LAD artery, we observed immediate ST-depressions in ECG leads, and observed immediate echocardiographic deterioration of the LV-function. The mean aortic pressure was maintained at 49 mmHg through the valve pump at level 2 and power at steady 6 Watt. The amplitude of the LV pressures steadily decreased, the right sided hemodynamics remained unchanged. 127 seconds after LAD occlusion ventricular tachycardia occurred, followed by ventricular fibrillation 29 seconds later. During this phase the valve pump was kept at steady speed at level 2, without presence of any alarms, septal suction or changes in power consumption (remained at stable 6 Watt). After 55 further seconds the heart went into cardiac arrest, with complete drop of all pressures. The timeline of this dynamic phase is demonstrated in the Graph 5 below. While keeping the valve pump running at level 2 the ECC support was fully reinitiated and the LAD occlusion removed. To restore the normal sinus rhythm, we had to shock at 50 Joules seven times. After 20 minutes of reperfusion, we weaned off the ECC support, whilst maintain the valve pump running at speed level 2.

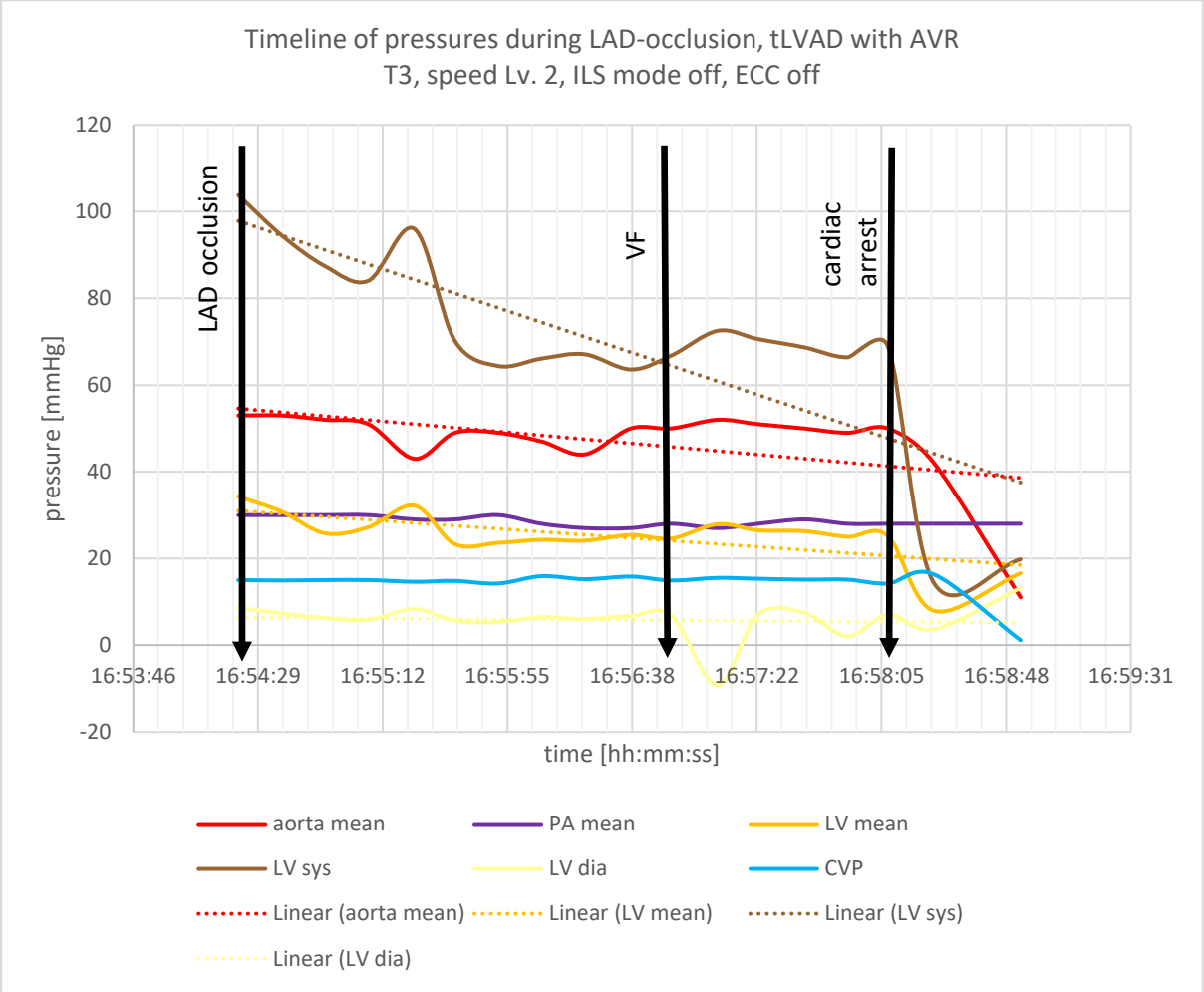


*Graph 5. Timeline of pressures during LAD-occlusion, timepoint T3, tLVAD with AVR*
*(Legend: aorta mean: mean aortic pressure; LV mean: mean left ventricular pressure; LV sys: systolic left ventricular pressure; LV dia: diastolic left ventricular pressure, PA mean: mean pulmonary pressure; CVP: central venous pressure; linear refers to linear trendline of the respected variable)*

As the heart function recovered, and the heart rhythm had remained in stable sinus we measured the hemodynamics. The cardiac output was 4.4 L/min, which equivalents to CI of 2.91 $L \cdot min^{-1} \cdot m^{-2}$, and TPR of 836 $dyn \cdot sec \cdot cm^{-5}$. The average pressures in aorta were 42/56/31 mmHg (m/s/d), in LV 12/36/3 mmHg (m/s/d), in PA 21/30/17 (m/s/d), and CVP at 17 mmHg.

With stable hemodynamic situation the second attempt of induction of acute heart failure with surgical ligation of the LAD artery was made. This second LAD-occlusion was performed at the mid-section of the LAD-artery. Prior to occlusion we switched off the valve pump, and measured the hemodynamics: average aortic pressure was at 48/68/39 mmHg (m/s/d), average LV pressure at 21/68/5 mmHg (m/s/d), average PA pressure at 25/35/19 mmHg (m/s/d) and average CVP at 19 mmHg, the average heart rate was at 81 /min.

A few seconds following the second induction of the mid-section LAD artery, the valve pump was turned on directly at speed level 3. This speed level was continued for two minutes, during which no ventricular arrythmias were observed and the hemodynamics remained stable. The power consumption remained stable at 7 Watt, the aortic pressure improved. The average aortic pressure during this phase was 55/75/47 mmHg (m/s/d), average LV pressure was 12/49/-2 mmHg (m/s/d), the average PA pressure was 26/41/9 mmHg (m/s/d), and average CVP was 24 mmHg. The pressure curves showed significant LV-pressure reduction as sign of LV unloading (Graph 4 Panel O).

After two minutes at speed level 3, the speed was increased at level 4. This speed level was continued for roughly four minutes, during which no ventricular arrythmias were observed and the hemodynamics remained stable. The power consumption remained stable at 11 Watt, the aortic pressures somewhat fluctuated. The average aortic pressure during this phase was 53/64/45 mmHg (m/s/d), average LV pressure was 14/38/3 mmHg (m/s/d), the average PA pressure was 19/30/17 mmHg (m/s/d), and average CVP was 19 mmHg. The cardiac output at this pump speed was 5.1 L/min, which equivalents to CI of 3.38 $L \cdot min^{-1} \cdot m^{-2}$, and TPR of 831 $dyn \cdot sec \cdot cm^{-5}$. The pressure curves showed significant LV pressure reduction as sign of LV unloading (Graph 4 Panel P).

The lactate levels after ECC support at time T0 remained stable throughout the duration of the experiment (12.21 mmol/L after first LAD occlusion).

This phase was followed by switching off the valve pump (timepoint T4), upon which the systolic LV pressures rose up to 108 mmHg, followed by ventricular fibrillation after a few seconds, with resulting drop of systemic and rise of pulmonary pressure. At this point we terminated the experiment, and euthanized the animal with intravenous systemic injection of pentobarbital and direct intracardiac injection of highly concentrated potassium.

## 4.2 Transvalvular RVAD in pulmonary position in native pulmonary valve (tRVAD)

In this second part of the experiment, the valve pump was used in pulmonary and in aortic position, without replacing the native pulmonary or aortic valve. This second part of the experiment was performed as a two-staged procedure on one animal model, by first implanting the valve pump through the pulmonary valve as an transvalvular RVAD, and testing its hemodynamics (Chapter 6.2). Afterwards the right ventricular valve pump was placed in through the native aortic valve, thus purposing as transvalvular LVAD (Chapter 6.3). The animal model was 90 kg heavy female adult pig, with BSA of 1.50 $m^2$.

The implantation of the tRVAD was performed under full support of ECC, but on a beating heart without aortic crossclamping and without cardioplegia. The ECC time for the implantation was 62 minutes. The time for the implantation of the tRVAD through the pulmonary valve was 15 minutes. The tRVAD was positioned through the pulmonary valve, whilst displacing the anterior cusp between the wall of the vessel and the valve pump.

Prior to cannulation and ECC start, the baseline hemodynamics were physiological, with average aortic pressure at 73/103/52 mmHg (m/s/d), pulmonary artery pressures at 27/33/22 mmHg (m/s/d), and CVP at 6 mmHg. The average heart rate was 58 /min. The PCWP was 13 mmHg, and the measured CO was 9.5 L/min. The calculated total peripheral resistance (TPR) (using the standard formula $TPR = \frac{MAP \times 80}{CO}$) was 615 dyn · sec · $cm^{-5}$, and the CI was 6.3 L· $min^{-1}$ · $m^{-2}$. The pressure curves were physiological, demonstrated in Graph 6 Panel A.

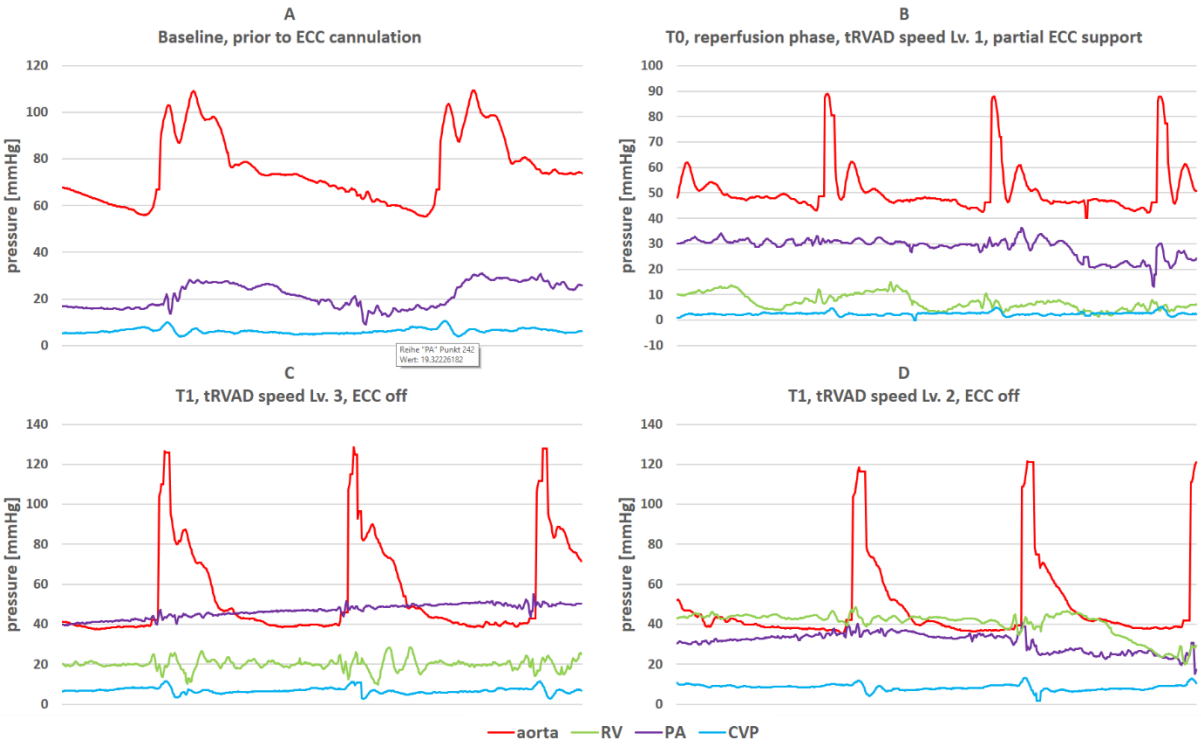


*Graph 6. Pressure curves at timepoints T0-T1 for tRVAD without PVR. Panels A-D.*
*Panel A: timepoint baseline, prior to cannulation for ECC. Panel B: timepoint T0, tRVAD at level 1, partial ECC support, reperfusion phase. Panel C: timepoint T1, tRVAD at level 3, ECC support off. Panel D: timepoint T1, tRVAD at level 2, ECC support off. (Legend: aorta: aortic pressure; RV: right ventricular pressure; PA: pulmonary artery pressure; CVP: central venous pressure).*

The heart was echocardiographically physiological, with visual LVEF of over 60 %, no aortic or mitral regurgitation, both pulmonary and aortic valves were physiological and tricuspid. The baseline hemoglobin was at 10.9 g/L, and baseline lactate at 3.31 mmol/L.

During the implantation under full support of ECC and beating heart, the hemodynamics were stable and no surgical complications were encountered. The average hemodynamics during this phase were MAP of 54 mmHg, mean PAP of 5 mmHg, CVP of 4 mmHg. During this phase we observed increase of lactate levels to 5.72 mmol/L, and a stable hemoglobin of 11.9 g/L.

After successful implantation of the valve pump as RVAD in pulmonary truncus, the heart was slowly weaned of the ECC support. During this weaning phase, the tRVAD pump was carefully turned on and gradually increased in its speed levels, while concurrently reducing the ECC-support.

As tRVAD pump was turned on to speed level 1, under partial ECC support, the RV pressure dropped from mean 31 mmHg to mean 9 mmHg, the mean PA pressure increased only minimally (from 28 mmHg to mean 30 mmHg), however with significant reduction in pulsatility. The aortic pressure did not change (Graph 6 Panel B). The heart rate was steady at 90/min. Power consumption at speed level 1 remained stable between 3 and 4 Watt, there was no septal suction or alarms.

After 2 minutes we increased the tRVAD pump speed to level 2 upon further reduction of the ECC support. The power consumption of the pump increased to 6 Watt. Throughout the weaning off phase we experienced difficulties in RV filling, as the RV pressures fluctuated almost periodically with increases and decreases of RV diastolic and systolic pressures. These correlated with the occurring ILS phases (during ILS phase the diastolic and systolic RV pressure increased, with echocardiographically better RV filling, upon termination of ILS phase the RV fillings decreased again). The mean aortic pressure remained stable, at 48 mmHg, the CVP pressure slightly increased to 6 mmHg. The mean RV pressure remained low at 13 mmHg, indicating RV-unloading by the tRVAD pump. The PA pressure remained linear, with mean pressure of 20 mmHg. The heart rate was steady at 90/min.

Afterwards we weaned off the ECC support entirely, whilst increasing the valve pump speed to level 3. The power consumption of the pump increased to 7 Watt. The mean aortic pressure remained stable, at 53 mmHg, the mean PA pressure remained unchanged at 21 mmHg, with a noticeable decrease in pulsatility (Graph 6 Panel C). The mean RV pressure increased to 22 mmHg, the CVP did not increase (7 mmHg). In trendlines we observed an immediate decrease of diastolic RV pressure upon increasing the speed level to 3, however with stabilization within 20 seconds. Echocardiographically the fluctuations of RV filling continued, however with notably better RV filling then during ECC support. The heart rate was steady at 85/min.

After 2 minutes at speed level 2, we decreased the PA pump valve to level 1. We observed an immediate increase of RV diastolic and systolic pressures (mean RV pressure 31 mmHg), which correlates to increased RV filling and/or worse RV unloading. Furthermore the mean PA pressure dropped significantly to 11 mmHg. The mean pressure difference between mean PA and mean RV pressure was calculated at 25 mmHg, indicating a possible functional stenosis in the RVOT due to implanted RV valve pump. The power consumption decreased to between 3 to 4 Watt. The mean aortic pressure remained unaffected (54 mmHg). Echocardiographically the fluctuations of RV filling continued, however with notably better RV filling then during ECC support. No septal suctions and no valve regurgitations were observed. The heart rate was steady at 86/min.

To further investigate this phenomenon further, we turned off the tRVAD pump after 2 minutes. We observed no significant difference in hemodynamics (mean aortic pressure 50 mmHg, mean PAP 12 mmHg, CVP 8 mmHg), however with further increase of mean RV pressure to 38 mmHg. We did however observe a light pulmonary regurgitation around the pump. The heart rate was steady at 90/min.

After 2 minutes, we turned on the tRVAD pump back to speed level 1. Interestingly, we observed an immediate RV distortion, with low RV diastolic pressures averaging at 22mmHg, systolic RV pressures at 52 mmHg, and mean RV pressures at 38 mmHg. The mean PAP was with 13 mmHg calculated 25 mmHg of pressure difference to RV mean pressure. The aortic pressure and CVP remained unchanged.

After 2 minutes, we increased the pump speed level to 2, upon we observed very low RV-filling, with mean RV pressure dropping as low as 7 mmHg. This phase lasted for approximately 20 seconds, upon which the hemodynamics stabilized. The mean aortic pressure was 49 mmHg, mean pulmonary pressure improved to 26 mmHg, and the pulmonary pulsatility decreased to a linear flow. This can be observed in the Graph 6 Panel D. The CVP remained unchanged at 7 mmHg, the heart rate was 93 /min. Power consumption of the valve pump remained at stable 6 Watt.

We concluded the testing of the valve pump in PA position as an RVAD. We reinitiated the full ECC-support and continued with the testing for valve pump as an LVAD in aortic position (Chapter 6.3).

## 4.3 Transvalvular LVAD in aortic position in the native aortic valve (tLVAD)

In this second part of the experiment, the valve pump was used in pulmonary and in aortic position, without replacing the native pulmonary or aortic valve. This second part of the experiment was performed as a two-staged procedure on one animal model, by first implanting the valve pump through the pulmonary valve as an RVAD, and testing its hemodynamics (Chapter 6.2). Afterwards the right ventricular valve pump was placed in through the native aortic valve, thus purposing as LVAD (Chapter 6.3). The animal model was 90 kg heavy female adult pig, with BSA of 1.50 $m^2$.

Prior to cannulation and ECC start, the baseline hemodynamics were physiological, with average aortic pressure at 73/103/52 mmHg (m/s/d), pulmonary artery pressures at 27/33/22 mmHg (m/s/d), and CVP at 6 mmHg. The average heart rate was 58 /min. The PCWP was 13 mmHg, and the measured CO was 9.5 L/min. The calculated total peripheral resistance (TPR) (using the standard formula $TPR = \frac{MAP \times 80}{CO}$) was 615 dyn · sec · $cm^{-5}$, and the CI was 6.3 L· $min^{-1}$ · $m^{-2}$. The pressure curves were physiological (Graph 7, Panel A).

The heart was echocardiographically physiological, with visual LVEF of over 60 %, no aortic or mitral regurgitation, both pulmonary and aortic valves were physiological and tricuspid. The baseline hemoglobin was at 10.9 g/L, and baseline lactate at 3.31 mmol/L.

After the implantation and testing of the valve pump in pulmonary position as RVAD, the full ECC support was reinstalled. After cross-clamping the aorta and administering Bretschneider© cardioplegia, the valve pump in pulmonary truncus was explanted, and implanted in the aortic position as an LVAD. The transvalvular left ventricular valve pump was positioned through the native aortic valve, whilst displacing the noncoronary cusp, between the aortic wall and the valve pump. The ECC time was 145 minutes, aortic cross-clamp time was 72 minutes. The time for the implantation of the valve pump through the pulmonary valve was 25 minutes.

During the implantation of tLVAD valve pump under the full support of ECC the hemodynamics were stable and no surgical complications were encountered. The during this second ECC support and cross-clamped aorta, average hemodynamics were MAP of 34 mmHg, mean PAP of -5 mmHg, CVP of -7 mmHg. During this phase we observed increase of lactate levels to 11.15 mmol/L, and a stable hemoglobin of 11.3 g/dL.

Upon successful implantation of the valve pump as tLVAD in ascending aorta, the aortic cross-clamp was removed and the heart slowly weaned off the ECC support, under concurrent support of the valve pump. During the weaning off the ECC support, the valve pump was gradually increased in its speed levels, under further reduction of ECC support.

As the aortic cross-clamp was removed and the valve pump was turned on to speed level 1, the heart was reperfused for 37 minutes. After 34 minutes of reperfusion under partial ECC support, we increased the valve pump speed to level 2, and weaned off the ECC support. The hemodynamics remained stable, with average aortic pressures of 51/107/34 mmHg (m/s/d), LV pressures of 30/173/-17 mmHg (m/s/d), PA pressures of 12/17/7 mmHg (m/s/d), and CVP of 8 mmHg. The power consumption remained stable at 4-5 Watt, the heart rate was paced at a steady 100 /min. The aortic pressures were pulsatile, the LV amplitudes showed a high range in pressure amplitudes, ranging from 192 mmHg systolic to -25 mmHg diastolic. The average pressure difference between systolic aortic and LV pressures averaged at 66 mmHg, The low diastolic pressures indicate a good LV-unloading, however the high systolic pressures and the high pressure difference between aorta and LV indicates a functional obstruction in LVOT due to the valve pump (Graph 7, Panel B). Echocardiographically, we observed a low-grade aortic regurgitation, but no septal suction or mitral regurgitation. The visual estimated RV function remained good.

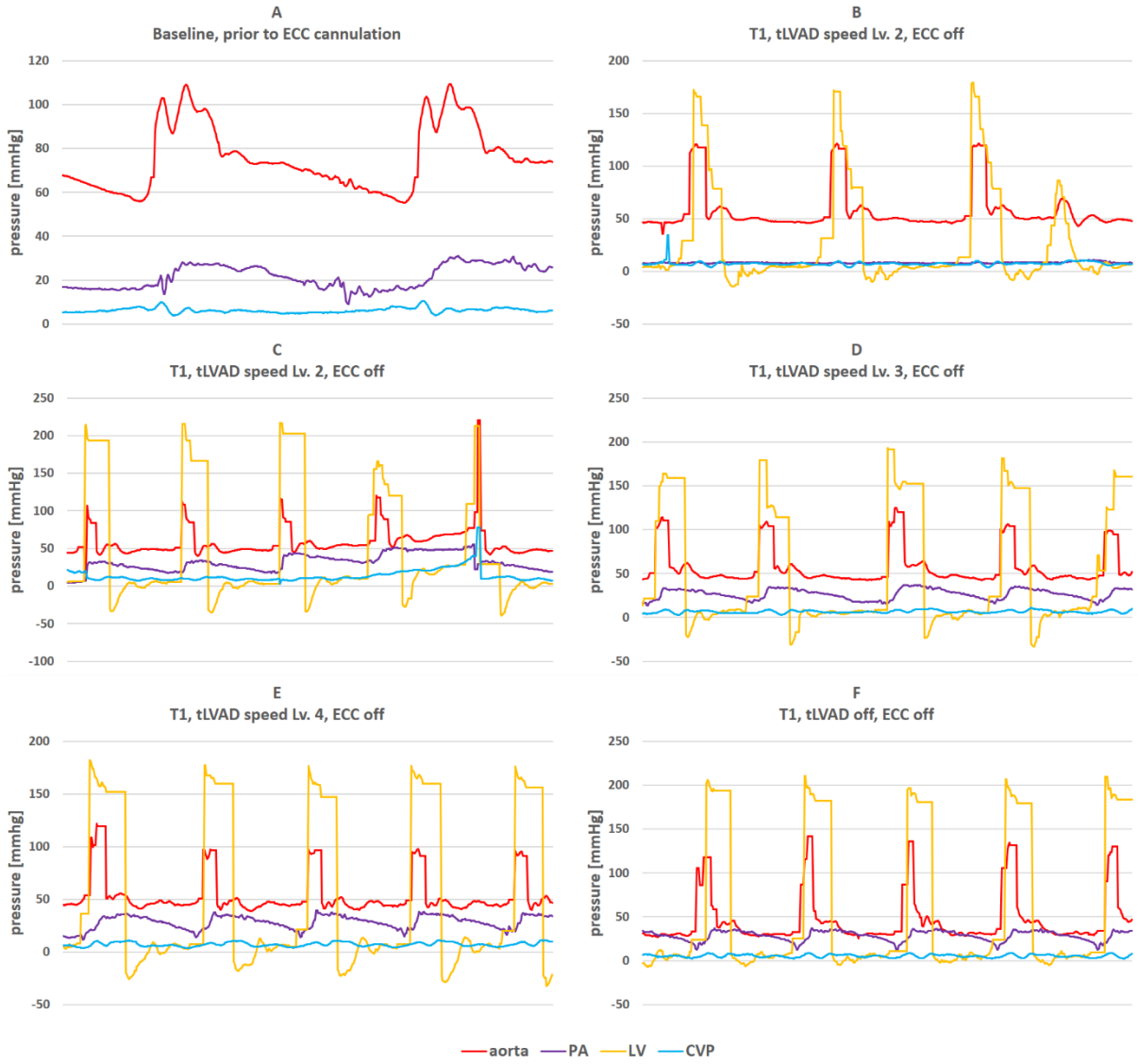


*Graph 7. Pressure curves at timepoints T0-T1 for tLVAD without AVR. Panels A-F.*
*Panel A: timepoint baseline, prior to cannulation for ECC. Panel B: timepoint T1, tLVAD at level 2, ECC support off. Panel C: timepoint T1, tLVAD at level 2, after switching off tLVAD minutes earlier (see text), ECC support off. Panel D: timepoint T1, tLVAD at level 3, ECC support off. Panel E: timepoint T1, tLVAD at level 4, ECC support off. Panel F: timepoint T1, tLVAD switched off, ECC support off. (Legend: aorta: aortic pressure; PA: pulmonary artery pressure; LV: left ventricular pressure; CVP: central venous pressure).*

After 5 minutes, we decreased the valve pump speed to level 1. The power consumption of the pump decreased to 3-4 Watt. The hemodynamics remained stable. The average aortic pressure was 51/121/32 mmHg (m/s/d), LV pressure was 34/181/-20 mmHg (m/s/d), PA pressure was 16/32/5 mmHg (m/s/d), and CVP was 6 mmHg. The CO was 6.10 L/min. The calculated total peripheral resistance (TPR) (using the standard formula $TPR = \frac{MAP \times 80}{CO}$) was 669 dyn · sec · $cm^{-5}$, and the CI was 4.07 L· $min^{-1}$ · $m^{-2}$. Echocardiographically there was a slight reduction of aortic regurgitation.

After 6 minutes, we increased the valve pump speed to level 2. The measured hemodynamics were 50/95/34 mmHg (m/s/d) for aortic pressure, 40/190/-23 mmHg (m/s/d) for LV pressure, 21/30/11 mmHg (m/s/d) for PA pressure, and 8 mmHg for CVP. The increased LVEDP was unchanged, with negative LVESP. The systemic pulsatility remained present (Graph 7, Panel C). The CO was 8.0 L/min. The calculated total peripheral resistance (TPR) (using the standard formula $TPR = \frac{MAP \times 80}{CO}$) was 500 dyn · sec · $cm^{-5}$, and the CI was 5.33 L· $min^{-1}$ · $m^{-2}$. Heart rate increased to 140 /min. Echocardiographically there was no worsening of the slight aortic regurgitation. No septal suction or mitral regurgitation was observed.

After 6 minutes, we increased the valve pump speed to level 3. The pump power consumption increased to 7-8 Watt. The measured hemodynamics were 55/115/39 mmHg (m/s/d) for aortic pressure, 43/179/-27 mmHg (m/s/d) for LV pressure, 26/36/12 mmHg (m/s/d) for PA pressure, and 6 mmHg for CVP. The LVEDP decreased slightly, and the diastolic LV pressure slightly decreased also, indirectly indicating to increased pump outflow (Graph 7, Panel D). The CO was 8.7 L/min. The calculated total peripheral resistance (TPR) (using the standard formula $TPR = \frac{MAP \times 80}{CO}$) was 506 dyn · sec · $cm^{-5}$, and the CI was 5.8 L· $min^{-1}$ · $m^{-2}$. Heart rate remained stable at 145 /min. Echocardiographically there was no worsening of the slight aortic regurgitation. No septal suction or mitral regurgitation was observed.

After 2 minutes, we increased the valve pump speed to level 4. The pump power consumption increased to 9-10 Watt. The measured hemodynamics were 56/109/39 mmHg (m/s/d) for aortic pressure, 42/179/-31 mmHg (m/s/d) for LV pressure, 27/37/11 mmHg (m/s/d) for PA pressure, and 6 mmHg for CVP. The pressure curves remained stable, with no significant changes to when operating at speed level 3 (Graph 7, Panel E). The CO was 8.1 L/min. The calculated total peripheral resistance (TPR) (using the standard formula $TPR = \frac{MAP \times 80}{CO}$) was 553 dyn · sec · $cm^{-5}$, and the CI was 5.4 L· $min^{-1}$ · $m^{-2}$. Heart rate remained stable at 145 /min. Echocardiographically there was no worsening of the slight aortic regurgitation, and no presence of septal suction or mitral regurgitation.

After 2 minutes, we turned the valve pump off. The measured hemodynamics remained stable: 55/132/31 mmHg (m/s/d) for aortic pressure, 46/196/-17 mmHg (m/s/d) for LV pressure, 27/37/11 mmHg (m/s/d) for PA pressure, and 6 mmHg for CVP. The increase in LV pressure was documented, and a drop in diastolic systemic pressure, with increased arterial pulsatility, however (Graph 7, Panel F). The CO was 6.0 L/min. The calculated total peripheral resistance (TPR) (using the standard formula $TPR = \frac{MAP \times 80}{CO}$) was 733 dyn · sec · $cm^{-5}$, and the CI was 4.0 L· $min^{-1}$ · $m^{-2}$. Heart rate remained stable at 142 /min. Echocardiographically there was no aortic regurgitation or mitral valve dysfunction.

### 4.3.1 LAD-Occlusion

The next step was the induction of acute heart failure via acute anterior ischemia induced by surgical occlusion of the LAD artery.

Prior to LAD occlusion the valve pump was turned back on, and set to speed level 2 to maintain a steady LV-unloading. Power consumption was stable at 5 Watt. The measured hemodynamics at valve pump at level 2 and prior to LAD occlusion were: 66/122/50 mmHg (m/s/d) for aortic pressure, 56/202/-15 mmHg (m/s/d) for LV pressure, 28/43/9 mmHg (m/s/d) for PA pressure, and 9 mmHg for CVP.

Throughout the LAD occlusion the valve pump was kept at speed level 2, without presence of alarms, septal suction or changes in power consumption (remained at stable 5 Watt). Hemodynamically, immediately after LAD occlusion the systolic LV started dropping (see Graph 8). Under valve pump support though, the aortic, pulmonary and venous hemodynamics remained stable. 120 seconds in the LAD occlusion, the heart developed asystole, with immediate drop of LV pressures (Graph 8). While keeping the valve pump running at level 2 the ECC support was fully reinitiated and the LAD occlusion removed. To restore the normal sinus rhythm, external defibrillation with 50 Joules was induced six times.

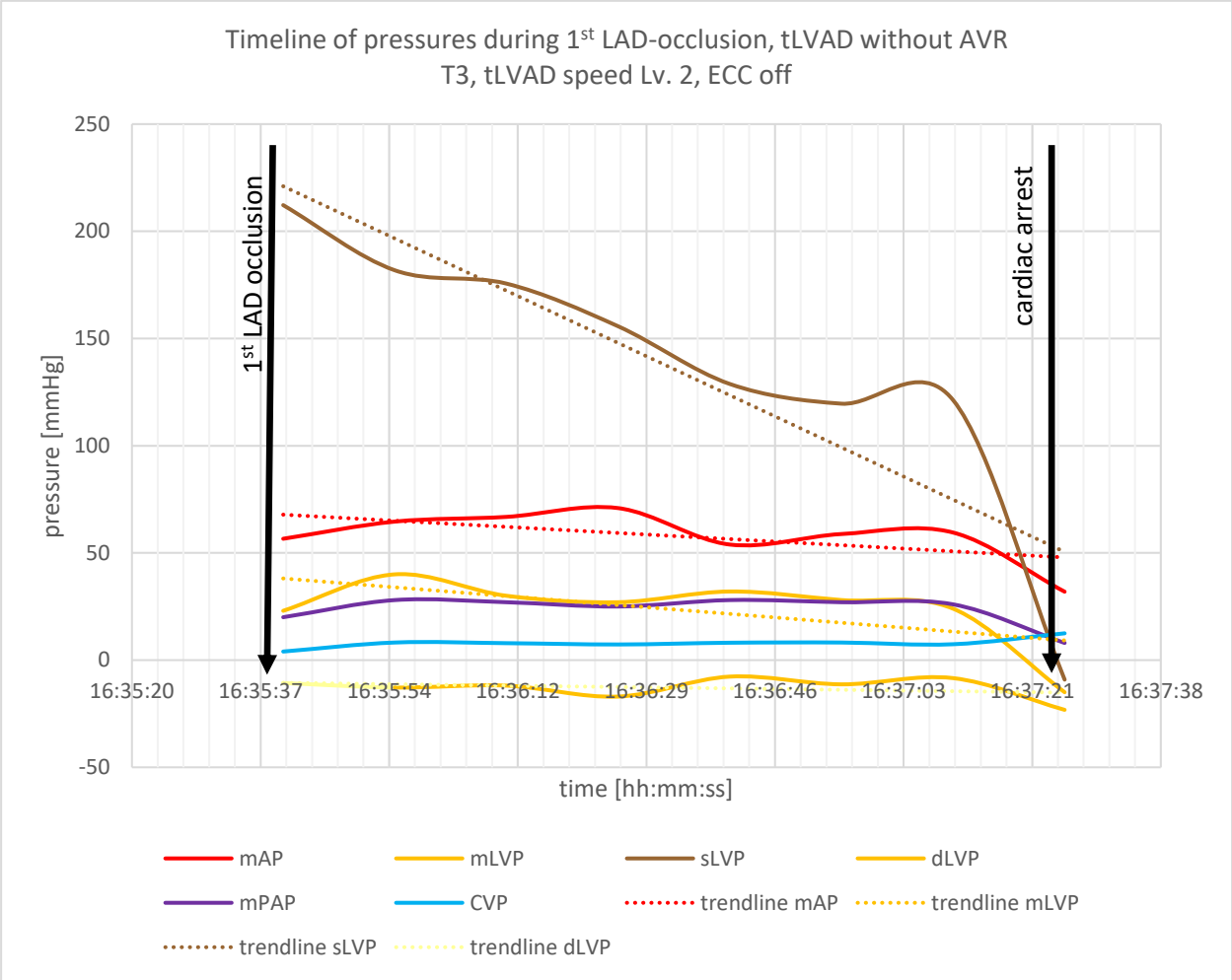


*Graph 8. Timeline of pressures during 1st LAD-occlusion, timepoint T3, tLVAD without AVR*
*(Legend: mAP: mean aortic pressure; mLVP: mean left ventricular pressure; sLVP: systolic left ventricular pressure; dLVP: diastolic left ventricular pressure, mPAP: mean pulmonary pressure; CVP: central venous pressure; trendline refers to linear trendline of the respected variable)*

After 7 minutes of reestablished partial ECC support, we were able to slowly wean off the ECC-support, whilst maintaining the LV support via the valve pump at speed level 2 (Graph 9, Panel A). The hemodynamics were stable at average pressures of 59/110/47 mmHg (m/s/d) in aorta, 41/193/-20 mmHg (m/s/d) in LV, 30/41/16 mmHg (m/s/d) in PA, and CVP of 6 mmHg, and steady sinus rhythm of 100 bpm. The cardiac output was 4.0 L/min, which equivalents to CI of 2.67 $L \cdot min^{-1} \cdot m^{-2}$, and TPR of 1180 $dyn \cdot sec \cdot cm^{-5}$. Echocardiographically, a slight central aortic regurgitation was observed, and no presence of mitral regurgitation and with good fillings of the LV without septal suction were observed. Pump presented no alarms, power remained stable at 5 Watt.

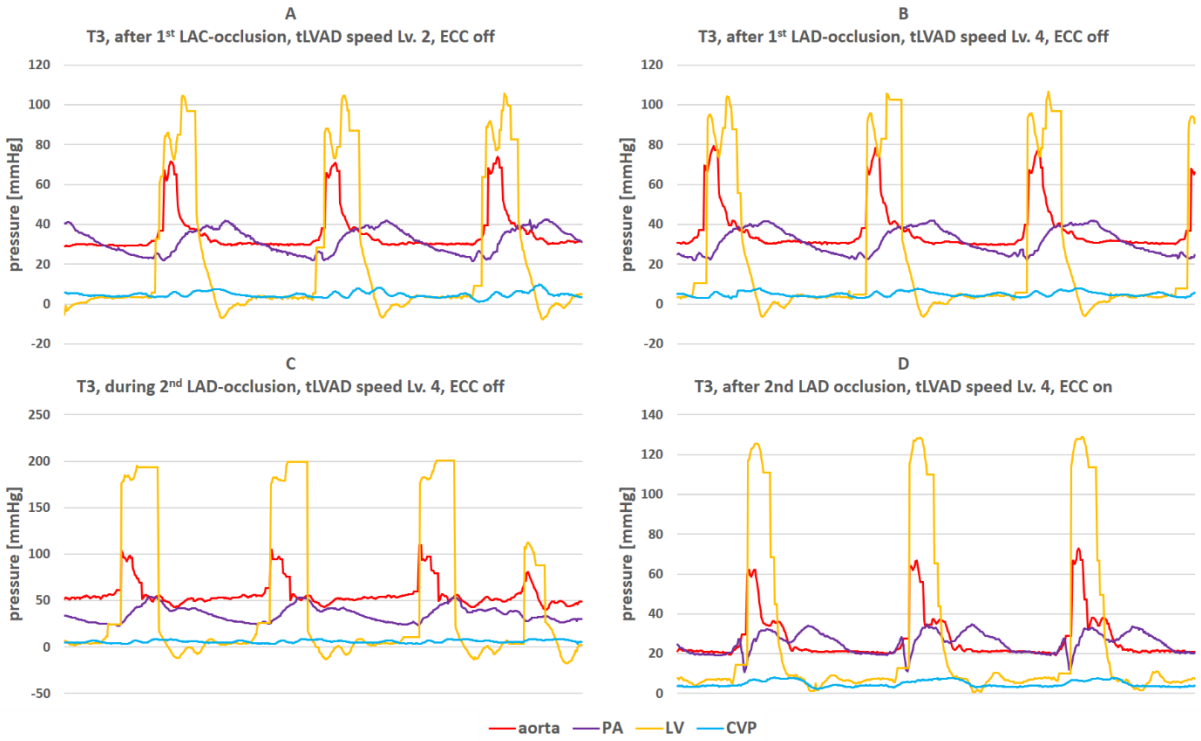


*Graph 9. Pressure curves at timepoint T3 for tLVAD without AVR. Panels A-D*
*Panel A: timepoint T3, after first LAD occlusion, tLVAD at level 2, ECC support off. Panel B: timepoint T3, after first LAD-occlusion, tLVAD at level 4, ECC support off. Panel C: timepoint T3, during second LAD-occlusion, tLVAD at level 4, ECC support off. Panel D: timepoint T3, after second LAD-occlusion, tLVAD at level 4, under partial ECC support. (Legend: aorta: aortic pressure; LV: left ventricular pressure; PA: pulmonary artery pressure; CVP: central venous pressure).*

To optimize the cardiac output and increase the LV unloading, the valve pump speed was increased to speed level 4. After initial drop of LV-filling with consecutive drop of LV pressure, and a less pulsatile aortic pressure curve, the hemodynamics improved within minutes. After 4 minutes on valve pump support at level 4, the aortic pressure pulsatility continued to be observed (Graph 9, Panel B). Hemodynamics stabilized, at average pressures of 59/112/40 mmHg (m/s/d) in aorta, 40/196/-24 mmHg (m/s/d) in LV, 35/55/22 mmHg (m/s/d) in PA, and CVP of 6 mmHg, and steady sinus rhythm of 95 bpm. The cardiac output increased to 7.4 L/min, which equivalents to CI of 4.93 $L \cdot min^{-1} \cdot m^{-2}$, and TPR of 638 $dyn \cdot sec \cdot cm^{-5}$. Echocardiographically, the stage one aortic regurgitation remained unchanged, and no mitral regurgitation and good fillings of the LV without septal suction. Pump presented no alarms, power remained stable at 9-10 Watt.

With stable hemodynamics, the second surgical induction of acute heart failure was performed via reapplying the LAD-occlusion (Graph 9 Panel C, Graph 10). For hemodynamic purposes, the aortic valve pump was kept at speed level 4, the power consumption remained stable at 9-10 Watt. No pump alarms and echocardiographically no septal suction was observed. Stage one aortic regurgitation was observed. Hemodynamically however, similarly as observed during first LAD occlusion, the systolic LV and systolic aortic pressures started decreasing (Graph 10), as a sign of impaired LV function.

The aortic pulsatility dropped, whilst maintaining a steady mean aortic pressure of 51 mmHg. The systolic LV pressure dropped for 141 mmHg, to 61 mmHg, equilibrating to the systolic aortic pressure. The systolic aortic pressure dropped for 52 mmHg, from 116 mmHg to 64 mmHg. Under valve pump support though, the mean aortic pressure, as well as pulmonary and venous hemodynamics remained stable, with average mean pressures of 53 mmHg in aorta, 32 mmHg in PA, and CVP of 6 mmHg, and sinus tachycardia at 110 bpm. The cardiac output decreased to 6.6 L/min, which equivalents to CI of 4.4 L· $min^{-1}$ · $m^{-2}$, and TPR of 618 dyn · sec · $cm^{-5}$.

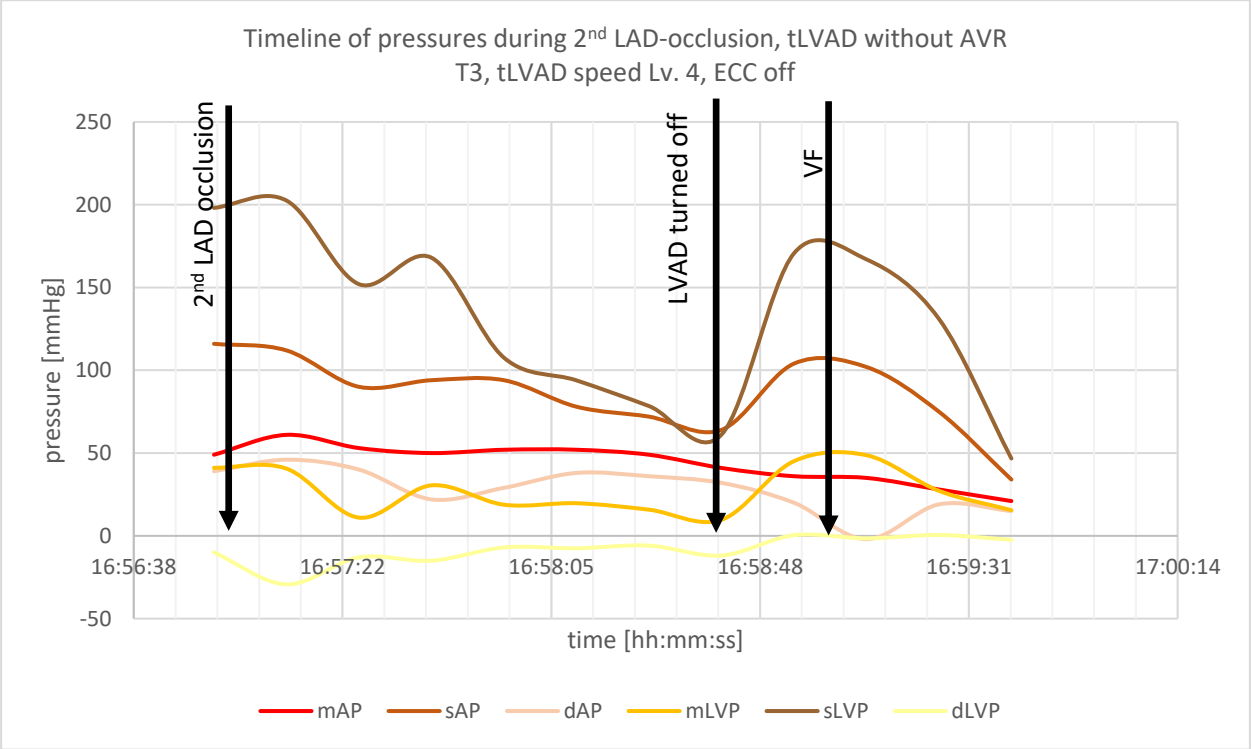


*Graph 10. Timeline of pressures during 2nd LAD-occlusion, timepoint T3, tLVAD without AVR*
*(Legend: mAP: mean aortic pressure; sAP: systolic aortic pressure; dAP: diastolic aortic pressure; mLVP: mean left ventricular pressure; sLVP: systolic left ventricular pressure; dLVP: diastolic left ventricular pressure)*

After 100 seconds since the induction of 2nd LAD occlusion, the aortic valve pump was turned off. Following the immediate initial increase in LV diastolic filling, the LV systolic pressure increased, followed by ventricular fibrillation 15 seconds after the aortic valve pump was turned off. The LAD occlusion was removed, the aortic valve pump was turned on to level 4, and the ECC support was fully reinstalled.

The LV function however did not recover, despite terminating the surgical occlusion of the LAD artery, under aortic valve pump support at level 4, as well as full ECC support (Graph 9, Panel D). We terminated the experiment, and euthanized the animal with intravenous systemic injection of pentobarbital and direct intracardiac injection of highly concentrated potassium.

# 5 Discussion

In advanced heart failure, mechanical circulatory support (MCS) devices have become a well-established treatment options. There are several classes of MCS devices, distinguished by hemodynamic characteristics of the pump, the sites from which blood is withdrawn and returned, the size of catheters and/or inflow and outflow conduits used, whether the insertion technique is percutaneous or surgical, whether the pump is intra-, para- or extracorporeal, and whether or not a gas exchange unit is used. Some devices are for short-term use, whereas others can be used for the duration of a patient's life. The aim of these devices is to improve the cardiac output, and reduce the ventricular load, but their specific features result in different overall hemodynamic effects.

While depending on the MCS used, the peak flow rates vary in average from 2.5 to 7.0 L/min. Depending on the etiology and mechanics of the heart failure, the circuit configurations may vary too, ranging from pumping from the right atrium (RA) or central vein to a systemic artery (i.e. ECLS/ECMO support), to pumping from the LV to a systemic artery (generally the aorta) in LVAD, or to pumping from RA or RV to pulmonary artery in RVAD. Flow rates and circuit configurations both have a major impact on their overall cardiac and systemic effects. Many other factors also affect the response to MCS, including: 1) the underlying pathology of the heart failure (e.g. ischemic, dilatative, restrictive or idiopathic cardiomyopathy (CMP)); 2) the acuteness of the heart failure (i.e., whether the patient has a prior history of chronic HF with a dilated, remodeled LV and/or RV, or whether it is a first event, with previously normal heart structure, thus acute HF); 2) the degree of acute ventricular recovery following initiation of MCS (e.g., potentially recoverable in some forms of acute coronary syndrome, but less likely recoverable with idiopathic cardiomyopathy); 3) right-sided factors, such as RV systolic and diastolic function and pulmonary vascular resistance; 4) the degree to which baro- and chemoreceptors are intact and can modulate vascular and ventricular properties; 5) concomitant medications, especially antiarrhythmics and catecholamines; and 6) metabolic factors, such as pH, lactate, $pO_2$, and $svO_2$ (mixed venous saturation), which, if corrected, could result in improved ventricular and vascular function. Finally, the characteristics of the pump (e.g., pulsatile, axial, or centrifugal flow) can also have an impact on several aspects of the hemodynamic responses to MCS.[68] [69]

It is therefore important to understand and distinguish between the direct hemodynamic effects of a device (i.e., the expected effects on pressures and flow in the absence of any change in native heart or vascular properties; e.g. direct increase of cardiac output generated by the device), and the resulting hemodynamic effects after accounting for the correction of secondary modulating factors following initiation of MCS (e.g. normalization of the end-organ dysfunction, as a result of increased cardiac output generated by the device). The response of a given patient to MCS must account for baseline preload, afterload, LV-contractility, and the flow rate of the MCS pump.

The minimalistic size and weight of the ventricular assist device specially designed to be placed transvalvularly through aortic (serving as LVAD) or pulmonary valve (serving as RVAD) is not a novel idea. First experimental setting with such blood pumps have been made in the early 90s (US Patent Number 5,888,241 by Jarvik in 1999[70]), and nowadays a short term transvalvular blood pump (e.g. Impella©, Hemopump©) is clinically used in patients presenting with either left- of right-sided acute heart failure.[49] The major limitation of the existing devices are however the durability, the short (and safe) support time, as well as the limitations associated the maximum pump flow of up to 5 L/min, as well as adverse events associated with higher flows (51.000 rpm at 5 L/min for Impella 5.0©) like hemolysis. As all percutaneous devices, they are intended for short-term support only. The investigated transvalvular VAD has the durable characteristics of its existing durable Jarvik LVADs. Similarly to other durable LVADs, it can reach mean flows of over 7 L/min.

The transvalvular VAD was adopted from the Jarvik 15mm© pediatric LVAD, and from the Jarvik 2000© Flowmaker adult LVAD, with combining the design of these pumps to the idea of positioning it through the aortic or pulmonary valve, thus providing LVAD or RVAD support, respectively.

As in each MCS device early in the development, the efficacy and safety of the medical product must be insured first. Before an extensive testing in a chronic animal model may proceed, the safety and efficacy in acute animal model needs to be tested. The animal model used, an adult pig weighing 90 and 100 kg, with estimated BSA of 1.58 and 1.5 m2, respectively, is a well-established animal model for the preclinical in vivo testing of novel MCS.

The animal model needed to correlate to humans in terms of anatomy and physiology of the heart and its main blood vessels. For this purpose two animal species most widely used as animal models in preclinical testing for novel MCS devices were evaluated. The inspected three calves weighing between 100-130 kg showed a short ascending aorta, and bicarotid truncus despite the larger size then in humans. With the transvalvular VAD ranging around 4 cm above the aortic anulus, we would risk a selective perfusion at the site of bifurcation, so implanting this transvalvular valve pump in calves was abandoned. A short ascending aorta should also represent an exclusion criterion for implantation of this valve. Similarly, implantation of this transvalvular pump in pulmonary position should be omitted in short pulmonary truncus of less then 4 cm above the pulmonary valve.

The six inspected porcine hearts showed a closer resemblance to humans, anatomically and in terms of size and mass. As the size of the heart and its main blood vessels in pigs correlates with its body mass, similar as in humans, adult pigs with body mass similar to an adult human patient was crucial. The inspected hearts were not weighed; however, the aortic anulus size in all hearts was between 19 and 23 mm, which correlates with size of the aortic anulus observed in most adult human patients of similar body mass. This led us to decision to use a 23mm size of the bioprosthetic aortic valve. The calculated BSA in both pigs was 1.51 $m^2$ in 100 kg pig, and 1.41 $m^2$ in 90 kg pig, using the adopted formula for adult farm pigs: $BSA = 0.0734 \times BW^{0.656}\ [kg]$.[71] This is slightly lower to the mean BSA of 1.71 m2 in adults,[72] using the commonly used Du Bois formula $BSA = 0.007184 \times BW^{0.425} \times BH^{0.725}$.

The transvalvular VAD was used as LVAD in aortic position in first and second animal model, and as RVAD in pulmonary position in second animal model. When concurrent native aortic valve replacement was performed in the first animal model, a 23 mm size aortic bioprosthetic aortic valve was used.

In our models, we did not observe any significant drops in hemoglobin throughout the duration of the experiment, as one of parameters typically decreasing in presence of hemolysis. The baseline lactate levels were high in both animal models. As the animals were healthy and had no signs of active infections, we were unable to explain these higher lactate levels. We did however observe a significant increase in lactate levels each time after weaning off the cardiopulmonary bypass. In all phases of experiments prior to induction of acute LV failure, the systemic hemodynamics remained stable, there were no oxygenation problems, and the support by vasoactive agents remained stable. As the surgery was not performed in mild hypothermia (normally around 34-32 °C), and during the cardiopulmonary bypass the systemic circulation was kept at mean aortic pressures of around 30-50 mmHg, we believe that the main reason for the increase in lactate levels was the possibly low microperfusion of the end-organs during these stages. The exact cause however remains unknown. The remaining blood results remained stable.

With the small size of 64 mm in length and 14 mm in outer diameter, the investigated VAD is on the smallest durable ventricular assist devices to this date, with the ability to fully unload the failing ventricle with flow of over 7 L/min.

The main LVAD related adverse events are major bleeding, major infection, major neurological dysfunction, device malfunction and pump thrombosis and hemolysis (MACCE). As the experiments were in acute setting, based to our experiments no statements on MACCE can be made at this point. Further investigations including chronic animal models are needed for further investigations.

## 5.1 Surgical feasibility

In the experiments we observed a smooth implantation of the transvalvular VAD without encountering any major surgical problems. With surgical implantation time at 25 min for both LVADs, and 15 min for RVAD, the simplicity of the surgical implantation is obvious. For the implantation of the transvalvular VAD in aortic position with replacement of the aortic valve, the ECC time was 167 min, in placement in aortic position without aortic valve replacement, and in implantation in pulmonary position, the ECC times were 145 min, and 62 min, respectively. The long ECC times are associated with A) world's first in vivo implantation of the device (and thus a lacking surgical pre-experience for this specific VAD), and B) the necessity to install the hemodynamic monitoring and perform regular cardiac output measurements and echocardiographic monitoring.

To avoid surgical problems, three crucial points need to be followed. Firstly, to position the transvalvular VAD through noncoronary aortic or anterior pulmonary cusp, respectively, whilst displacing the corresponding cusp between the pump and aortic or pulmonary wall. This step is crucial as a functional valve is detrimental. As sometimes observed in some LVAD patients, upon development of relevant aortic regurgitation under LVAD support, the shunting volume between the aorta and LV through aortic regurgitation may lead to severe deterioration of cardiac output and lead to further ventricular dilatation and pressure and volume overload, often resulting in pulmonary congestion and right-sided heart failure. As some patients present a relevant aortic regurgitation upon LVAD implantation, it is general consensus that it should be surgically addressed via aortic valve replacement with bioprosthetic valve at the time of LVAD implantation, to avoid the above stated problem.[73] For this purpose, a special bioprosthetic aortic valve was developed for the purpose of this study, with a special mounting mechanism for the transvalvular LVAD in the subvalvular apparatus of the valve – the device system termed prosthetic valve pump, or PVP. As the transvalvular LVAD can be mounted in this subvalvular apparatus simply via screwing it on the implanted bioprosthetic aortic valve until a click-tone is emitted, the implantation time of this method amounts mostly to the time of the surgical replacement of the aortic valve. Through this innovative principle, one can spare aortic crossclamp time in these severely ill patients, thus reducing the overall surgery time. The design of the prosthetic valve pump could be especially beneficial to selected patients with relevant aortic regurgitation (grade two aortic regurgitation or larger), with dilated cardiomyopathy and advanced heart failure.

Secondly, the transvalvular VAD needs to be fixated positioned carefully in its correct position. The orientation of the transvalvular pump should always be axial to the direction of the left or right ventricular outflow tract (LVOT/RVOT), to avoid injury to the ventricular septum, or to the anterior leaflet of the mitral valve, or to the tricuspid valve in RVAD, respectively. Great care must be given to avoid obstruction of the coronary arteries by the pump in left-ventricular setting. Also, in cases of severe hypertrophic septum, as seen in HOCM (hypertrophic obstructive cardiomyopathy), the obstructing subvalvular ventricular septal myocardium should be surgically resected (i.e. using the surgical myectomy by Morrow), to avoid later septal suctions. The transvalvular pump should be positioned through the aortic or pulmonary valve at its narrowest part. This allows for the valve cusps to open and close, as well as providing enough outflow area at annular level, to allow blood to be ejected through the aortic or pulmonary valve.

Thirdly, the transvalvular VAD needs to be fixated firmly in that position, using three or four fixating points: two thick non-resorbable sutures enhanced with Teflon pledges positioned around the pump at two marked points supraannularly, through the wall of the aorta or pulmonary truncus, respectively. The third fixating point is the driveline cable, which exits the aortic lumen at the initial aortotomy incision, which also needs to be fixated with non-resorbable sutures with Teflon pledges. Accordingly, it is positioned lastly, upon closure of the aorta. In case of transvalvular LVAD with concomitant aortic valve replacement, the fourth mounting point is in the subvalvular apparatus of the bioprosthetic valve, which is short in pig. A displacement or migration of the transvalvular VAD needs to be prevented in every way.

The surgical approach via median sternotomy allows for possible concomitant procedures, e.g. valve replacement or coronary artery bypass surgery. In theory, the transvalvular LVAD could be implanted in aortic position, with or without aortic valve replacement (AVR), through a mini sternotomy, as performed in minimally invasive AVR. Different than in other durable LVADs, as the transvalvular LVAD is positioned through the aortic valve, the aorta needs to be cross-clamped, and the heart needs to be arrested through cardioplegic solution. In patients with advanced HF however, arresting the heart in LVAD implantations in the LV apex is often omitted, through induction of ventricular fibrillation, as it was shown it reduces the myocardial oxygen consumption. With only 25 minutes of aortic cross-clamp time in both LVAD implantations however, the implantation time is significantly shorter then in LVAD implantations performed clinically. The implications however are unclear and need to be further investigated in chronical models. Furthermore, the classical implantation of durable LVADs in the LV-apex may allow, in very selected cases, and under specific considerations, the implantation of the LVAD without aortic crossclamp and without cardiopulmonary bypass. This technique cannot be applied in for the implantation of the investigated transvalvular LVAD.

For the implantation of the transvalvular RVAD in pulmonary truncus position, there are two possible implantation techniques. The VAD can be implanted in the pulmonary position without administering cardioplegia, on beating heart, however under bicaval cannulation and full ECC support while implanting the transvalvular RVAD. Through this technique, the right ventricle is fully unloaded. The other implantation technique is through administering the aortic cross-clamp and arresting the heart with cardioplegic solution. With surgical implantation time at 15 minutes, the overall stress on the myocardium is kept at a minimum. A two-stage venous cannula for the ECC may be used, however is not recommended as it may cause air blocks while pulmonary truncus is opened.

Upon following these principles, there was no septal suction observed at any phase of the experiment. There was no observed low-flow alarm, power consumption remained stable at all times. The inspection of the explanted transvalvular VAD upon termination of the experiments showed no signs of pump thrombosis. However, protamine was not administered during any of the experiments, and the in vivo time of the VAD was maximum 5 hours.

The major cardiovascular and cerebral events (MACCE), as well as other major adverse events in LVAD patients (major bleeding, major infection, driveline infection, device malfunctions, pump thrombosis, right-heart-failure) were not investigated, due to the acute design of the experiment.

## 5.2 Hemodynamics

To assess the hemodynamic properties under VAD support, the understanding of the physiological volume-pressure loop is crucial, which is determined by the end-systolic pressure-volume relationship (ESVPR) and end-diastolic pressure-volume relationship (EDPVR).[69]

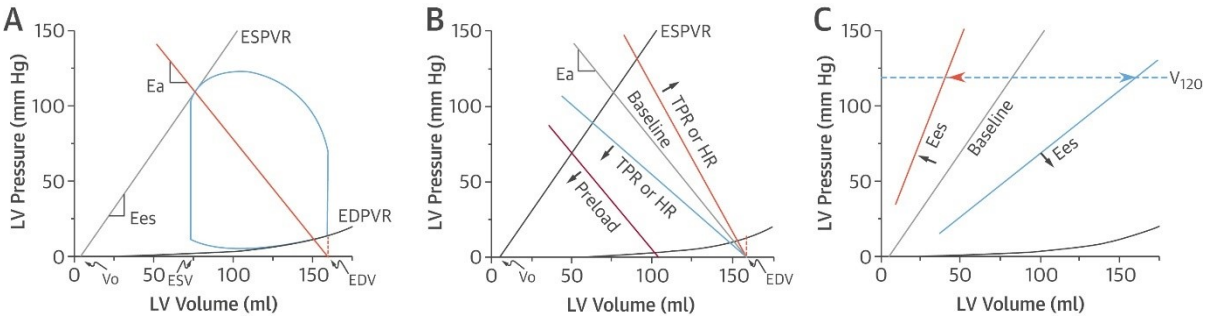


*Image 12. Overview of pressure-volume curves and its relations.*
*Panel A: normal pressure–volume loop (PVL), is bounded by the end-systolic pressure–volume relationship (ESPVR) and end-diastolic pressure–volume relationship (EDPVR). ESPVR correlates linearly with slope end-systolic elastance (Ees) and volume–axis intercept (Vo). Effective arterial elastance (Ea) is the slope of the line extending from the end-diastolic volume (EDV) point on the volume axis through the end-systolic pressure–volume point of the loop. Panel B: slope of the Ea line depends on total peripheral resistance (TPR) and heart rate (HR), and its position depends on EDV. Panel C: the ESPVR shifts with changes in ventricular contractility, which can be a combination of changes in Ees and Vo. ESV = end-systolic volume; LV = left ventricular. (Adopted and modified from [69])*

The preload can be defined as end-diastolic pressure (EDP), which relate to average myocardial sarcomere stretch. Afterload is determined by the hemodynamic properties of the vascular system against which the ventricle contracts, it is more simply indexed by total peripheral resistance (TPR), the ratio between mean pressure and flow. Afterload can also be depicted on the pressure–volume plane by the "effective arterial elastance" (Ea) line (Image 12, Panel A).[74] When TPR, heart rate, or preload volume changes, the Ea line changes accordingly (Image 12 Panel B). This construct is the basis of ventricular–vascular coupling, which describes how SV, MAP, and other key cardiovascular parameters are determined by preload, afterload, and contractility. When ESPVR changes, so does the ventricular contractility (Image 12, Panel C).[75] Increases and decreases in contractility are associated with leftward and rightward shifts of the ESPVR, respectively. The EDPVR is nonlinear and defines the passive diastolic properties of the ventricle. Clinically it correlates with the diastolic stiffness. Stiffness is the change in pressure for a given change in volume (dP/dV). The diastolic stiffness varies with filling pressure, increasing as EDP increases.[69]

In LVAD support, the continuous pumping of blood directly from the LV results in loss of the normal isovolumic periods. This transforms the PVL from its normal trapezoidal shape to a triangular shape (Image 13, Panel A).[69]

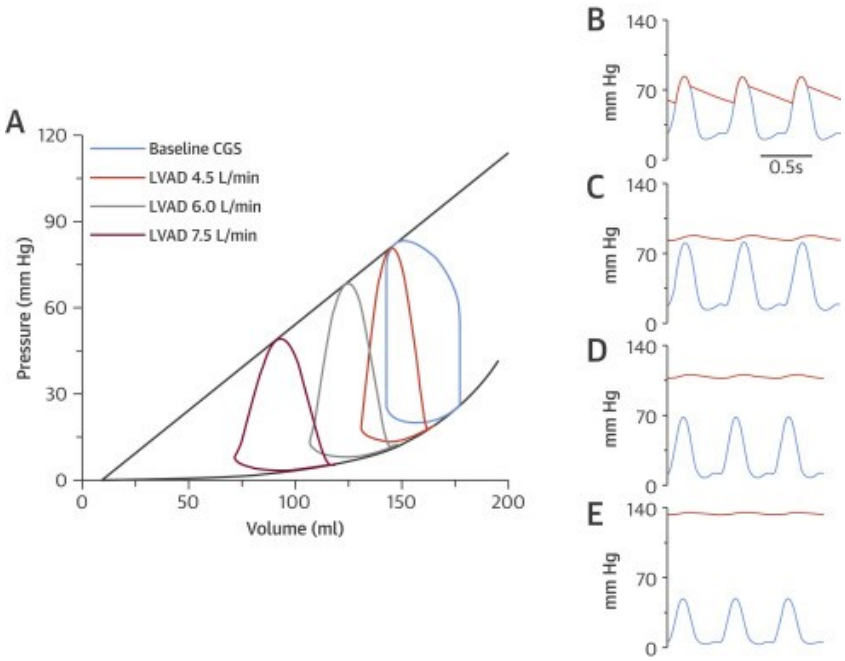


*Image 13. Ventricular effects of LV-MCS. Panels A-E.*
*Panel A: pressure-volume curve at LV-MCS pump-flows at 4.5, 6.0, and 7.5 L/min, respectively. Panels B-E: arterial (red) and left-ventricular (blue) pressure curves at different pump-flows, corresponding to the LV-unloading by the LV-MCS. (Adopted and modified from [69].)*

Unlike the other forms of support, removal of blood from the LV is not dependent on ejection through the aortic valve. As pump flow rate increases, the LV becomes increasingly unloaded (progressive leftward shifted PVL), and following the Frank-Starling mechanism, the systolic and diastolic LV pressure decreases, resulting in decreasing the myocardial oxygen consumption. Concurrently, arterial pressure increases, the aortic pulsatility decreases, and the mean aortic and systolic LV pressures become increasingly dissociated (Image 13; Panels B to E). This direct LV unloading also decreases the LA and wedge pressures, thus reducing the right ventricular afterload. However, through the increased cardiac output generated by the LVAD, there is an increased preload returning to the right ventricle through systemic circulation, thus increasing the myocardial stress to the right ventricle.

### 5.2.1 Transvalvular LVAD

In our models, we measured the pressures and the overall cardiac output. As the ventricular volume and flow was not directly measured, an exact comparison to the pressure volume loop discussed earlier cannot be fully made.

In both our LVAD models (with AVR and with native aortic valve), the observed hemodynamics were similar.

Upon LVAD support throughout the phases of the experiments the mean aortic as well as mean LV pressures dropped. Upon increase of the pump speed, the pump flow increased, resulting in increase of the cardiac output (CO). With the increase of the pump speed, we also observed a corresponding drop in LV pressures, with diastolic LV pressures sometimes falling to negative values, indicating passively an “under-pressure” in the LV through the LVAD. However, there were no septal suctions or LVAD low-flow alarms observed.

The LVAD was approximately 14 mm in outer diameter, resulting in surface area of 1.54 $cm^2$, the LVAD inflow diameter is 7 mm (resulting in inflow surface area 0.38 $cm^2$). The 23 mm bioprosthetic aortic valve has an outer diameter of 23 mm, resulting in surface area of approximately 4.15 $cm^2$. This means by definition there will be a certain obstruction of the outflow area due to the placed LVAD, thus presenting hemodynamically similar as aortic stenosis. This phenomenon was observed in both LVAD implantations – with and without aortic valve replacement (AVR).

In the case of concomitant AVR, the tLVAD produced aortic stenosis. When the LVAD was switched off, the observed mean transaortic gradient was 11 mmHg (and maximum systolic pressure gradient of 36 mmHg). Under all criteria, this is considered a low-grade aortic stenosis. During LVAD support, these pressure gradients decreased due to ventricular unloading by the LVAD. However, the increasing peak-to-peak systolic LV and aortic pressure gradient indicates the drop in produced peak LV-pressure with increasing LVAD speed, whilst maintaining a stable mean pressure gradient. This is important, as it is a secondary sign to an effective ventricular volume unloading, whilst allowing the ventricle to produce enough pressure to maintain a steady mean LV-pressure. In a transvalvular LVAD, the mean aortic gradient cannot be interpreted as in physiologic heart, as the blood pump is actively unloading the ventricle via continuous flow, and through the negative suction produced in the LV by the blood pump, the mean LV pressure drops. This phenomenon is observed in all continuous flow LVADs placed in the LV, as illustrated above. (Image 13, Panels B-E). At speed level 5 however, we observed a reversal of the mean and systolic aortic pressure gradients: 35 mmHg mean pressure gradient, and 11 mmHg aortic pressure gradient during systole. This however is due to an overall decrease of the LV filling and decrease of the LV preload (as the LVAD output increases), resulting in lower LV filing and LV contractility – according to the Frank-Starling mechnism.

In the animal model where the native aortic valve was not replaced but left in place, and the LVAD placed transaortically through the acoronary cusp, the hemodynamics observed were similar, however with significantly higher aortic pressure gradients. At baseline, when the LVAD was switched off, the mean transaortic pressure gradient was 9 mmHg, but the systolic pressure gradient was 64 mmHg. During LVAD support, the transaortic pressure gradients remained constant, despite the LV-unloading by the LVAD. While the mean aortic gradient remains low (technically a low-grade aortic stenosis), the systolic maximum aortic gradients indicate a severe aortic stenosis. Also, the LV pressure curves are flattened systolically, indicating the typical pressure phenomenon in the presence of aortic stenosis. This correlates to the typical pressure curve in LV measured invasively through left-side catheter in patients with severe aortic stenosis.[76]

What is unknown is whether the obstruction caused by the investigated transvalvular pump (tVAD) is caused only due to the cross-section area of the pump, or also due to the length of the entire pump, thus as a functional LVOT obstruction. The tVAD reaches about 3 cm inside the ascending aorta. Since the ascending aorta only measures about 4 cm in length from the aortic annulus to the first aortic branch in pigs (right subclavian artery), and since the porcine aortas are overall shorter than usually seen in humans, the tVAD pump fills out most of the volume of the ascending aorta – and in such creating an obstruction in the outflow tract. This obstruction could be regarded as a stenosis of the left-ventricular outflow tract, comparable to a stenosis of the aortic valve. In addition, it is plausible that pump reduces the Windkessel-effect through the volume taken by the pump.

The second animal model had a BSA of 0.1 $m^2$ lower then the first animal model (1.41 $m^2$ vs. 1.51 $m^2$). Echocardiographically, the aortic anular size was not determined preoperatively, it was the subjective opinion of the implanting surgeon that the aortic valve area was similar to that of the first animal model. However, no exact statement may be made whether the difference in systolic aortic pressure gradient is only due to difference in the aortic valve size (accordingly to the Hagen-Poisseuille law of hemodynamics; $\Delta P = \frac{8\mu LQ}{\pi R^4}$), or whether it is a mechanical obstruction problem present due to the positioning of the LVAD. Further investigations would be needed to further address this problem. It can be said though, that the presence of a severe aortic stenosis, of mechanical cause or other, is associated with detrimental decrease on the overall survival outcome. Such a high hemodynamic enddiastolic and midsystolic stress on the LV should not be present after LVAD implantation.

Another important factor to consider is the opening of the aortic valve. As the pump speed was steadily increased, the LV-pressure dropped accordingly due to the increased pump output resulting in enddiastolic decrease of the LV-preload. The observed phenomenon resulted in steady decrease of the LVEDP. If the LVEDP is below the diastolic aortic pressure, the aortic valve per definition cannot open. The opening of the aortic valve has prognostic values especially on a longer-term LVAD support. A non-opening aortic valve during LVAD support has been shown to be associated with development of aortic regurgitation, valve leaflet fusion, aortic root thrombosis, and gastrointestinal bleeding.[77 78 79 80 81 82]

In the animal model where the AVR was concurrently performed, the aortic valve continued opening during LVAD support until speed level 4 was reached. At speed levels 4 and 5 the aortic valve opening was only intermittently present during ILS phases. Importantly, there was no observed aortic regurgitation, indicating a functional aortic valve.

Thus the importance of the intermittend low speed mode (ILS mode), as it allows for recurrent decreases of the pump output and thus in those short phases increase in the LV filling, thus resulting in increased LVEDP and LV output. Echocardiographically, as the LVAD speed was increased, the LV-pressure decreased accordingly, due to increased output through the LVAD, and thus reducing the preload for the LV-output. Accordingly to the Frank-starling-mechanism, with decrease of preload of the LV, the LV output and contractility decrease. As the decrease of the preload decreases the LV wall stress, it also decreases the myocardial oxygen consumption. These intermittent ventricular fillings are important for the wash-out effect for the ventricular ejection, as well as for intermittent loading of the ventricle and thus its training, playing a role in possible ventricular recovery in a long-term support. When the ILS mode was switched off, this wash-out phenomenon was not observed at higher LVAD speeds. The effects however would need to be further investigated in chronic animal models.

In the animal model where only the LVAD was implanted without AVR, the aortic valve was opening at all speed modes under LVAD support. However, a major problem observed was the continuous presence of aortic regurgitation. Echocardiographically, the aortic regurgitation was only low-grade, however with reduced echocardiographic quality due to the shadowing by the pump. Hemodynamically however, the aortic pressure amplitudes remained high at all phases of the experiment, indicating the presence of a relevant aortic regurgitation. The diastolic aortic pressure averaged between 30 – 40 mmHg, during the baseline when the LVAD was switched off, as well as during all phases of LVAD support. The presence of relevant aortic regurgitation is associated with poor outcomes in LVAD patients. It means that with each cardiac cycle, a certain proportion of the aortic blood regurgitates to the LV, causing a continuous LV wall stress and volume overload. This also decreases the functional cardiac output, as a part of the ejecting volume is continuously regurgitating in the LV. The overall lower CO in this animal model compared to the animal model that underwent a concurrent AVR with resulting functional aortic valve corresponds to this. Furthermore, in the animal model without concurrent AVR, there was an observed functional severe aortic stenosis, if classified by the systolic aortic pressure gradient. This means that in latter animal model there was presence of functional severe aortic stenosis as well as relevant aortic regurgitation.

In both animal LVAD models, concurrent echocardiographic assessment on the mitral regurgitation and LV filling was performed at each stage of the experiments. In both animal models, we observed, parallel to the increase of the LVAD pump speed, a decrease of the LV pressure. Even negative LV pressures were observed at speed levels 4 and 5. Negative ventricular diastolic pressures are dangerous however, as the risk of ventricular or septal suction is greater. We observed the echocardiographic “kissing phenomenon” at speed levels 3 and 4 in the animal model with concurrent AVR, as sign of low LV-filling – within seconds later intermittent septal suctions were observed. The preload in a low flow alarm with septal suction was addressed with administering volume and decreasing the pump speed. Upon further increase of the pump speed, no further septal suctions were observed – indicating the importance of sufficient volume status of the animal. In the LVAD animal model where the AVR was not performed, the phenomenon of negative diastolic LV pressures was only briefly observed, and no septal suctions or low flow alarms were observed. This is mostly due to regurgitating volume through the insufficient aortic valve.

The hemodynamics of the right-sided heart system and the pulmonary circulation remained stable in both LVAD animal models. There was a minimum increase of the mean pulmonary pressure, correlating to the increase in LVAD speed and thus increase in the CO. With the increase of the LVAD speed, preload of the LV decreases, resulting in decrease of the pulmonary afterload. In addition, the cardiac output increases, thus resulting in increased preload for the right ventricle, hemodynamically correlating to increase in central venous pressure. As it is a feasibility study however, the animal models all had physiological biventricular cardiac function and anatomy prior to surgery, meaning the RV-function was not impaired. In the clinical setting however, patients who receive durable LVAD in advanced end-stage heart failure often have concurrent impairment of the RV-function with/without the presence of pulmonary hypertension. In such patients, an acute right-sided heart failure may occur upon increasing the RV-preload through the increased cardiac output by the implanted LVAD. As the RV-function was not impaired preoperatively, the RV failure did not occur.

The interpretation of the hemodynamic measurements during acute phases like during LAD occlusion, but also during weaning of ECC, is multifactorial and thus difficult to interpret. Amongst main factors are the titration of the catecholamine and other vasoactive agents, the external cardiac pacing, the speed of the weaning, and the level of LVAD support, as well as the pre- and afterload of the ventricles, also influenced by the presence or absence of functional aortic stenosis and/or regurgitation. However it is to be stressed out that the intravascular volume, the ventricular volumes (i.e. filling of the heart) as well as the afterload influenced by the constantly changing dosages of medications (catecholamine, amiodarone, lidocaine, etc.) were constantly changing. Especially during and after the LAD-occlusions the catecholamine support were very high and consequently all the parameters in this way modified. As a highly dynamic process therefore, further analyses of these variables would have to be performed on future animal models.

#### *5.2.1.1 Induction of acute heart failure by surgical LAD-occlusion*

The significant drop in CO as well as all pressures during LAD occlusion is an indicator of a successful induction of acute heart failure in the perfusion area distal to the occlusion (namely the septum and anterior LV wall), resulting in immediate impairment of the LV ejection fraction echocardiographically. In all phases of the experiments where LAD occlusion was performed, the heart switched to ventricular fibrillation followed by cardiac arrest within minutes. As the surgical ligation of the LAD artery is performed without concurrent measurements of the coronary flow before and after the occlusion, the severity and effectiveness of the LAD occlusion is subjective to the operating surgeon. Thus, the overall success of the occlusion is highly subjective. Furthermore, a complete and sudden occlusion of a major heart vessel on a prior healthy und non-preconditioned heart often results in sudden cardiac death, as the ventricle has no mechanisms to compensate. Therefore, a better option could be an indirect measurement of the coronary flow distal to the occlusion, allowing for more controlled and only partial occlusion of the vessel. Our surgeon has performed a complete occlusion of the mid-section of the LAD artery, and thus disrupting the blood flow distal to the occlusion. As the LAD occlusion resulted in ventricular fibrillation in all models, probably the LAD occlusion should ideally result in subtotal stenosis and high flow obstruction, but not a complete flow obstruction as induced in our models. This setting would require however a live measurement of the post-stenotic LAD flow.

During LAD occlusion, the LV systolic pressures dropped and the diastolic LV pressure increased, as a secondary sign of increased LV wall stress in a progressively distended LV due to sudden ligation of a major artery. The increased ventricular filling follows the Frank-Starling principle with initial increase in contractility, and thus increase in myocardial stress and oxygen consumption. As the main inflow of oxygen rich blood is impaired through the occluded artery, the progressively distended ventricle cannot cope for long. This mismatch between myocardial oxygen demand and supply results in cardiac shock, followed by VF and cardiac arrest.

Under the LVAD support however, a constant ventricular unloading is provided through the supporting LVAD. This further decreases the ventricular oxygen consumption, while maintaining sufficient output and systemic pressures. With increasing LVAD speed, the cardiac output increased accordingly. As a major part of the LV was deprived of oxygen through the LAD occlusion, the ventricular fibrillation occurred nonetheless. For the duration of LVAD support during LAD occlusion, the systemic hemodynamics remained stable.

### 5.2.2 Transvalvular RVAD

The feasibility of implanting the RVAD in pulmonary position was technically not challenging. In severely ill patients with right-sided heart failure, the investigated transvalvular RVAD through the pulmonary valve can be implanted without aortic crossclamping on a beating heart, under established cardiopulmonary bypass circulation, further decreasing the myocardial operative stress as well as the overall surgical time, and thus giving the possible advantage for use in high-risk patients. In our RVAD model, due to a first ever implantation and as a feasibility study, the implantation was performed in a crossclaped aorta and under full cardiopulmonary bypass, with nonetheless short implantation time of 15 minutes, and cardiopulmonary bypass time of 62 minutes.

Similarly as in the LVAD animal model where the valve replacement was not performed, the pulmonary valve was left in place. The right heart system with pulmonary circulation is a lower-pressure system compared to the systemic circulation. The pulmonary regurgitation after RVAD implantation was low-grade at most when the blood pump was switched off, and decreased accordingly to slight pulmonary regurgitation as the blood pump was turned on. The regurgitation remained stable throughout the experiment, also the remaining echocardiographic parameters observed no RV-filling problems or suction phenomenon. As the physiologic pulmonary circulation has lower pressure then the systemic circulation, the RV afterload is in general lower than the systemic one. As the pulmonary pressure is physiologically lower, the pulmonary valve needs to withstand lower pressure gradients, thus resulting in hemodynamically less functional pulmonary regurgitation.

Upon RVAD support throughout the phases of the experiments, the RV-unloading increased as the pump speed increased, with consecutive drop in RV-pressures. Correlating with the increase of the pump speed, the pulmonary pressure increased accordingly. At blood pump speed levels ≥ 2, the pulmonary artery pressure curve became non-pulsatile. This correlates to a functioning model for right ventricular support, with sufficient unloading of the RV, and sufficient cardiac output for the systemic hemodynamics to remain unchanged. The decrease in pulsatility correlates with the increased output by the RVAD. The non-pulsatility at lower speed levels indicated that in our RV-model, the pump flow needed for full unloading of the RV is lower than in the left-ventricular model.

As the pump speed decreased, the RV-unloading decreased, and the RVEDP increased. Differently than in LVAD animal model, the maximum systolic RV pressure never exceeded the diastolic pulmonary pressure. This is an indirect sign to successful RV-unloading by the RVAD, resulting in lower RV wall stress and lower RV myocardial consumption. No pulmonary edema was clinically observed, and no ventilation problems occurred, indicating a well-maintained pulmonary perfusion and oxygenation.

However, we observed a significant drop in pulmonary pressure, indicating either a significant decrease in the pulmonary resistance and severe pulmonary vasodilatation (which is unlikely at stable and unchanging systemic hemodynamics as well as unchanged respiratory parameters), or a significant decrease in the RV function. A significant increase in transpulmonary pressure gradient of around 25 mmHg was observed during phases of low speed level support of the RVAD, or when the RVAD support was not turned on. This indirectly suggests a pulmonary flow obstruction by the implanted RVAD, either in the right ventricular outflow tract (RVOT), or in the pulmonary truncus, or a combination of both. The mechanism is probably similar to the observed functional stenosis in tLVAD model, as described in Chapter 7.2.1. As a low pressure system, a mean transvalvular pressure gradient of 25 mmHg, especially in a chronic setting is likely associated with poor overall prognosis, as it significantly impairs the RV-function through increase of the RV-afterload, causing a volume overload. However, this was only observed under low RVAD support or under no RVAD support. Under sufficient RVAD support, the RV was continuously unloaded. However, this may present a problem in selected cases where the RV-function recovers sufficiently for the RVAD to be gradually weaned-off and explanted.

The systemic hemodynamics remained stable and unchanged during the entire duration of RVAD experiment. The cardiac output remained stable throughout the testing of the RVAD. It is to be taken into consideration that the RV function was not impaired prior to RVAD implantation, and that no induction of RV failure was performed. Thus, the RV had sufficient coping mechanisms to keep up with the increased RVEDP, right-ventricular maximum pressure and subsequent volume overload during low support of the RVAD or when it was switched off.

As the right heart failure has a greatly negative prognosis on the overall survival in heart failure patients, the right sided heart failure is not to be underestimated. While it is true that the majority of patients with advanced heart failure have a leading left-sided heart problem, and after LVAD implantation the end-organ perfusion increases due to pump flow, this sudden increase in “cardiac” output after LVAD implantation may result in an acute volume overload of the right ventricle, leading to increases of RV-preload, CVP, RVEDP, and RVEDV. In such patients, the main limitation often remains the impaired right-sided heart failure presenting with congestion and functional shortness of breath. For selected patients with biventricular heart failure, or for selective patients with isolated advanced right-sided heart failure and pulmonary hypertension, a selective RVAD support with less invasive RVAD through a small incision in the pulmonary truncus may potentiate the RV recovery or functionally unload the failing right ventricle. However, further investigations are needed before any such statements for the investigated transvalvular ventricular assist device may be made.

## 5.3 Implications for the future

Before any recommendations may be made, further investigations in acute and chronic heart failure animal models need to be made, to assess the feasibility as well as efficacy and patient safety for the transvalvular ventricular assist device, in long-term follow-up. Upon initial investigation described in this dissertation, there is a wide window of possibilities how and in what setting the described VAD may be further developed and used.

In selected patients who have either acute or chronic end-stage left-sided heart failure refractory to maximum medical therapy, and who also present with a significant aortic regurgitation, a concomitant aortic valve replacement is recommended by the current guidelines by Feldman et at in 2013.[83] In the investigated blood pump in the setting with concomitant aortic valve replacement, the transvalvular LVAD may be mounted in the subvalvular apparatus of the implanted valve. Thus, the aortic crossclamp time may be significantly reduced to the time necessary for the aortic valve implantation. Especially in marginal patients of INTERMACS stadiums 1 and 2, the operating time and aortic crossclamp time is aimed at being reduced to as short as possible during LVAD implants. These patients may benefit the most from the investigated blood pump.

The specially developed bioprosthetic valve with subvalvular apparatus (subvalvular screw locking device) for the transvalvular VAD to be mounted and secured in position could be developed further, also to allow possible detachment of the blood pump from the valve, allowing for an easy and quick explantation later, should the ventricular recovery occur.

A further implication for the future could be a less invasive transapical approach. The tri-leaflet tissue valve and a miniature VAD would be combined into a stented product, and implanted via transapical way through minimal thoracotomy at the left ventricular apex, with cable exiting the heart at the LV apex cannulation site. Particularly in the elderly patients and the ones too sick to undergo a cardiopulmonary bypass surgery, the advantage is the implantation of a valved LVAD without the use of cardiopulmonary bypass. A combined tri-leaflet tissue valve and a miniature VAD is inserted via a small incision in the apex through the transapical catheter approach and positioned under continuous transillumination and continuous x-ray into correct position by means of expandable stent fixation – thus a TAVR-LVAD.

Furthermore, the bioprosthetic valve could be modified to be placed percutaneously via specially modified transapical aortic valve replacement (TAVR). This would allow the LVAD to be implanted either surgically (as a two-stage-procedure following TAVR implantation), or percutaneously through transapical approach directly after TAVR implantation. As the device is 14 mm in outer diameter, the percutaneous approach would have to be performed through a surgical cutdown of the left subclavian artery with/without a end-to-side arm prosthesis (e.g. 16 mm Dacron® prothesis), or more likely, through a transapical approach.

A major problem for the percutaneous approach via surgical cutdown especially in mid- and long-term LVAD support is the limitation of the driveline cable. This cable could be tunneled subcutaneously from the vessel cannulation site, where it is secured and sealed to the vessel wall with pledged sutures, to the cutaneous exit site. This could also allow later explantation of the device without the necessity of median sternotomy and risks associated with reoperation, simply through a vessel dissection and stepwise explantation of the device.

Another possible limitation for the percutaneous approach could be the danger of a migration of the percutaneous stented valve, as the sheer wall stress on the aortic wall and aortic annulus may be significantly higher if the stented valve needs to hold the blood pump in place. A migration or dislocation either of the valve or of the blood pump would have detrimental effects and would most likely be associated with high mortality. A possible aspect of this problem is to develop special mounting mechanism that would fixate the transvalvular blood pump in the center of the intraluminal aortic space. Such could be achieved through a specially designed supravalvular stented mounting mechanism, as a special adaptation of the existing TAVR stented mechanism, for example with a self-expanding aortic wall stent. Such approach however could only implemented in selected patients that have no significant aneurysm of ascending aorta.

In selected patients with biventricular end-stage heart failure, the investigated device could be used as biventricular assist devices, concomitantly implanting LVAD, followed by the RVAD implantation. The best surgical approach in theory could be first the implantation of the LVAD in crossclamped aorta under full cardiopulmonary bypass, followed by aortic declamping, and then followed by RVAD implantation in a beating heart under partial cardiopulmonary bypass. This staged operative strategy would in theory shorten the aortic crossclamping time as well as the cardiopulmonary bypass time in these selected BiVAD implantation. However, no investigations have been performed to this date on the efficacy and safety of the BiVAD approach, and would need to be further investigated.

Another further development may be aimed at eliminating the driveline cable to implantable internal batteries, which could be recharged through transdermal transduction charging (i.e. TET-system – transcutaneous energy transfer), but further technological advancement needs to be made in this field before this technology becomes safe for patient use.

# 6 Conclusions

To conclude, patients with acute heart failure with cardiogenic shock, defined as the acute cardiac hemodynamic instability with end organ hypoperfusion resulting from a primary cardiac disorder[84], which is refractory to maximum medical therapy, should be evaluated for mechanical circulatory support. The short-term mechanical circulatory support devices may be used in selected cases where ventricular recovery is possible, or in acute critical setting with the purpose to stabilize the patient, allowing time to recovery or further therapy decisions.[85] Up to this date, many devices have been developed and are in clinical use today, the most frequently used being the intra-aortic balloon pump (IABP), extracorporeal membrane oxygenation (ECMO) and percutaneous short-term ventricular assist devices like Impella©.

The investigated device is a second generation axial continuous flow ventricular assist device, and is a miniaturized version of existing durable assist devices Jarvik 2000© Flowmaker LVAD and Jarvik 15mm© LVAD. It allows for a special implantation through the aortic or pulmonary valve, and potentiates a long-term support.

The investigated transvalvular ventricular assist device (tVAD) for mechanical circulatory support in end-stage heart failure, as LVAD or as RVAD was evaluated for the world's first in vivo implantation. For this purpose, two acute adult porcine animal models were used. The LVAD for left-sided heart support was positioned through the aortic valve in first and second animal model, and as RVAD in pulmonary position in second animal model. When concurrent native aortic valve replacement was performed in the first animal model, a 23 mm size aortic bioprosthetic aortic valve was used.

With the small size of 64 mm in length and 14 mm in outer diameter, the investigated VAD is on the smallest durable ventricular assist devices to this date, with the ability to fully unload the failing ventricle with flow of over 7 L/min. We could show the surgical feasibility for the implantation of the device as LVAD and as RVAD. No major surgical complications occurred, and no device failure or other technical device problems occurred throughout the duration of the experiments.

During the VAD support in both LVAD and in RVAD model, the cardiac output was sufficiently supported by the investigated assist device. The systemic hemodynamics remained stable during VAD support at speed level 2 or higher. At lower speed levels, the lower ventricular unloading by the VAD allowed for better ventricular output, however indicated the presence of relevant ventricular outflow tract obstruction by the implanted VAD in situ. Native aortic and pulmonary valves remained functional throughout the duration of the experiments. During induction of the acute left ventricular failure through surgical ligature of the left ascending coronary artery showed a significant deterioration of the left ventricular function. During this phase, the ventricular unloading by the LVAD assisted in maintaining stable systemic hemodynamics. Further investigations need to be made to further assess the postoperative outcomes, as well as the overall outcomes. In the short intraoperative setting, the expected operative safety and efficacy standards were met. However, further long-term investigations will be needed before any statements regarding the overall surgical safety, efficacy and feasibility for the investigated VAD can be made.

# 7 Acknowledgments

I would like to thank my mentor and dear friend professor Paolo Brenner for putting his trust and support in me to be a part of this exciting experimental project of the investigated novel device. I have initially approached Prof. Brenner after returning from the medical elective in a major LVAD center in Houston, Texas, as a young inexperienced but eager to learn medical student. Through his support and vision, I was able to become part of the surgical research team at the prestigious Walter Brendel Center for Experimental Medicine, including the work on the pig-to-baboon xenotransplantation project, led by the world renowned cardiac surgeon and professor emeritus Bruno Reichart. With group efforts, we were able to complete many projects, past and ongoing, and throughout the years he has provided me with innovative ideas, ever-present support and many constructive advices. Without his full support, these experiments, as well as many more would not have been possible.

In fact, the entire team at the Walter Brendel Center at LMU Campus Grosshadern in Munich has been ever-supporting throughout the years. I would like to condole my special and sincere thanks to colleagues Jan Michael Abicht, Matthias Längin and Sonja Güthoff for their continuous support for this project, and others. Especially in the past few years they have shown unprecedented support in the making of this dissertation, and were kind enough to provide me valuable and constructive advices and ideas throughout the years.

As mentioned above, many thanks go to professor Bruno Reichart, who has granted me his support throughout the years, and has supported me with his words of wisdom and advices since we met, 9 years ago. He was kind enough, together with everyone at the Walter Brendel Center, to have let me in their inner and professional circles, and have allowed me – through their vision and advices – to grow in so many ways. I would also like to express my deepest gratitude and appreciation to professor of cardiac surgery and department head Christian Hagl, who has supported me with his trust and honest advices regarding this project and beyond throughout the years, and continues to do so.

My very deepest gratitude and appreciation goes to my mentor, trusted friend and colleague professor Igor Gregoric, chief of cardiac surgery at Memorial Hermann Hospital at the world-renowned Texas Medical Center. Ever since we first met at your lecture so many years ago, when I was still a high school student, you have blessed me with your fullest support and honest advices in all my steps towards fulfilling my dream as a cardiac surgeon, and you continue to do so. It is difficult to sum up in words the magnitude of appreciation I have towards your trust, support, and belief in me, when you have supported me as your protégé throughout the years. In regards to this project, I sincerely thank you for sharing your in-depth understanding in the field of experimental testing of novel ventricular assist devices on large animal models, through your decades long experience at the world renowned Texas Heart Institute and your joint work in the field of mechanical circulatory support with Dr. Bud Frazier.

I would also like to thank Dr. Robert Jarvik for choosing the institution as world's first to investigate the developed blood pump, and for giving us his professional and personal trust to perform the experiments.

A special appreciation goes to my teacher and mentor, professor Thierry Carrel, chief of cardiac surgery at the University Hospital Bern, who has given me the opportunity to train under his direct supervision as a young resident in cardiac surgery for all these years. Writing this work was not an easy task, since we all have to dedicate all our time and efforts to the treatment of our patients. Sometimes in late hours we then occupy ourselves with various ongoing research projects, and in the end not much time is left for the completion of this dissertation. I thank you from my heart for all your support and patience throughout this time.

Last but not least, I would like to show my greatest and most sincere gratitude to my entire family, but especially to my mom, and foremost to my beloved partner for showing me your everlasting support in all the steps of my life, and through the entire medical studies and during completion of this thesis. Thank you for simply being there whenever I need you the most. In moments of joy and sorrow alike, in times of great stress and exertion, you have continued to enrich me with your presence, belief and love. This work is dedicated to you, and without you, none of this would have been possible.

# 8 Appendix

## 8.1 List of Abbreviations

| | |
|---|---|
| ACC | American College of Cardiology |
| AHA | American Heart Association |
| AHF | advanced heart failure |
| AKI | acute kidney injury |
| AP | arterial pressure |
| AVR | aortic valve replacement |
| BiVAD | biventricular assist device |
| BSA | body surface area |
| BTT | bridge to transplant |
| BR | bridge to recovery |
| CAD | coronary artery disease |
| CI | cardiac index |
| CO | cardiac output |
| CMP | cardiomyopathy |
| CPB | cardiopulmonary bypass |
| CRT | cardiac resynchronization therapy |
| DT | destination therapy |
| ECC | extracorporeal circulation |
| ECMO | extracorporeal membrane oxygenation |
| EDPVR | enddiastolic pressure-volume relationship |
| ESVPR | endsystolic pressure-volume relationship |
| HF | heart failure |
| HOCM | hypertrophic obstructive cardiomyopathy |
| ICD | implantable cardioverter-defibrillator |
| ILS | intermittent low speed |
| LAD | left anterior descending artery |
| LV | left ventricle |
| LVAD | left ventricular assist device |
| LVEDP | left ventricular enddiastolic pressure |
| LVESP | left ventricular endsystolic pressure |
| LVOT | left ventricular outflow tract |
| LVP | left ventricular pressure |
| MAP | mean arterial pressure |
| MACCE | major adverse cardiovascular and cerebral events |
| MCS | mechanical circulatory support |
| MI | myocardial infarction |
| MOF | multi-organ failure |
| NYHA | New York Heart Association |
| PA | pulmonary artery |
| PAP | pulmonary artery pressure |
| PCWP | pulmonary capillary wedge pressure |
| PVR | pulmonary valve replacement |
| RV | right ventricle |
| RVAD | right ventricular assist device |
| RVEDP | right ventricular enddiastolic pressure |
| RVESP | right ventricular endsystolic pressure |
| RVOT | right ventricular outflow tract |
| RVP | right ventricular pressure |
| tLVAD | transvalvular left ventricular assist device |
| tRVAD | transvalvular right ventricular assist device |
| tVAD | transvalvular ventricular assist device |
| TAH | total artificial heart |
| TIA | transitory ischemic attack |
| TPR | total peripheral resistance |
| VAD | ventricular assist devic |

## 8.2 Index of Images

Image 1. Jarvik 7 total artificial heart (TAH). ..... 4
Image 2. Dr. Robert Jarvik holding the Jarvik 2000 Flowmaker LVAD in a heart model ..... 4
Image 3. Jarvik 2000© Flowmaker LVAD compared to a standard AA battery ..... 8
Image 4. Jarvik 15 mm© LVAD and Jarvik 2000© Flowmaker LVAD compared in size ..... 9
Image 5. Components of the Jarvik 2000© Flowmaker LVAD system. ..... 9
Image 6. Jarvik 2000© Flowmaker LVAD. ..... 10
Image 7. Image 2. Schematic illustration on the placement of Impella for left-sided ventricular support. ..... 12
Image 8. The basic design of the investigated transvalvular VAD. Panels a and b. ..... 14
Image 9. Positioning of the investigated transvalvular VAD in aortic position in a three-dimensional illustration. 16
Image 10. Evaluation of ex-vivo bovine hearts; a-f. ..... 21
Image 11. Evaluation of porcine ex-vivo hearts. a-i. ..... 22
Image 12. Overview of pressure-volume curves and its relations. ..... 52
Image 13. Ventricular effects of LV-MCS. Panels A-E. ..... 53

## 8.3 Index of Graphs

Graph 1. tLVAD with AVR. Pressure curves at baseline ..... 29
Graph 2. tLVAD with AVR. Timeline of pressures after increase to level 3, T1, tLVAD at level 3. ..... 30
Graph 3. Pressure curves at timepoints T0-T3 for tLVAD with AVR, Part I, Panels A-H. ..... 33
Graph 4. Pressure curves at timepoints T0-T3 for tLVAD with AVR, Part II, Panels I-P. ..... 34
Graph 5. Timeline of pressures during LAD-occlusion, timepoint T3, tLVAD with AVR ..... 36
Graph 6. Pressure curves at timepoints T0-T1 for tRVAD without PVR. Panels A-D. ..... 38
Graph 7. Pressure curves at timepoints T0-T1 for tLVAD without AVR. Panels A-F. ..... 42
Graph 8. Timeline of pressures during 1st LAD-occlusion, timepoint T3, tLVAD without AVR ..... 44
Graph 9. Pressure curves at timepoint T3 for tLVAD without AVR. Panels A-D ..... 45
Graph 10. Timeline of pressures during 2nd LAD-occlusion, timepoint T3, tLVAD without AVR ..... 46

## 8.4 Index of Tables

Table 1. Speed and flow characteristics of the investigated transvalvular VAD ..... 15
Table 2. Intraoperative parameters assessed at timepoints baseline, T0, T1, T2, T3, T4 ..... 28

## 8.5 Index of Publications

None.

## 8.6 “Eidesstattliche Versicherung”

# Eidesstattliche Versicherung

Mihalj Maks
(Name, Vorname)

Ich erkläre hiermit Eides statt,

dass ich die vorliegende Dissertation mit dem Titel

*“Novel transvalvular ventricular assist device (VAD) as new surgical treatment strategy in acute terminal heart failure, as LVAD or RVAD, in acute adult porcine models – initial experiences”*

selbständig verfasst, mich außer der angegebenen keiner weiteren Hilfsmittel bedient und alle Erkenntnisse, die aus dem Schrifttum ganz oder annähernd übernommen sind, als solche kenntlich gemacht und nach ihrer Herkunft unter Bezeichnung der Fundstelle einzeln nachgewiesen habe.

Ich erkläre des Weiteren, dass die hier vorgelegte Dissertation nicht in gleicher oder in ähnlicher Form bei einer anderen Stelle zur Erlangung eines akademischen Grades eingereicht wurde.

Bern, den 26.06.2021 _____MAKS MIHALJ____
(Ort, Datum) (Unterschrift Doktorand)

# 9 References


[1] Go AS, Mozaffarian D, Roger VL, et al. Executive summary: heart disease and stroke statistics – 2013 update, a report from the American heart association. Circualation. 2013;127:143-52.

[2] McMurray JJ, Petrie MC, Murdoch DR, et al. Clinical epidemiology of heart failure: public and private health burden. Eur Heart J. 1998;19(Suppl P) P9-16.

[3] Djousse L, Driver JA, Gaziano JM. Relation between modifiable lifestyle factors and lifetime risk of heart failure. JAMA, 302 (2009), pp. 394-400

[4] Dornquast C, Kroll LE, Neuhauser HK, et al. Regional Differences in the Prevalence of Cardiovascular Disease. Dtsch Arztebl Int. 2016 Oct 21;113(42):704-711. doi: 10.3238/arztebl.2016.704.

[5] Roger VL, Weston SA, Redfield MM, et al. Trends in heart failure incidence and survival in a community-based population. JAMA, 292 (2004), pp. 344-350

[6] Loehr LR, Rosamond WD, Chang PP, et al. Heart failure incidence and survival (from the Atherosclerosis Risk in Communities study). Am J Cardiol, 101 (2008), pp. 1016-1022

[7] Ammar KA, Jacobsen SJ, Mahoney DW, et al. Prevalence and prognostic significance of heart failure stages: application of the American College of Cardiology/American Heart Association heart failure staging criteria in the community. Circulation, 115 (2007), pp. 1563-1570

[8] Krumholz HM, Merrill AR, Schone EM, et al. Patterns of hospital performance in acute myocardial infarction and heart failure 30-day mortality and readmission. Circ Cardiovasc Qual Outcomes, 2 (2009), pp. 407-413

[9] Go AS, Mozaffarian D, Roger VL, et al. Heart disease and stroke statistics–2013 update: a report from the American Heart Association. Circulation, 127 (2013), pp. e6-245

[10] Fonarow GC, Stough WG, Abraham WT, et al. Characteristics, treatments, and outcomes of patients with preserved systolic function hospitalized for heart failure: a report from the OPTIMIZE-HF Registry. J Am Coll Cardiol, 50 (2007), pp. 768-777.

[11] Jessup M, Brozena S. Heart failure. N Engl J Med 2003;348:2007-18

[12] Hunt SA, Abraham WT, Chin MH, et al. 2009 Focused update incorporated into the ACC/AHA 2005 guidelines for the diagnosis and management of heart failure in adults: a report of the American College of Cardiology Foundation/American Heart Association Task Force on Practice Guidelines. J Am Coll Cardiol, 53 (2009), pp. e1-e90

[13] The Criteria Committee of the New York Heart Association. Nomenclature and criteria for diagnosis of diseases of the heart and great vessels (9th edition), Little & Brown, Boston, Mass (1994)

[14] Braunwald E. Heart Disease: A Textbook of Cardiovascular Medicine. Fifth. Philadelphia, PA: WB Saunders Company; 1997. pp. 783–801.

[15] Jessup M, Abraham WT, Casey DE, et al. 2009 focused update: ACCF/AHA Guidelines for the Diagnosis and Management of Heart Failure in Adults: a report of the American College of Cardiology Foundation/American Heart Association Task Force on Practice Guidelines: developed in collaboration with the International Society for Heart and Lung Transplantation. Circulation. 2009 Apr 14; 119(14):1977-2016.

[16] Richardson P, McKenna W, Bristow M, et al. Report of the 1995 World Health Organization/International Society and Federation of Cardiology Task Force on the Definition and Classification of Cardiomyopathies. Circulation, 93 (1996), pp. 841-842

[17] Maron BJ, Towbin JA, Thiene G, et al. Contemporary Definitions and Classification of the Cardiomyopathies; An American Heart Association Scientific Statement From the Council on Clinical Cardiology, Heart Failure and Transplantation Committee; Quality of Care and Outcomes Research and Functional Genomics and Translational Biology Interdisciplinary Working Groups; and Council on Epidemiology and Prevention. Circulation. 2006;113:1807-1816.

[18] Remme WJ, Swedberg K. Comprehensive guidelines for the diagnosis and treatment of chronic heart failure. Task force for for the diagnosis and treatment of chronic heart failure of the European society of cardiology. Eur J Heart Fail. 2002;4:11-12.

[19] Hunt SA, Frazier OH. Mechanical circulatoy support and cardiac transplantation. Circulation. 1998;97:2079-2090.

[20] Lund LH, Khush KK, Cherikh WS, et al. The Registry of the International Society for Heart and Lung Transplantation: Thirty-fourth Adult Heart Transplantation Report—2017; Focus Theme: Allograft ischemic time. The Journal of Heart and Lung Transplantation, Vol 36, No 10, October 2017. http://dx.doi.org/10.1016/j.healun.2017.07.019

[21] Rose EA, Gelijns AC, Moskowitz AJ, et al. Randomized Evaluation of Mechanical Assistance for the Treatment of Congestive Heart Failure (REMATCH) Study Group. N Engl J Med. 2001 Nov 15; 345(20):1435-43.

[22] https://www.eurotransplant.org/cms/index.php?page=annual_reports

[23] Fauci AS. Harrisons innere Medizin. McGraw-Hill, London.

[24] Herold G. 2013. Innere Medizin 2014. Herold Gerd, Köln.

[25] Stewart GC, Givertz MM. Mechanical circulatory support for advanced heart failure: patients and technology in evolution. Circulation 2012;125:1304–1315.

[26] Lietz K, Miller LW. Patient selection for left-ventricular assist devices. Curr Opin Cardiol 2009;24:246–251.

[27] Giridharan GA, Lee TJ, Ising M et al. Miniaturization of mechanical circulatory support systems. Artif Organs 2012;36:731–739.

[28] Starling RC, Moazami N, Silvestry SC, et al. Unexpected abrupt increase in left ventricular assist device thrombosis. N Engl J Med. 2014 Jan 2; 370(1):33-40.

[29] Maltais S, Kilic A, Nathan S, et al. PREVENT Study Investigators. PREVENtion of HeartMate II Pump Thrombosis Through Clinical Management: The PREVENT multi-center study. J Heart Lung Transplant. 2017 Jan; 36(1):1-12.

[30] Jessup M, Brozena S. Heart Failure. N Engl J Med 2003;348:2007-18

[31] Rose EA, Gelijns AC, Moskowitz AJ, et al., for the Randomized Evaluation of Mechanical Assistance for the Treatment of Congestive Heart Failure (REMATCH) Study Group. Long-Term Use of a Left Ventricular Assist Device for End-Stage Heart Failure. N Engl J Med 2001; November 15, 2001. 345:1435-1443. DOI: 10.1056/NEJMoa012175

[32] Kirklin JK, Naftel DC, Kormos RL, et al. Seventh INTERMACS annual report: 15,000 patients and counting. J Heart Lung Transplant. 2015;34:1495–1504

[33] Mehra MR, Goldstein DJ, Uriel N, et al. MOMENTUM 3 Investigators. Two-Year Outcomes With a Magnetically Levitated Cardiac Pump in Heart Failure. N Engl J Med, 378 (15), 1386-1395 2018 Apr 12.

[34] Morgan JA, Brewer RJ, Nemeh HW, et al. Stroke while on long-term left ventricular assist device support: incidence, outcome, and predictors.ASAIO J. 2014; 60:284–289. doi: 10.1097/MAT.0000000000000074

[35] Bashir J, Legare JF, Freed DH, et al. Multicentre Canadian experience with the HeartWare ventricular assist device: concerns about adverse neurological outcomes.Can J Cardiol. 2014; 30:1662–1667. doi: 10.1016/j.cjca.2014.07.746.

[36] Roever L, Resende ES, Mehra MR. Vulnerable Brain and Ventricular Assist Devices. Stroke. 2016 Nov;47(11):2677-2678.

[37] https://www.jarvikheart.com/products/duration-of-support/ accessed on June 3rd 2019.

[38] Jarvik R, Scott V, Morrow M, et al. Belt worn control system and battery for the percutaneous model of the Jarvik 2000 Heart. Artif Organs, 23 (1999), pp. 487-489

[39] Siegenthaler MP, Martin J, Gutwald R, et al. Anterior approach to implant the Jarvik 2000 with retroauricular power supply. Ann Thorac Surg. 2005 Aug;80(2):745-7. Doi:10.1016/j.athoracsur.2004.02.117

[40] Brenner P, Wirth TJ, Liebermann A, et al. First Biventricular Jarvik 2000 Implants (Retroauricular Version) Via a Median Sternotomy. Exp Clin Transplant. 2016 Apr;14(2):215-23. doi: 10.6002/ect.2015.0053.

[41] Jarvik Heart, I., 333 West 52nd Street, 10019 New York. “User Manual Guide” The Jarvik 2000; Version March 2009.

[42] Burzotta F, Trni C, Doshi SN, et al. Impella ventricular support in clinical practice: Collaborative viewpoint from a European expert user group. Int J Cardiology. Volume 201, 15 December 2015, Pg 684-691. https://doi.org/10.1016/j.ijcard.2015.07.065

[43] Rihal CS, Naidu SS, Givertz MM, et al. 2015 SCAI/ACC/HFSA/STS Clinical Expert Consensus Statement on the Use of Percutaneous Mechanical Circulatory Support Devices in Cardiovascular Care (Endorsed by the American Heart Association, the Cardiological Society of India, and Sociedad Latino Americana de Cardiologia Intervencion; Affirmation of Value by the Canadian Association of Interventional Cardiology-Association Canadienne de Cardiologie d'intervention). J Card Fail. 2015; 21(6):499–518. [PubMed: 26036425]

[44] O'Neill WW, Schreiber T, Wohns DH, et al. The current use of Impella 2.5 in acute myocardial infarction complicated by cardiogenic shock: results from the USpella Registry. J Interv Cardiol. 2014; 27(1):1–11.

[45] Lauten A, Engstrom AE, Jung C, et al. Percutaneous left-ventricular support with the Impella-2.5assist device in acute cardiogenic shock: results of the Impella-EUROSHOCK-registry. Circ Heart Fail. 2013; 6(1):23–30.

[46] Cheng JM, den Uil CA, Hoeks SE, et al. Percutaneous left ventricular assist devices vs. intra-aortic balloon pump counterpulsation for treatment of cardiogenic shock: a meta-analysis of controlled trials. Eur Heart J. 2009; 30(17):2102–2108.

[47] Seyfarth M, Sibbing D, Bauer I, et al. A randomized clinical trial to evaluate the safety and efficacy of a percutaneous left ventricular assist device versus intra-aortic balloon pumping for treatment of cardiogenic shock caused by myocardial infarction. J Am Coll Cardiol. 2008; 52(19):1584–1588.

[48] Thiele H, Sick P, Boudriot E, et al. Randomized comparison of intra-aortic balloon support with a percutaneous left ventricular assist device in patients with revascularized acute myocardial infarction complicated by cardiogenic shock. Eur Heart J. 2005; 26(13):1276–1283.

[49] Stretch R, Sauer CM, Yuh DD, Bonde P. National trends in the utilization of short-term mechanical circulatory support: incidence, outcomes, and cost analysis. J Am Coll Cardiol. 2014; 64(14): 1407–1415.

[50] Monreal G, Sherwood L, Sobieski MA, et al. Large Animal Models for Left Ventricular Assist Device Research and Development. ASAIO Journal. 60(1):2-8, January/February 2014. DOI: 10.1097/MAT.0000000000000005

[51] Weaver ME, Pantely GA, Bristow JD, Ladley HD: A quantitative study of the anatomy and distribution of coronary arteries in swine in comparison with other animals and man. Cardiovasc Res 20: 907–917, 1986.

[52] Sahni D, Kaur GD, Jit H, et al. Anatomy and distribution of coronary arteries in pig in comparison with man. Indian J Med Res 127: 564–570, 2008.

[53] Hill AJ, Iazzio PA. Comparative Cardiac Anatomy, in Iaizzo PA (ed.), Handbook of Cardiac Anatomy, Physiology, and Devices. New York, Springer, 2009.

[54] Michaelsson M, Ho SY. Introduction: Normal hearts—A comparison, in Michaelsson M, Ho SY (eds), Congenital Heart Malformations in Mammals. London, Imperial College Press, 2000

[55] Tuzun E, Narin C, Gregoric ID, et al. Ventricular assist device outflow-graft site: effect on myocardial blood flow. J Surg Res 171: 71–75, 2011.

[56] Naimark WA, Lee JM, Limeback H, et al. Correlation of structure and viscoelastic properties in the pericardia of four mammalian species. Am J Physiol 263(4 pt 2): H1095–H1106, 1992.

[57] Sands MP, Rittenhouse EA, Mohri H, et al. An anatomical comparison of human pig, calf, and sheep aortic valves. Ann Thorac Surg 8: 407–414, 1969.

[58] Crick SJ, Sheppard MN, Ho SY, et al. Anatomy of the pig heart: Comparisons with normal human cardiac structure. J Anat 193 (pt 1): 105–119, 1998

[59] Farrar DJ, Bourque K, Dague CP, et al. Design features, developmental status, and experimental results with the HeartMate III centrifugal left ventricular assist system with a magnetically levitated rotor. ASAIO J 53: 310–315, 2007

[60] Slaughter MS, Giridharan GA, Tamez D, et al: Transapical miniaturized ventricular assist device: Design and initial testing. J Thorac Cardiovasc Surg 142: 668–674, 2011

[61] Shinbane JS, Wood MA, Jensen DN, et al. Tachycardia-induced cardiomyopathy: A review of animal models and clinical studies. J Am Coll Cardiol 29: 709–715, 1997

[62] Bartoli CR, Giridharan GA, Litwak KN, et al: Hemodynamic responses to continuous versus pulsatile mechanical unloading of the failing left ventricle. ASAIO J 56: 410–416, 2010

[63] Litwak KN, McMahan A, Lott KA, et al. Monensin toxicosis in the domestic bovine calf: A large animal model of cardiac dysfunction. Contemp Top Lab Anim Sci 44: 45–49, 2005

[64] Bartoli CR, Sherwood LC, Giridharan GA et al. Bovine model of chronic ischemic cardiomyopathy: implications for ventricular assist device research. ASAIO J 59: 221–229, 2013

[65] Schmitto JD, Mokashi SA, Lee LS, et al. A novel, innovative ovine model of chronic ischemic cardiomyopathy induced by multiple coronary ligations. Artif Organs 34: 918–922, 2010

[66] Siefert AW, Rabbah JP, Koomalsingh KJ, et al. In vitro mitral valve simulator mimics systolic valvular function of chronic ischemic mitral regurgitation ovine model. Ann Thorac Surg 95: 825–830, 2013

[67] Yoshitake I, Hata M, Sezai A, et al. The effect of combined treatment with Impella(®) and landiolol in a swine model of acute myocardial infarction. J Artif Organs 15: 231–239, 2012

[68] Moazami N, Fukamachi K, Kobayashi M, et al. Axial and centrifugal continuous-flow rotary pumps: a translation from pump mechanics to clinical practice. J Heart Lung Transplant, 32 (2013), pp. 1-11

[69] Burkhoff D, Sayer G, Doshi D, et al. Hemodynamics of Mechanical Circulatory Support. JACC, Volume 66, Issue 23, 15 December 2015, Pages 2663-2674. https://doi.org/10.1016/j.jacc.2015.10.017

[70] Jarvik R. Cannula pumps for temporary cardiac support and methods of their application and use. United States Patent, Nr. 5,888,241. Date Mar 30, 1999.

[71] Swindle MM, Makin A, Herron J, et al. Swine as Models in Biomedical Research and Toxicology Testing. Veterinary Pathology 49(2) 344-356. The American College of Veterinary Pathologists 2012. doi: 10.1177/0300985811402846

[72] Sacco JJ, Botten J, Macbeth F, et al. The Average Body Surface Area of Adult Cancer Patients in the UK: A Multicentre Retrospective Study. PLoS One. Jan 28, 2010; 5(1): e8933. doi: 10.1371/journal.pone.0008933

[73] Feldman D, Pamboukian SV, Teuteberg JJ, et al. The 2013 International Society for Heart and Lung Transplantation Guidelines for mechanical circulatory support: Executive summary. The Journal of Heart and Lung Transplantation. Volume 32, Issue 2, February 2013, Pages 157-187. https://doi.org/10.1016/j.healun.2012.09.013

[74] Sunagawa K, Maughan WL, Burkhoff D, et al. Left ventricular interaction with arterial load studied in isolated canine ventricle. Am J Physiol, 245 (1983), pp. H773-H780

[75] Burkhoff D, Mirsky I, Suga H. Assessment of systolic and diastolic ventricular properties via pressure-volume analysis: a guide for clinical, translational, and basic researchers. Am J Physiol Heart Circ Physiol, 289 (2005), pp. H501-H512

[76] Carabello BA, Paulus WJ. Aortic stenosis. Lancet. 2009 Mar 14;373(9667):956-66. doi: 10.1016/S0140-6736(09)60211-7. Epub 2009 Feb 21.

[77] Cowger J, Pagani FD, Haft JW, et al. The development of aortic insufficiency in left ventricular assist device-supported patients. Circ Heat Failure 2010;3:668-74

[78] Crestanello JA, Orsinelli DA, Firstenberg MS, et al. Aortic valve thrombosis after implantation of temporary left ventricular assist device. Interact Cardiovasc Thorac Surg 2009;8:661-2.

[79] Mudd JO, Cuda JD, Halushka M, et al. Fusion of aortic valve commissures in patients supported by a continuous axial flow left ventricular assist device. J Heart Lung Transplant 2008;27:1267-74.

[80] Crow S, John R, Boyle A, et al. Gastrointestinal bleeding rates in recipients of nonpulsatile and pulsatile left ventricular assist devices. J Thorac Cardiovasc Surg 2009;137:208-15.

[81] Balcioglu O, Engin C, Yagdi T, et al. Effect of aortic valve movements on gastrointestinal bleeding that occurred in continuous flow left ventricular assist device patients. Transplant Proc 2013;45:1020-1.

[82] Slaughter MS, Pagani FD, Rogers JG, et al. Clinical management of continuous-flow left ventricular assist devices in advanced heart failure. J Heart Lung Transplant 2010;29:S1-39.

[83] Feldman D, Pamboukian SV, Teuteberg JJ, et al. The 2013 International Society for Heart and Lung Transplantation Guidelines for mechanical circulatory support: Executive summary. The Journal of Heart and Lung Transplantation. Volume 32, Issue 2, February 2013, Pages 157-187. https://doi.org/10.1016/j.healun.2012.09.013

[84] Goldberg RJ, Makam RC, Yarzebski J, et al. Decade-Long Trends (2001-2011) in the Incidence and Hospital Death Rates Associated with the In-Hospital Development of Cardiogenic Shock after Acute Myocardial Infarction. Circ Cardiovasc Qual Outcomes 2016;9:117-25.

[85] Csepe TA, Kilic A. Advancements in mechanical circulatory support for patients in acute and chronic heart failure. J Thorac Dis 2017;9(10):4070-4083. doi: 10.21037/jtd.2017.09.89